Structural studies of two outer membrane proteins: OmpT from *Escherichia coli* and NspA from *Neisseria meningitidis*

Structurele studies aan twee buitenmembraaneiwitten: OmpT van *Escherichia coli* en NspA van *Neisseria meningitidis*

(met een samenvatting in het Nederlands)

Proefschrift

ter verkrijging van de graad van doctor aan de Universiteit Utrecht
op gezag van Rector Magnificus, Prof. Dr. W.H. Gispen,
ingevolge het besluit van het College voor Promoties
in het openbaar te verdedigen op maandag
13 oktober 2003 des middags te 4.15 uur

door

Lucy Vandeputte-Rutten

geboren op 5 augustus 1974 te Leiden

Promotoren: **Prof. Dr. P. Gros**
Prof. Dr. M.R. Egmond

Beide verbonden aan de Faculteit Scheikunde
van de Universiteit Utrecht

Het in dit proefschrift beschreven onderzoek werd uitgevoerd bij de vakgroep Kristal- en Structuur Chemie, Bijvoet Centrum, Universiteit Utrecht, Padualaan 8, 3584 CH Utrecht, Nederland
Het onderzoek werd gefinanceerd door de Nederlandse organisatie voor Wetenschappelijk Onderzoek (NWO), Gebied Chemische Wetenscappen (CW).

ISBN: 90-393-3489-7

Aan mijn ouders

Lay-out: Audiovisuele dienst Chemie,
Universiteit Utrecht

Reproductie: Labor, Utrecht

Contents

1

General introduction

Bacteria

Bacteria are unicellular organisms that range in size from 0.5 μm to about 20 μm. They are subdivided into two classes according to the Gram-staining (Popescu & Doyle, 1996). Gram-positive and Gram-negative bacteria differ in the composition of their cell-envelope. Both classes contain an inner membrane with a cross-linked peptidoglycan layer on top of it. In Gram-positive bacteria this layer is thicker and forms the outer surface of the bacterium, whereas Gram-negative bacteria have an additional membrane at the outside, which is called the outer membrane (Figures 1.1 and 1.2).

Whereas most bacteria pose no threat to human health, a number of them can be pathogenic (Table 1.1), causing infectious diseases. A number of these infections can be prevented by the administration of vaccines, non-toxic antigens derived from the causative bacterium, that activate the host humoral immune system. In addition, due to the wide use of antibiotics since the 1950s, bacterial infectious diseases ceased to be a major threat to public health in the western world. In the last two decades, however, it has become clear that bacterial infectious diseases are all but eradicated.

The emergence of drug-resistance in pathogenic bacteria is an important cause of the reappearance of infectious diseases in the developed world. Tuberculosis is a striking example of an infectious disease which had almost been eliminated but which reappeared, leading to many deaths worldwide (Zumia & Grange, 2001). This reappearance was due to the development of *M. tuberculosis* strains that were multidrug-resistant as a result of the uncontrolled use of antibiotics. Another example is the methicillin-resistant *Staphylococcus aureus* (MRSA) strain, which causes considerable problems in many hospitals (Haddadin *et al.*, 2002).

Due to the growing mobility of the world population, as well as the increasingly massive character of many manifestations the risk of outbreaks has also significantly increased. In The Netherlands for example, there have been recent outbreaks of Legionnaires disease (Hoepelman, 1999), caused by *Legionella pneumophila* and meningococcal meningitis, caused by *Neisseria meningitidis*. A large-scale vaccination program has been initiated to prevent meningococcal infections in children. Unfortunately, this vaccine does not provide protection against all pathogenic meningococcal strains.

These recent developments, challenge new lines of research on novel drugs and vaccines against bacterial infections. In the case of Gram-negative bacteria, the focus on outer membrane proteins (OMPs) as therapeutic targets may be a promising strategy for developing these novel compounds. Three-dimensional structures of proteins have, in a number of cases, been crucial for the design of drugs (reviewed by Kuhn *et al.* (2002)). For example, the structure of HIV-1 protease has led to the development of an inhibitor

Table 1.1 **pathogenic Gram-negative bacteria**

pathogen	reservoir	main disease	virulence factors	prevention/ treatment
Borrelia burgdorferi	white-footed mouse/ ticks	Lyme disease	Outer surface protein/ adhesins	antibiotics in early disease (doxycyline, amoxicille)
Yersinia spp. (e.g. *Yersinia pestis*)	fleas, rodents, cats	bubonic/ pneumonic plague	toxins, omptin	rodent control, antibiotics
Pseudomonas auruginosa	water/ soil and plants	variety of opportunistic infections	adhesins/ LPS/toxins	No vaccine, antibiotic resistance rising
Legionella pneumophila	amoebae in soil and water/ air-conditioning	Legionnaires disease	proteolytic enzymes	no vaccine, antibiotics
Helicobacter pylori	human stomach	gastric ulcers	adhesins/ toxin/LPS	no vaccine/ antibiotics
Vibrio cholerae	infected humans	cholera	toxin	no vaccine
Salmonella species	human carriers, livestock animals	typhoid fever/ gastroenteritis	adhesions/ LPS	vaccine against S. typhi antibiotics
Escherichia coli	human colon	diarrhea/ urinary tract infections/sepsis and meningitis	adhesions/ OmpT/ toxins	antibiotics, antibiotics are not used against diarrhea
Neisseria meningitidis	human throat and nose	epidemic meningitis	adhesions (Opa, OpcA)	vaccine available against some serotypes/antibiotics if administered early
Chlamydia trachomatis	infectected humans	cervical infection/ enfertility		antibiotic treatment

Not all pathogenic bacteria, possible reservoirs, related diseases, virulence factors or prevention and treatment methods are listed, but a relevant selection is made based on Bacterial Pathogenesis, A molecular approach by A. A. Salyers and Dixie D. Whitt.

of this protease (Wlodawer & Vondrasek, 1998), which is part of a cocktail of drugs administered to people suffering from AIDS (Gulick, 2003). Another example is neuraminidase (Wade, 1997), an enzyme isolated from influenza viruses. Its structure was crucial for the design of drugs that are used to prevent common flu. Whereas structure-based drug design is becoming an established method, the development of vaccine compounds, including peptides, is still mainly performed through classical methods. Recently, a new approach for vaccine development, which involved a structure-based design of a putative peptide-vaccine, has proven to be successful in eliciting bactericidal antibodies in mice (Oomen *et al.*, 2003).

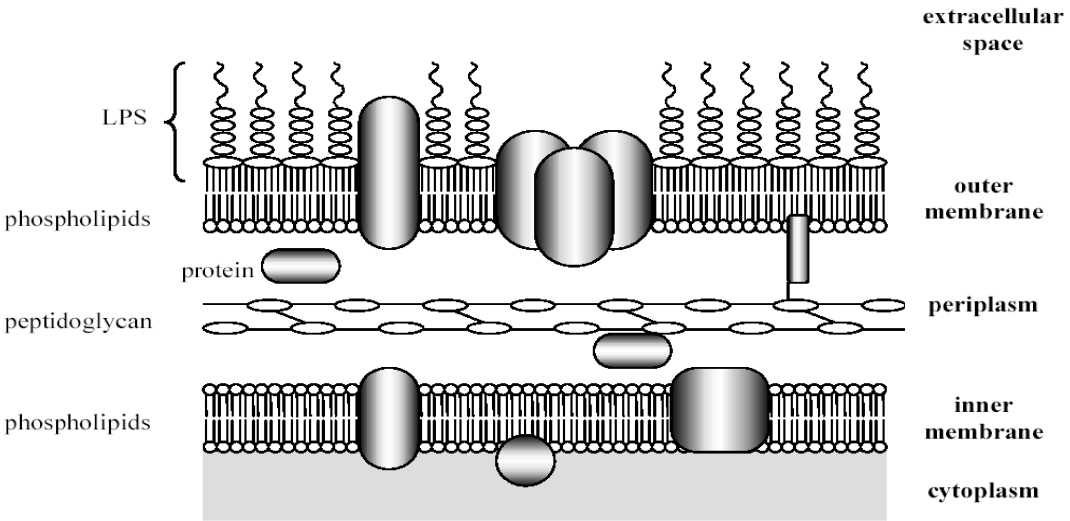

Figure 1.1 **Schematic representation of the Gram-negative cell-envelope.**
The Gram-negative cell envelope consists of three layers, i.e. the inner membrane, the peptidoglycan layer and the outer membrane. The inner membrane, also called the cytoplasmic or plasma membrane, is composed of a bilayer of phospholipids. Between the inner and the outer membranes in Gram-negative bacteria a fluid gel-like zone is present, called the periplasmic space. This space contains a cross-linked peptidoglycan layer and many soluble proteins involved in processes such as protein secretion and the uptake of nutrients. Like the inner membrane the outer membrane also consists of an inner leaflet and an outer leaflet. However, the lipid bilayer of the outer membrane has an asymmetric organization. It is composed of phospholipids (70-80% phosphatidylethanolamine, 20-30% phospatidylglycerol, and cardiolipin) and lipoproteins in the inner leaflet and mainly lipopolysaccharides (LPS) and sometimes also phospholipids in the outer leaflet, such as in *N. meningitidis*.

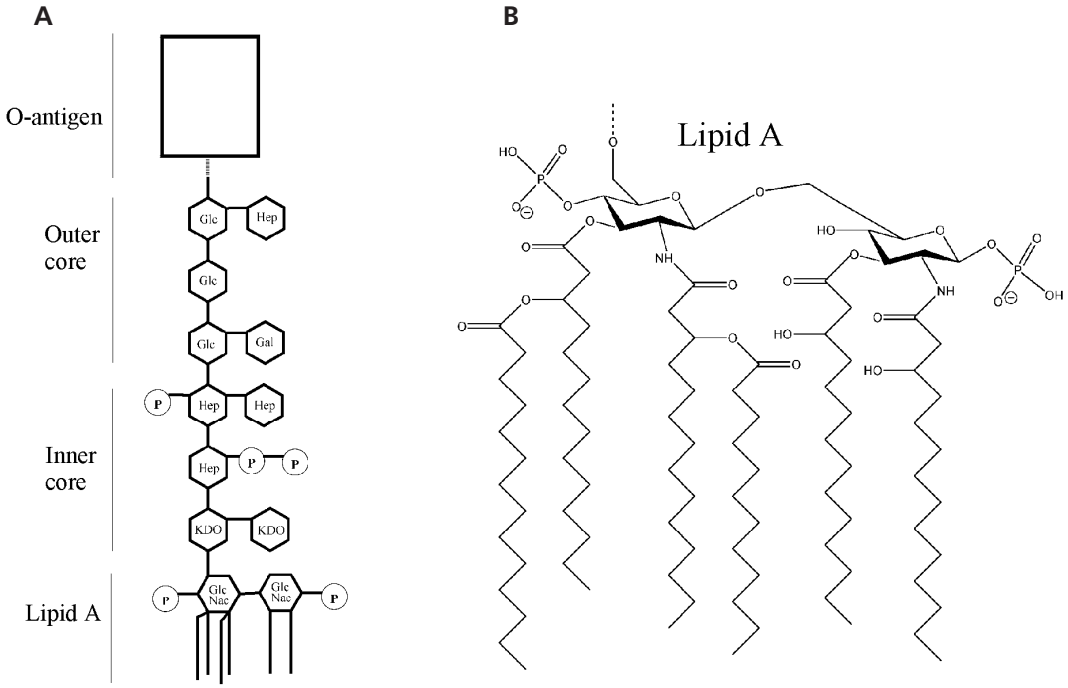

Figure 1.2 **Lipopolysaccharide.**
A) Lipopolysaccharide (LPS) from *Escherichia coli* strain K-12. LPS is built up of three components, the lipid A part, the core region and the O-antigen. The core region can be divided into the inner and the outer core. The O-antigen is not present in *Escherichia coli* strain K-12 and some other Gram-negative bacteria. GlcNac = *N*-acetyl-D-glucosamine, Kdo = 3-deoxy-D-*manno*-oct-2-ulopyranosonic acid, Hep = L-*glycero*-D-*manno*-heptose, Glc = D-glucose, Gal = D-galactose, P = phosphate or aminoethyl phosphate. *N. meningitidis* LPS, which is also referred to as lipooligosaccharide (LOS), contains a shorter tail of core carbohydrates than *E. coli*. LPS B) Structure of the Lipid A part of LPS. The dotted line indicates where the core sugars are attached.

Escherichia coli

Escherichia coli are Gram-negative rods and contain flagella that are necessary for motility. Classification of *E. coli* strains is based on the reactivity of highly variable bacterial surface molecules with different antibodies (Orskov & Orskov, 1992). The O-antigen of LPS identifies the serogroup of the strain and the H-antigen of flagella identifies the serotype. Some *E. coli* strains contain a polysaccharide capsule (the K-antigen), which is also used for classification. Most *E. coli* strains are nonpathogenic and

are commensally present in human intestines. *E. coli* can grow under aerobic and anaerobic conditions and do not posses very special nutritional requirements. Therefore, *E. coli* has been used as a model organism for studying many biological phenomena. A number of different *E. coli* strains, however, can cause diseases, including diarrhoea, dysentery, kidney failure, urinary tract infections, septicaemia, pneumonia and meningitis. For example, the production of powerful endotoxins by serotype O157:H7 has been found to be an important cause of severe diarrhoea (traveller's diarrhoea) and kidney failure (Peacock *et al.*, 2001)

Uropathogenic *E. coli* strains (UPEC) are responsible for 70-95% of urinary tract infections acquired outside hospitals (Mulvey *et al.*, 2000). The ability of these *E. coli* strains to adhere to the bladder mucosae in order to colonize the bladder is thought to be a key feature of such strains, because non-adhered bacteria are discharged from the bladder via urination before they can multiply in large quantities. In addition, uropathogenic *E. coli* strains multiply much faster than other *E. coli* strains in urine, again facilitating the colonization of the urinary tract (Gordon & Riley, 1992). Possibly, uropathogenic *E. coli* are resistant to bactericidal defensins, like protamine, that are excreted by the epithelial cells of the urinary tract (Stumpe *et al.*, 1998). This resistance may be mediated by the action of the protease OmpT present in the outer membrane of *E. coli* (Stumpe *et al.*, 1998). Other factors involved in virulence of the uropathogenic *E. coli* strain include LPS, which induces an inflammatory response, α-hemolysin, which forms pores in host cell membranes, and the K-antigen capsule, which protects the bacterium from phagocytosis.

Neisseria meningitidis

The Gram-negative diplococcus *N. meningitidis* is the main cause of life-threatening meningitis, which is the inflammation of the meninges, the membranes surrounding the brain. In addition, infection by *N. meningitidis* can cause sepsis, leading to a septic shock. The bacterium is continuously present in the mucosae of the naso-pharynx of approximately 10% of the population, without causing any symptoms (Pollard & Frasch, 2001). Only when it enters the blood stream, it can cause infection. Meningococcal meningitis and sepsis can be treated with antibiotics, if recognized early enough. However, early diagnosis of meningococcal infection is difficult, because patients often present with non-specific symptoms, such as fever and headaches. Even when treated, the mortality caused by *N. meningitidis* infections is 10% and even if people survive, lifelong complications may remain such as amputations, loss of sight or impaired hearing.

N. meningitidis strains contain a polysaccharide capsule around the outer membrane. Based on these capsular polysaccharides *N. meningitidis* strains are divided in 12 serogroups, which are further divided into sub-serogroups. Five of these serogroups,

designated A, B, C, Y and W-135, account for 90% of the disease-producing isolates (Cripps *et al.*, 2002). Diseases caused by serogroups B and C predominate all over the world. Vaccines containing meningoccocal polysaccharides are currently available for A, C, Y and W-135, but are only effective in children above 2 years of age (Wildes & Tunkel, 2002). Vaccines that are more effective against *N. meningitidis* serogroup C consist of C-polysaccharide conjugated to tetanus toxoid or a nontoxic mutant of diphtheria toxin, to enhance the immunogenicity of the vaccine (Fairley *et al.*, 1996). No vaccine is commercially available yet against serogroup B, which is responsible for half of the meningococcal infections in the developed countries. Capsular polysaccharides of serogroup B cannot be used as a vaccine because they are poorly immunogenic, probably because these polysaccharides contain sialic acid residues, which are also present on the surface of most human cells (Moe & Granoff, 2001).

Researchers have started to explore the possibility of using outer membrane vesicles (OMVs) containing immunogenic outer membrane proteins (OMPs) for vaccine development (Morley & Pollard, 2001). Much progress has been made using PorA, derived from different meningococcal B strains, in outer membrane vesicles as potential vaccine. A hexavalent PorA outer membrane vesicle preparation was shown to elicit bactericidal antibodies in human (Peeters *et al.*, 1996). PorB and Opc are also being explored as potential vaccine candidates (Rosenqvist *et al.*, 1995; Wright *et al.*, 2002). A disadvantage of using the highly immunogenic OMPs, such as PorA, PorB and Opc as vaccines, is that these proteins are hypervariable in sequence. Hypervariability of certain genes is caused by the high mutation and recombination rate of *N. meningitidis*, which results in the occurrence of novel antigen sequences. As a result, strains with novel antigen sequences may not be recognised anymore by the antibodies raised against the original OMPs. Therefore, efforts have been made to identify outer membrane proteins that are more conserved in sequence. One of the successes has been the identification in 1997 of a highly conserved OMP, NspA, which is therefore an attractive vaccine candidate (Martin *et al.*, 1997).

Outer membrane proteins

Bacterial outer membrane proteins (OMPs) perform a range of important functions. They can form channels, which are involved in the uptake of nutrients and the export of proteins. They can function as adhesins, which mediate the adherence of bacteria to host cells. Other OMPs are enzymes, involved in lipopolysaccharide modification, phospholipid degradation or proteolysis of extracellular proteins. Because OMPs are exposed at the surface of the bacterium they are potential targets for antimicrobial drugs and vaccine development.

Overall structure of OMPs

A number of OMP structures have been solved using X-ray crystallography and, in a few cases, NMR spectroscopy. These studies have revealed the general architecture of OMPs and in addition indicate that, despite the different functions performed by OMPs, their structures are much less diverse than those of water-soluble proteins. Whereas inner membrane proteins are solely made up of α-helices with long stretches of hydrophobic residues, outer membrane proteins exclusively contain next-neighbour anti-parallel β-strands, forming closed barrels, referred to as β-barrels.

β-Barrels of OMPs come in different sizes and forms (Figure 1.3). Structures of OMPs solved to date, revealed β-barrels containing 8 up to 22 β-strands (Table 1.2), assembled as monomer or in some cases, multimers. Viewed from the extracellular side, the β-strands are arranged in a clockwise fashion around the central axis of the beta-barrel (Figure 1.4). The tilt angle of the strands with respect to the barrel axis is also clockwise. The diaphragm of the barrel depends on this tilt, which is on average 45° and which itself depends on the shear number of the strands. The shear number gives the number of amino acids the strand goes up when the next neighbour hydrogen bonded residues are followed until reaching the starting strand again.

In the membrane-spanning region of the β-barrel, all main chain hydrogen bond donor and acceptors participate in inter-strand hydrogen bonding. Also within the same region, hydrophobic residues point towards the membrane whereas hydrophilic residues point to the inside of the β-barrel (reviewed by Schulz *et al.* (Schulz, 2002). In water-soluble proteins this is the reverse. Most OMPs contain girdles of aromatic residues at the membrane boundaries that probably stabilize the position of the protein in the outer membrane. Furthermore, OMPs contain short turns (called T1, T2, …) at the periplasmic side of the barrel and long loops (called L1, L2, …) at the extracellular side of the barrel. The N-terminal and C-terminal regions of the protein are always located at the periplasmic side.

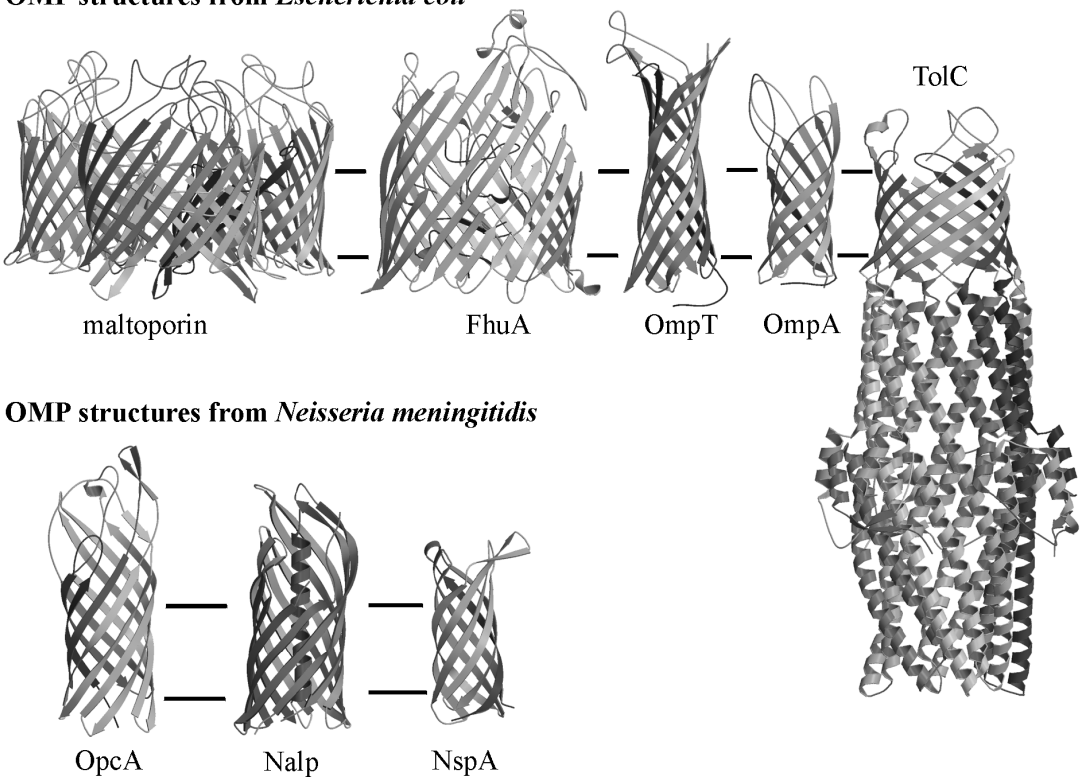

Figure 1.3 **Structures of OMPs with different sizes.** The hydrophilic/hydrophobic boundaries of the outer membrane are indicated with black lines. All OMPs are shown as ribbon representations and are at the same scale. The upper panel shows some *E. coli* OMP structures, whereas the lower panel shows all OMP structures known from *N. meningitidis*. The *E. coli* OMPs are Maltoporin (Schirmer *et al.*, 1995), FhuA (Ferguson *et al.*, 1998), OmpT (described in this thesis (Vandeputte-Rutten *et al.*, 2001)), OmpA (Pautsch & Schulz, 1998) and TolC (Koronakis *et al.*, 2000). The OMPs from *N. meningitidis* are OpcA (Prince *et al.*, 2002), NalP (Oomen, submitted) and NspA (described in this thesis (Vandeputte-Rutten *et al.*, 2003))

Table 1.2 **OMPs with known structure.**

No. of β-strands	name	Species	function
8	OmpA (Pautsch & Schulz, 1998)	*Escherichia coli*	membrane-anchor to periplasm
	OmpX (Vogt & Schulz, 1999)	*Escherichia coli*	Adhesin
	PagP (Hwang *et al.*, 2002)	*Escherichia coli*	LPS modification
	NspA (Vandeputte-Rutten *et al.*, 2003)	*Neisseria meningitidis*	function not known yet
10	OmpT (Vandeputte-Rutten *et al.*, 2001)	*Escherichia coli*	protease
	OpcA (Prince *et al.*, 2002)	*Neisseria meningitidis*	Adhesin
12	OMPLA (Snijder *et al.*, 1999)	*Escherichia coli*	phospholipase
	TolC (Koronakis *et al.*, 2000)	*Escherichia coli*	protein transport
	NalP (Oomen *et al.*, submitted)	*Neisseria meningititidis*	Autotransporter
16	porin (Weiss *et al.*, 1990)	*Rhodobacter capsulatus*	porin
	ompF (Cowan *et al.*, 1992)	*Escherichia coli*	porin
	PhoE (Cowan *et al.*, 1992)	*Escherichia coli*	porin
	porin (Kreusch *et al.*, 1994)	*Rhodopseudomonas blastica*	porin
	porin (Hirsch *et al.*, 1997)	*Paracoccus denitrificans*	porin
	OmpK36 (osmoporin) (Dutzler *et al.*, 1999)	*Klebsiella pneumoniae*	porin
	anion selective Omp32 (Zeth *et al.*, 2000)	*Comamomonas acidovorans*	porin
18	Maltoporin (Schirmer *et al.*, 1995)	*Escherichia coli*	porin
	Maltoporin (Meyer *et al.*, 1997)	*Salmonella typhimurium*	porin
	Sucrose specific ScrY porin (Forst *et al.*, 1998)	*Salmonella typhimurium*	porin
22	FhuA (Ferguson *et al.*, 1998)	*Escherichia coli*	iron-siderophore uptake
	Ferric enterobacterin receptor (fepA) (Buchanan *et al.*, 1999)	*Escherichia coli*	iron-siderophore uptake
	ferric citrate transporter (FecA)(Ferguson *et al.*, 2002)	*Escherichia coli*	iron- siderophore uptake

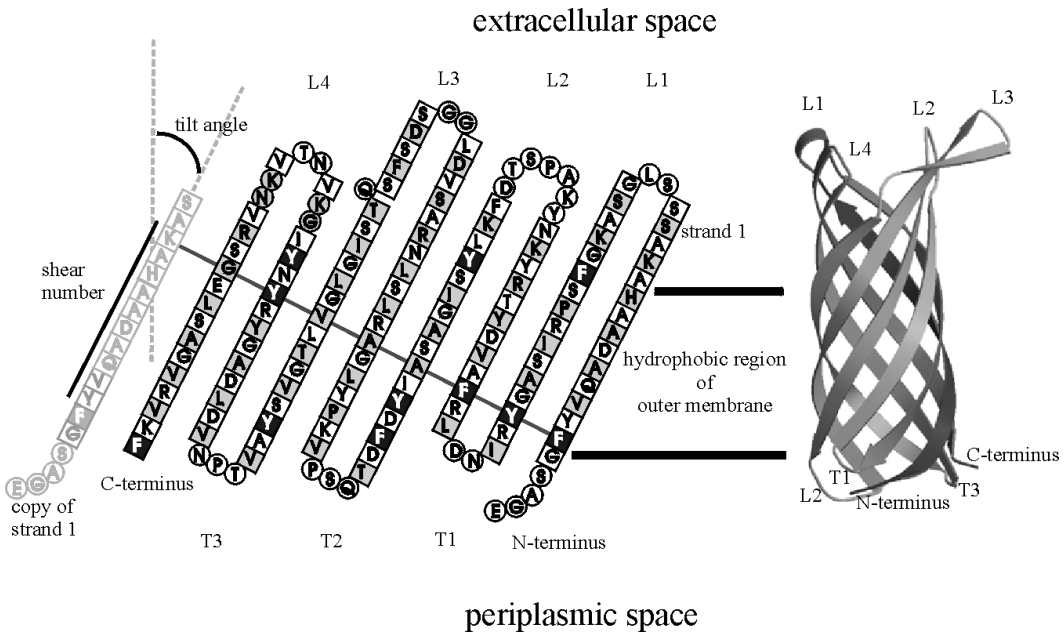

Figure 1.4 **Topology model and structure of NspA, an example of the architecture of OMPs.**
The view of the topology model (left panel) is from outside the β-barrel. A copy of the N-terminal strand is placed next to the C-terminal strand. Residues are indicated with one-letter codes. The residues that point to the outside of the β-barrel are with a grey shaded or black background, whereas the residues that point to the inside of the β-barrel have a white background. The hydrophobic/hydrophilic boundaries of the outer membrane are indicated with black lines. Aromatic residues present at these boundaries are indicated with a black background. The short periplasmic turns are numbered T1, T2, and T3, whereas the longer extracellular loops are numbered L1 to L4. Using the copy of the N-terminal strand, the definitions of the shear number and the tilt angle are shown. In the case of NspA, the shear number is 10.

Transport and insertion into the OM

In vivo, OMPs are synthesized with a leader peptide or signal sequence preceding the mature protein sequence. This peptide is required for the recognition by the Sec chaperone system, which transports the unfolded OMPs across the inner membrane (Danese & Silhavy, 1998) into the periplasm. There, the signal peptide is cleaved off after which the protein is folded into the outer membrane. Voulhoux *et al.* recently showed that Omp85, a conserved 85-kDa outer membrane protein, is likely to play an important part in this latter process (Voulhoux *et al.*, 2003). The lack of long hydrophobic stretches

in OMPs is probably related to their requirement for transport across the inner membrane, which would otherwise be hampered, because the OMPs would get stuck in the inner membrane.

Recombinant production of OMPs

Determining the crystal structure of proteins heavily depends on obtaining pure protein in sufficient amounts. For a long time this has been difficult for membrane proteins, because they are low abundant. Fortunately, many OMPs can be recombinantly expressed in bacteria, without their leader sequence. This often leads to the formation of large amounts of inclusion bodies, insoluble protein aggregates in the bacterium, which consist for more than 90% of the desired protein. Inclusion bodies can be solubilized using 8M urea and the protein can subsequently be refolded to the native state in an appropriate detergent solution (Buchanan, 1999). Refolding of OMPs can be monitored by non-denaturing SDS-PAGE because folded OMPs have different mobility than if they are unfolded (Beher *et al.*, 1980). This is referred to as heat-modifiability. Expression using inclusion bodies typically yields milligram amounts of the desired protein of high purity, which facilitates further purification by means of ion-exchange chromatography. During all steps of purification, OMPs have to stay in detergent containing solution to keep them soluble.

OMP structures of E. coli and N. meningitidis

More than half of the OMP structures, which are 22 in total solved to date are from *E. coli*. Although many *E. coli* OMPs have homologous counterparts in other Gram-negative bacteria, this is not always the case. For example, many important adhesin molecules, such as Opa from *N. meningitidis,* are not conserved in *E. coli*. In addition, for structure-based vaccine development, it is necessary to determine the structure of the loops of OMPs, as these are the targets of bactericidal antibodies. OMP loops are generally not highly conserved. It is therefore not surprising that the number of structures solved of OMPs from other Gram-negative bacteria is increasing.

Structures of three OMPs from *N. meningitidis*, OpcA, NalP and NspA, have been solved. OpcA is an adhesin, which facilitates binding of the bacterium to human cells. One of the ligands for OpcA is the plasma glycoprotein vitronectin, which adheres to human cells. The structure of OpcA, which comprises a 10-stranded β-barrel, reveals a positively charged binding cleft, possibly constituting the binding site for vitronectin (Prince *et al.*, 2002; Virji *et al.*, 1994).

NalP is a member of the family of autotransporters, which transport their own N-terminal domain across the OM. This domain, 'the passenger domain', is often an important virulence factor. The crystal structure of the translocator domain of NalP

revealed a 12-stranded barrel with a central N-terminal α-helix inside (Oomen *et al.* submitted). This structure forms the basis for a proposed mechanism for translocation, which does not require ATP. In this thesis the structure of NspA from *N. meningitidis* is discussed.

Outer membrane enzymes

Four different types of outer membrane enzymes have been identified and characterized to date, OmpT, OMPLA, PagP and PagL. Of the first three, structures have been solved, which of the structure of OmpT is discussed in this thesis. OMPLA is an enzyme that breaks down phospholipids presented at the outer leaflet of the OM. In *E. coli*, these phospholipids are normally only present in the inner leaflet of the membrane, but can be translocated to the outer leaflet when the OM is disrupted. The crystal structures of OMPLA in complex with and without a substrate analogue have been solved (Snijder *et al.*, 1999). These structures provide detailed insight into the activation, which is dependent on calcium and dimerization. The catalytic site containing Ser-His-Asn resembles the classical serine hydrolases catalytic triads, but the contribution of the asparagine to catalysis is only modest (Kingma *et al.*, 2000).

PagP is an enzyme that transfers a palmitate residue from the sn-1 position of a phospoholipid to the N-linked 3-hydroxymyristate on the proximal unit of lipid A. This modification of LPS is thought to provide resistance against anti-microbial peptides. An NMR structure has been solved for PagP (Hwang *et al.*, 2002). The NMR structure shows that PagP is an 8-stranded β-barrel, with an N-terminal α-helix, having very flexible extra-cellular loops. The proposed catalytic site, consisting of a classical Ser-His-Asp triad is not intact in the structure, but it is proposed that stabilization of the tetrahedral transition state compensates for the energy needed for substrate binding. Recently, another enzyme involved in LPS modification has been identified, named PagL (Trent *et al.*, 2001). This enzyme cleaves off one acyl chain of LPS. No structure is as yet available for this enzyme.

Proteases

Proteases, also referred to as proteinases, proteolytic enzymes, peptidases or peptide hydrolases, catalyse the hydrolysis of peptide bonds. Proteases can be divided into two categories, exopeptidases and endopeptidases. Exopeptidases act only near the N- or C-terminini of the polypeptide chains, whereas endopeptidases act in the inner regions of substrates. Some proteases have a high specificity for certain amino acids, whereas others are much less specific and cleave at multiple sites. Proteases are involved in a multitude of processes, such as degradation of unfolded or misfolded proteins, activation of other

enzymes and protein transport. To date, proteases are classified, based on their catalytic mechanism, into four major classes. These are serine peptidases, cysteine peptidases, aspartic acid peptidases and metallopeptidases, named after key residues or cofactor involved in the enzymatic reaction. Some proteases that contain a threonine as the nucleophile, are classified as a group in the serine peptidases sub-class, and others that have a glutamic acid are grouped among the aspartic proteases.

The residues in substrates are numbered according to their position with respect to the cleavage site (Schechter & Berger, 1967). The residues away from the cleavage site towards the N-terminal direction are numbered P1, P2, …, and the residues away from the cleavage site towards the C-terminal direction are number P1', P2', …. A similar numbering exists for the substrate binding sub-sites in the protease. The numbering of these sub-sites are S1, S2, … and S1', S2', ….

Catalysis by serine proteases

Classical serine proteases contain a Ser-His-Asp catalytic triad in a special rearrangement. The mechanism used by serine proteases involves two major stages, the acylation stage (stage 1) and the deacylation stage (stage 2) (Figure 1.5). In the absence of substrate, one of the nitrogens in the side chain of the histidine is protonated. The aspartic acid stabilizes the proton at the Nε1 position, such that during the first step of acylation of the substrate, the histidine acts as a base abstracting a proton from the OH-group of the serine residue, which then performs a nucleophilic attack on the carbonyl carbon of the substrate. The four atoms bonded to the carbonyl carbon are then arranged as in a tetrahedron, resulting in a tetrahedral intermediate. The tetrahedral intermediate is stabilized by binding of the carbonyl oxygen in a positively charged hole, the oxyanion hole. This positive oxyanion hole, which is usually made up of two backbone amides, makes the carbonyl oxygen more negatively charged by attracting an electron, whereas the carbonyl carbon becomes more positively charged and therefore becomes more vulnerable to nucleophilic attack. In the next step of the acylation stage, the acyl-enzyme intermediate is formed. The extra electron at the carbonyl oxygen returns to its original position and the proton at the histidine abstracted from the serine, is donated to the amine part of the substrate. In the second stage in the hydrolysis of a peptide bond, the acyl-enzyme intermediate is hydrolysed by water. The amine component diffuses away from the active site and is replaced by water. The histidine now abstracts a proton from the water molecule making the water molecule nucleophilic towards the carbonyl carbon. Like in the first stage, again a tetrahedral transition state is formed, followed by the release of the acid part of the substrate and donation of the proton of the histidine back to the serine, regenerating the native enzyme species.

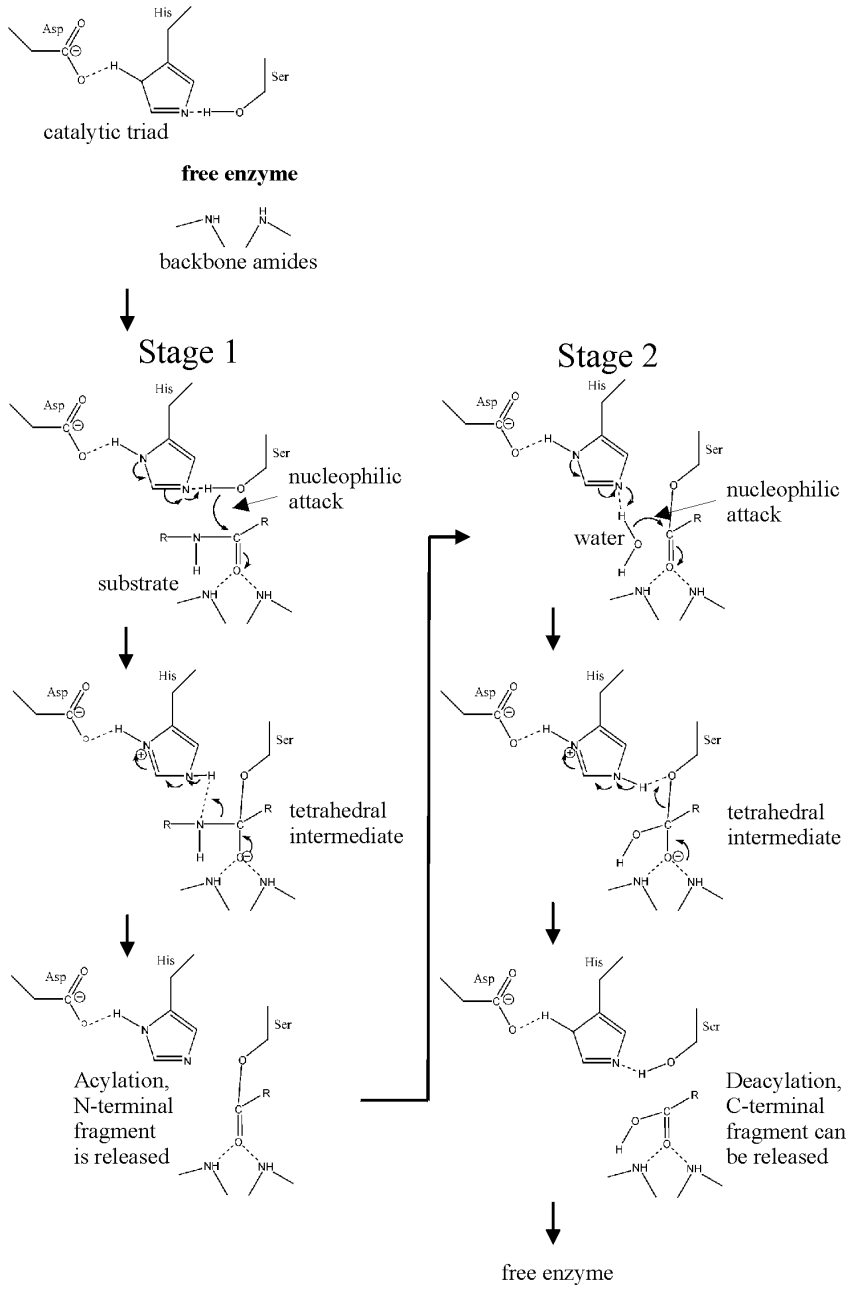

Figure 1.5 **Proposed catalytic mechanism for serine proteases containing the classical Ser/His/Asp catalytic triad**. The dotted lines show hydrogen bonds, whereas the solid lines are covalent interaction made up of electron pairs. The arrows indicate the movement of the electron pairs.

Omptins

Omptins are a family of integral outer membrane proteases present in a number of pathogenic Gram-negative bacteria. Characterized members of the omptin family include OmpT and OmpP from *Escherichia coli* (Kaufmann *et al.*, 1994), Pla from *Yersinia pestis* (Sodeinde & Goguen, 1989), PgtE from *Salmonella thyphimurium* (Grodberg & Dunn, 1989; Yu & Hong, 1986) and SopA from *Shigella flexneri* (Egile *et al.*, 1997). A homology blast in the genomic sequence database yielded additional homologs of omptins in e.g. *Mesorhizobium loti*, *Salmonella typhi*, *Salmonella paratyphi*, and *Leuconostoc pneumophila*, and *Yersinia pestis*. The omptin family is still growing as the number of bacterial genomes that is sequenced, is increasing. Interestingly, omptins are not present in all Gram-negative bacteria, for example *Neisseria meningitidis* lacks an omptin homologue.

A number of studies have suggested a role for the omptin family in bacterial pathogenicity. For example Pla from *Yersinia pestis* the causative agent of bubonic plague, was shown, by Sodeinde *et al.*, to act as an important virulence factor. They showed that inactivation of this gene resulted in a million-fold increase of the median lethal dose of the bacteria for mice. (Sodeinde *et al.*, 1992). In addition, several studies have reported a positive correlation between the presence of the OmpT gene in *E. coli* and severe urinary tract disease as well as neonatal meningitis (Webb & Lundigran, 1996) (Johnson *et al.*, 2002).

Functions of omptins

Omptins have been implicated in the hydrolysis of various peptides and proteins *in vitro*. Many of these include recombinant proteins overexpressed in *E. coli* that are degraded by OmpT (Grodberg & Dunn, 1988; Hammarberg *et al.*, 1990; Henderson *et al.*, 1994; Sugimura & Higashi, 1988; White *et al.*, 1995; Zhao & Somerville, 1993) and are not likely targets *in vivo*. However, a number of studies have identified host proteins or peptides that are related to bacterial invasion and immunity, which are candidate targets for the omptin family.

Defense against innate immune system

OmpT has been found to cleave the antimicrobial cationic peptide protamine, which is excreted by epithelial cells of the urinary tract (Stumpe *et al.*, 1998). Likewise, PgtE of *Salmonella typhimurium* promotes resistance to α-helical cationic antimicrobial peptides (α-CAMPs) (Guina *et al.*, 2000). In both cases, the bacterium is protected in this way against the innate immune system, which is the first line of defense against bacterial infection. In addition, it was also reported that Pla from *Yersinia Pestis* cleaves complement C3, which is the central complement factor, on which all three complement pathways converge (Sodeinde *et al.*, 1992).

Plasminogen activation

It is likely that the most important function of Pla is to cleave plasminogen, a property it shares with OmpT from *E. coli* (Leytus *et al.*, 1981) and PgtE from *Salmonella thyphimurium*. The specific cleavage of the zymogen plasminogen results into the active protease plasmin, which mediates lysis of fibrin, which is normally deposited around the bacterium to trap the bacterium after infection. In this way omptins may act to breach barriers to enhance the spread of the bacterium. This theory is supported by the finding that intact *E. coli* cells containing OmpT are capable of dissolving a fibrin film, whereas an OmpT mutant does not (Lundrigan & Webb, 1992).

Additional functions of Pla

Pla displays additionally coagulase activity, i.e. blood clotting activity (Sodeinde & Goguen, 1989). Blood clotting in the meal of the flea, which results in ejection of the meal including the plague bacterium into the host, is an important step in spreading of the bacterium from rodents to human. Therefore, Pla is most likely also involved in this process, although the proteolytic target of Pla in this process has yet to be identified. In addition, an adhesive function for Pla has also been observed (Kienle *et al.*, 1992), since expression of Pla of *Yersinia pestis* enhances bacterial attachment to the mammalian extracellular matrix (Lahteenmaki *et al.*, 1998).

Release of passenger domain of autotranporters

SopA (IcsP) of *Shigella flexneri*, the bacterium, which causes severe dysentery, has been found to cleave the extracellular part of (VirG) IcsA, an autotransporter, of which the transported extracellular domain binds to actin-filaments inside cells. Cleavage of IcsA by SopA was thought to be responsible for the motility of *Shigella flexneri* inside host cell (Egile *et al.*, 1997). However, Shere *et al.* showed that *Shigella flexneri* strains lacking the gene coding for SopA have accelerated motility (Shere *et al.*, 1997). Endogenous OmpT is able to release recombinant passenger domains by cleavage in the linker region between the passenger domain and the autotransporter b-barrel domain, which is inserted in the outer membrane (Klauser *et al.*, 1992; Maurer *et al.*, 1997), but no endogenous autotransporters have been found to be cleaved by OmpT.

OmpT

The gene encoding for the OmpT protein was discovered in 1976 (Manning & Reeves, 1976). OmpT is biochemically the best-characterized member of the omptin family. OmpT expression is temperature dependent, i.e. expression is higher at temperatures above 30°C, hence the T, which stand for temperature, in the name OmpT (Manning & Reeves, 1976) (Rupprecht *et al.*, 1983). The mature OmpT protein consists

of 297 amino acid residues, with a calculated mass of 33.5 kDa (Grodberg *et al.*, 1988). Proteolytic activity by OmpT has in many cases hampered overexpression and subsequent purification of recombinant proteins in *E. coli*. For this reason, novel *E. coli* strains, such as the widely used BL21(DE3) strains, were engineered that lack the gene encoding OmpT (Studier & Moffatt, 1986). Reports on cleavage of recombinant proteins by OmpT lead to the consensus that OmpT proteolytic activity shows preference for two consecutive basic amino acids. Using spatially addressed peptide libraries, OmpT substrate specificity was investigated in further detail, revealing the necessity of a positively charged residue at the P1 position of the peptide, whereas OmpT has a broader allowance for residues at the P1' position, except for negatively charged residues, cysteines, tryptophans and tyrosines (Dekker *et al.*, 2001). The activity of OmpT is dependent on the presence of lipopolysaccharide (LPS), which is normally abundantly present in the outer membrane of gram-negative bacteria (Kramer *et al.*, 2000b). Of the LPS the lipid A part is the minimal requirement for OmpT activity. Furthermore, the core phosphates are also important for activity (Kramer *et al.*, 2002). OmpT contains no conserved sequence motif typical for any of the protease families, making classification of OmpT difficult. Most commonly used protease inhibitors, including chloromethylketones, EDTA, leupeptin and antipain do not inhibit proteolytic activity of OmpT (Sugimura & Nishihara, 1988). However, high concentrations of the serine protease inhibitors diisopropylfluoro-phosphate (DFP) and phenylmethylsulfonyl fluoride (PMSF), do inhibit OmpT activity (Sugimura & Nishihara, 1988). Mainly based on these findings, omptins were classified as a new serine protease family (S18 in the enzyme database (omptins: EC 3.4.21.87)). The catalytic site of serine proteases typically consists of a serine-histidine-aspartate catalytic triad. Site directed mutagenesis of the conserved serines and histidines of OmpT and Pla, resulted in the identification of possible catalytic residues. The S99A mutation in OmpT reduced catalytic activity approximately 500 times whereas the H212A mutation led to a reduction in activity of ~10.000 times (Kramer *et al.*, 2000a). OmpT activity was found to have a pH optimum at high pH (Kramer *et al.*, 2000b). These two findings further supported the classification of OmpT as a serine protease. Later studies, however, contradict the earlier findings that the serine protease specific inhibitors PMSF and DFP can inhibit OmpT, since no effect of PMSF and DFP on OmpT activity could be detected, even at higher concentrations (Hollifield *et al.*, 1978; Sugimura & Higashi, 1988; White *et al.*, 1995). These conflicting results warranted further research into the catalytic mechanism used by the omptin family.

Neisserial surface protein A (NspA)

Neisserial surface protein A (NspA) was identified in 1997 by Martin et al. (Martin *et al.*, 1997) while searching for a potential vaccine candidate against *Neisseria meningitidis*. They immunized mice with different combinations of OM preparations in order to obtain hybridoma clones secreting mAbs specific for highly conserved surface antigens. One mAb (Me-1) was selected, because it cross-reacted with all nine meningococcal OM preparations tested. The mAb exhibited bactericidal activity against all meningococcal strains tested and passively protected mice against experimental meningococcal infection. Western blotting experiments indicated that Me-1 recognized protein bands with apparent molecular weights of 22-kDa and 18-kDa. Both bands appeared to correspond to a single protein, which was called Neisserial surface protein A (NspA).

NspA is highly conserved in sequence and is present and expressed in all strains of *Neisseria meningitidis* and *Neisseria gonorrhoeae*, tested so far (Cadieux *et al.*, 1999; Martin *et al.*, 1997; Moe *et al.*, 1999; Moe *et al.*, 2001; Plante *et al.*, 1999). The vaccine potential of NspA was investigated by using recombinant NspA protein expressed in *E. coli* (BL21(DE3)). This recombinant NspA was found to be present in the outer membrane as well as secreted in the culture supernatant, where it is present in outer membrane blebs (Martin *et al.*, 1997) (Moe *et al.*, 1999). Martin et al. (Martin *et al.*, 1997) purified the recombinant NspA from the culture supernatant using affinity chromatography and showed that this NspA shared enough immunological characteristics with the native protein, to induce bactericidal antibodies. Moe et al., (Moe *et al.*, 1999) however, found that recombinant NspA elicited antibodies that cross-reacted with only 65% of 17 genetically diverse meningococcal strains. Only 73% of these strains that were recognized were susceptible to anti-NspA complement-mediated bacteriolysis. A later study, in which mice and guinea pigs were sequentially immunized with three doses of OMVs prepared from genetically different meningococcal strains, showed that an NspA-based vaccine prepared from protein expressed by Neisseria itself did elicit broadly protective antibodies (Moe *et al.*, 2002).

Mature NspA protein is a relatively small protein consisting of only 155 amino acids. Like other OMPs, the NspA protein is heat-modifiable, which explains the observation that NspA runs as two bands on a SDS-PAGE gel. The 18-kDa band corresponds to the unfolded protein, whereas the 22-kDa band corresponds to the folded form. NspA shares significant homology with neisserial Opa proteins (Martin *et al.*, 1997; Moe *et al.*, 1999), which are important adhesins in *N. meningitidis*. A number of Opa proteins can bind to the human CEACAM (carcinoembryonic antigen cell adhesion molecule) family of receptor glycoproteins, thereby allowing the entry of Neisseriae into human cells (Virji *et al.*, 1996). The function of NspA has not been discovered yet. NspA does not seem to be essential for causing bacteremia, as an NspA knockout was highly virulent in infant

rats (Moe *et al.*, 2001). Nevertheless, the observation that NspA is highly conserved among different neisserial strains suggests an important function and makes it an attractive vaccine candidate.

Protein crystallography

Three-dimensional structures of proteins are a valuable tool to study protein functions, interaction between macromolecules and can be used for drug design. Three techniques can be used to obtain three-dimensional structural information, X-ray crystallography, nuclear magnetic resonance spectroscopy (NMR), and electron microscopy. Most three-dimensional atomic models of proteins are determined using X-ray crystallography and nuclear magnetic resonance (NMR) spectroscopy. Whereas NMR-spectroscopy does not require a protein crystal and reveals information about the dynamics of the molecule, it cannot be used for large protein molecules or complexes and does not yield structures to a resolution as high as for most crystal structures. Using X-ray crystallography, structures of large proteins or protein complexes can be solved to high resolutions (~3.5 Å-~1.2 Å). A striking example of a huge macromolecular complex that has been solved using x-ray crystallography in recent years is the structure of the ribosome (Ramakrishnan, 2002). A drawback of crystallography is that the method requires good quality protein crystals (Figure 1.6), which are not always easy to obtain. Crystallization of proteins, which requires milligrams of very pure protein, can take place when they are precipitated very slowly under the right conditions, which have to be searched for by trial-and-error.

Diffraction theory

Crystals are made up of three-dimensional arrays of identical repeating units, called unit cells. When protein crystals are placed in an X-ray beam, the X-rays will be scattered in all directions by the electron clouds of the atoms in the crystal. In analogy with the scattering of visible light by a two-dimensional grid, due to the repetitive building blocks (unit cells) of crystals, the scattered waves may be enhanced or completely extincted. The enhanced waves result in discrete diffraction and can be visualized, using a detector, as diffraction spots with different intensities that form a regular pattern (Figure 1.7). W. L. Bragg showed that X-ray diffraction by crystals can be regarded as if it were reflection from sets of parallel, equivalent planes of atoms in the crystal. When x-rays with wavelength λ impinge on a set of planes with indices hkl and interplanar spacing d at an angle θ, reflection at the same angle occurs, only if θ meets the condition $2d\sin\theta=n\lambda$, where n is an integer (Bragg's law). Reflection can thus only occur if the difference of distance travelled by the X-rays reflected by successive planes equals a whole number

times the wavelength λ of the incident beam. Using Bragg's law, the positions of the diffraction spots on the detector can be used to determine the size and characteristics of the unit cell. To obtain all possible reflections, the crystal is rotated, to ensure that all planes have been in reflection orientation.

The X-rays that arrive at the detector can be described by the structure factors (F_{hkl}), which is a fourier summation of all atomic scattering factors. Whereas diffraction by electrons in a crystal can be translated by a fourier transform into structures factors, structure factors are in turn used to calculate the electron density using again a fourier transform. In the calculated electron density a protein model can be built. The structure factor includes the amplitude of the resultant diffracted X-ray waves as well as their phases. The amplitude of the structure factor can be derived from the measured intensity of the reflection, whereas, unfortunately, the phase of the reflected X-rays cannot be measured. This crystallographic problem is referred to as the 'phase problem'.

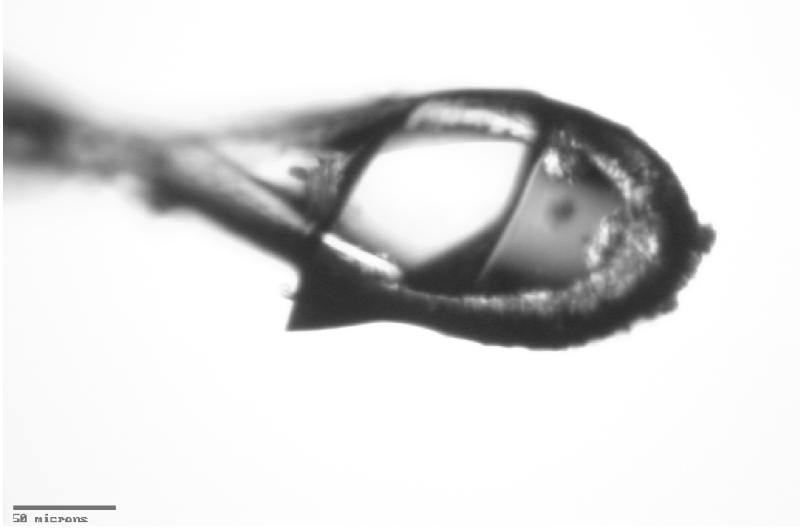

Figure 1.6 **OmpT crystal in a loop.** A crystal is usually placed into the X-ray beam in a loop and cooled to a temperature of 100K. The bar indicates 50 μm.

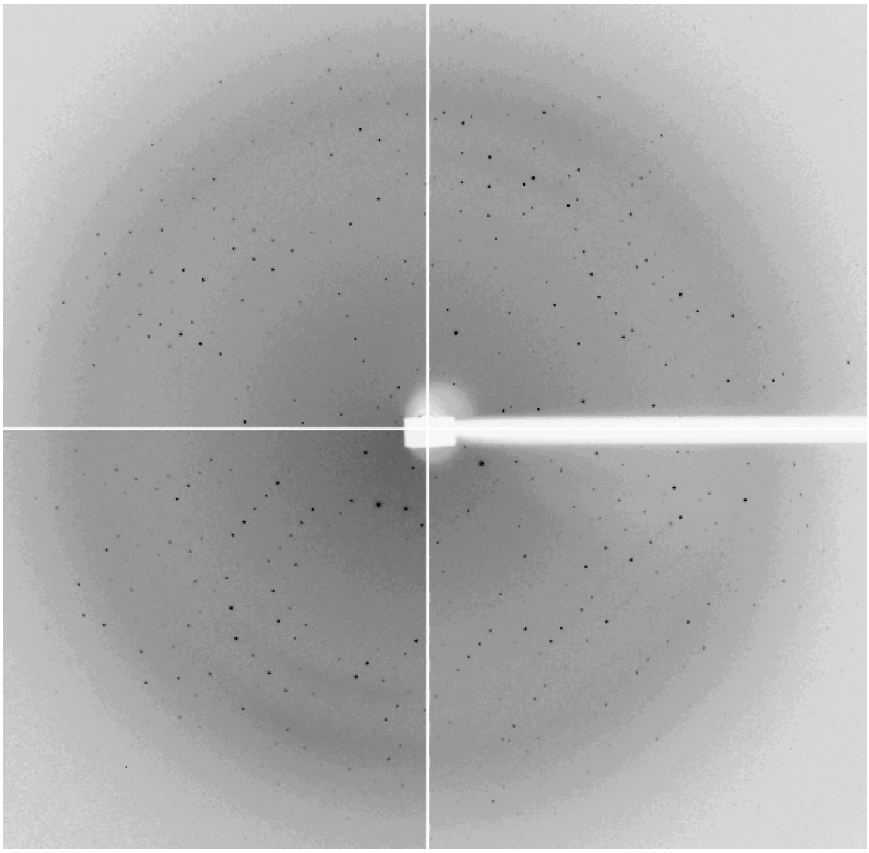

Figure 1.7 A diffraction pattern from a protein crystal. Reflections which form a regular pattern are visible as discreet dark spots with varying intensities. The white vertical and horizontal lines are a feature of the detector, which consist of four square Charge Coupled Devices (CCDs). The broader white horizontal region at the right and the white region in the middle are caused by the beamstop, which blocks the primary beam behind the crystal.

Phasing

To determine the phase of the structure factor a few methods can be used, e.g. multiple isomorphous replacement (MIR), molecular replacement (MR), multiple-wavelength anomalous dispersion (MAD) and single-wavelength anomalous dispersion (SAD). For multiple isomorphous replacement (MIR), which is the most classical method for determining phases in protein crystallography, a native crystal and at least two crystals with heavy atoms bound to the protein have to be measured. The differences of the intensities between the native and other diffraction patterns are caused by the heavy

atoms and can be used to determine the position of the heavy atoms using the Patterson function, and subsequent phase determination. As the name isomorphous replacement indicates, all crystals measured must be isomorphous, a criterion which is not always easy to satisfy.

Molecular replacement (MR) is often the most rapid method, but can only be used if the protein of interest has sufficient structural homology to a protein of known structure. This method uses the phases of the known structure, first applying a rotation search and than a translation search.

In recent years, anomalously scattering atoms are exploited for structure determination using multiple- or single-wavelength anomalous dispersion methods (MAD and SAD). Anomalous scattering atoms cause the intensities of the Friedel pairs, h,k,l and –h,-k,-l, which are normally identical, to differ slightly, which provides information for the calculation of protein phases. Since the anomalous differences are generally very small, data have to be measured very accurately, which is facilitated by measuring redundant data. A main advantage of MAD and SAD is that only one crystal is used to obtain enough information for structure determination. Selenium is often used as anomalous scatterer, because it can be incorporated into recombinant produced proteins in the form of selenomethionines, which replace the normal methionines in the protein. Using MAD with at least three wavelengths, protein phases can unambiguously be determined, whereas with SAD, which uses data from only one wavelength, the phase distributions for each reflection are bimodal. To discriminate between the right and the wrong phases obtained by SAD, density modification, including for example solvent flattening, is a very powerful tool. An advantage of SAD compared with MAD, is that less data need to be collected, resulting in less radiation damage to the crystal. Additionally, usage of a tuneable synchrotron X-ray beamline, which are nowadays overbooked due to the popularity of the MAD method, is often not required.

The phases determined by these methods together with the intensities of the reflection are used to calculate an 'experimental' electron density map in which the protein model can be built. The process of model building is validated by the so-called R-factor, which is a measure of the overall agreement between the amplitudes of the observed structure factors and those of the structure factors calculated from the built model. Because this agreement is initially rather poor, due to errors in phase determination, the structure is refined in an iterative process, such that the *R*-factor will decrease. This refinement includes the adjustment of the positional parameters of all atoms and their thermal vibration, which is given by the temperature factor, also referred to as *B*-factor.

Scope of this thesis

In this thesis, structural studies are described of two outer membrane proteins, OmpT and NspA, using X-ray crystallography. OmpT is an outer membrane protease from *Escherichia coli*. Although outer membrane protease T (OmpT) has been classified as a novel serine protease, this classification is controversial. OmpT activity is dependent on the presence of lipopolysaccharide (LPS), which is a feature of OmpT that has not been observed for other proteases before. What the exact role of LPS in catalysis is, is unclear. In order to gain more insight into the catalytic mechanism and into LPS activation we solved the crystal structure of OmpT, which is described in **chapter 2**. In order to identify the catalytic site unambiguously, residues essential for catalysis were identified, using site directed mutagenesis. Important serines and histidines had been identified previously, whereas the identification of important aspartic acid and glutamic acid residues is described in **chapter 3**. All conserved acidic residues had been separately mutated into alanines and residual activities were determined for all these OmpT mutants. On the basis of the results described in **chapter 2** and **chapter 3** we proposed a novel catalytic mechanism for OmpT. Because zinc is a potent inhibitor of OmpT, the crystal structure of a OmpT/Zn^{2+} complex was solved in order to gain more insight into the active site of OmpT. This complex structure is described in **chapter 4**. **Chapter 5** describes the crystal structure of another outer membrane protein, Neisserial surface protein A (NspA) from *Neisseria meningitidis*. NspA is a vaccine candidate against *N. meningitidis*, because it is highly conserved and elicits bactericidal antibodies. A crystal structure of this protein would provide a possible basis for vaccine development using the structure-based peptide vaccine design. Additionally, a clue about the function of NspA, which is as yet unknown, may be derived from the crystal structure. In **chapter 6** the results and conclusions described in this thesis are summarized.

References

Beher, M.G., Schnaitman, C.A. & Pugsley, A.P. (1980). Major heat-modifiable outer membrane protein in gram-negative bacteria: comparison with the OmpA protein of *Escherichia coli*. *J Bacteriol,* ***143*** *(2):* 906-913.

Buchanan, S.K. (1999). Beta-barrel proteins from bacterial outer membranes: structure, function and refolding. *Curr Opin Struct Biol,* ***9*** *(4):* 455-461.

Buchanan, S.K., Smith, B.S.,Venkatramani, L., Xia, D., Esser, L., Palnitkar, M., Chakraborty, R.,Van Der Helm, D. & Deisenhofer, J. (1999). Crystal structure of the outer membrane active transporter FepA from *Escherichia coli*. *Nat Struct Biol,* ***6*** *(1):* 56-63.

Cadieux, N., Plante, M., Rioux, C.R., Hamel, J., Brodeur, B.R. & Martin, D. (1999). Bactericidal and cross-protective activities of a monoclonal antibody directed against *Neisseria meningitidis* NspA outer membrane protein. *Infect Immun,* ***67*** *(9):* 4955-4959.

Cowan, S.W., Schirmer, T., Rummel, G., Steiert, M., Ghosh, R., Pauptit, R.A., Jansonius, J.N. & Rosenbusch, J.P. (1992). Crystal structures explain functional properties of two *E. coli* porins. *Nature,* ***358*** *(6389):* 727-733.

Cripps, A.W., Foxwell, R. & Kyd, J. (2002). Challenges for the development of vaccines against *Haemophilus influenzae* and *Neisseria meningitidis*. *Curr Opin Immunol,* ***14*** *(5):* 553-557.

Danese, P.N. & Silhavy, T.J. (1998). Targeting and assembly of periplasmic and outer-membrane proteins in *Escherichia coli*. *Annu Rev Genet,* ***32*** 59-94.

Dekker, N., Cox, R.C., Kramer, R.A. & Egmond, M.R. (2001). Substrate specificity of the integral membrane protease OmpT determined by spatially addressed peptide libraries. *Biochemistry,* ***40*** 1694-1701.

Dutzler, R., Rummel, G., Alberti, S., Hernandez-Alles, S., Phale, P., Rosenbusch, J., Benedi, V. & Schirmer, T. (1999). Crystal structure and functional characterization of OmpK36, the osmoporin of *Klebsiella pneumoniae*. *Structure Fold Des,* **7** *(4):* 425-434.

Egile, C., D'hauteville, H., Parsot, C. & Sansonetti, P.J. (1997). SopA, the outer membrane protease responsible for polar localization of IcsA in *Shigella flexneri*. *Mol Microbiol,* ***23*** *(5):* 1063-1073.

Fairley, C.K., Begg, N., Borrow, R., Fox, A.J., Jones, D.M. & Cartwright, K. (1996). Conjugate meningococcal serogroup A and C vaccine: reactogenicity and immunogenicity in United Kingdom infants. *J Infect Dis,* ***174*** *(6):* 1360-1363.

Ferguson, A.D., Chakraborty, R., Smith, B.S., Esser, L.,Van Der Helm, D. & Deisenhofer, J. (2002). Structural basis of gating by the outer membrane transporter FecA. *Science,* ***295*** *(5560):* 1715-1719.

Ferguson, A.D., Hofmann, E., Coulton, J.W., Diederichs, K. & Welte, W. (1998). Siderophore-mediated iron transport: crystal structure of FhuA with bound lipopolysaccharide. *Science,* ***282*** *(5397):* 2215-2220.

Forst, D., Welte, W., Wacker, T. & Diederichs, K. (1998). Structure of the sucrose-specific porin ScrY from *Salmonella typhimurium* and its complex with sucrose. *Nat Struct Biol,* ***5*** *(1):* 37-46.

Gordon, D.M. & Riley, M.A. (1992). A theoretical and experimental analysis of bacterial growth in the bladder. *Mol Microbiol,* ***6*** *(4):* 555-562.

Grodberg, J. & Dunn, J.J. (1988). ompT encodes the *Escherichia coli* outer membrane protease that cleaves T7 RNA polymerase during purification. *J Bacteriol,* ***170*** *(3):* 1245-1253.

Grodberg, J. & Dunn, J.J. (1989). Comparison of *Escherichia coli* K-12 outer membrane protease OmpT and *Salmonella typhimurium* E protein. *J Bacteriol,* ***171*** *(5):* 2903-2905.

Grodberg, J., Lundrigan, M.D., Toledo, D.L., Mangel, W.F. & Dunn, J.J. (1988). Complete nucleotide sequence and deduced amino acid sequence of the *ompT* gene of *Escherichia coli* K-12. *Nucleic Acids Res,* ***16*** *(3):* 1209.

Guina, T., Yi, E.C., Wang, H., Hackett, M. & Miller, S.I. (2000). A PhoP-regulated outer membrane protease of *Salmonella enterica serovar typhimurium* promotes resistance to alpha-helical antimicrobial peptides. *J Bacteriol,* ***182*** *(14):* 4077-4086.

Gulick, R.M. (2003). New antiretroviral drugs. *Clin Microbiol Infect,* ***9*** *(3):* 186-193.

Haddadin, A.S., Fappiano, S.A. & Lipsett, P.A. (2002). Methicillin resistant *Staphylococcus aureus* (MRSA) in the intensive care unit. *Postgrad Med J,* ***78*** *(921):* 385-392.

Hammarberg, B., Moks, T., Tally, M., Elmblad, A., Holmgren, E., Murby, M., Nilsson, B., Josephson, S. & Uhlen, M. (1990). Differential stability of recombinant human insulin-like growth factor II in *Escherichia coli* and *Staphylococcus aureus*. *J Biotechnol,* ***14*** *(3-4):* 423-437.

Henderson, T.A., Dombrosky, P.M. & Young, K.D. (1994). Artifactual processing of penicillin-binding proteins 7 and 1b by the OmpT protease of *Escherichia coli*. *J Bacteriol,* ***176*** *(1):* 256-259.

Hirsch, A., Breed, J., Saxena, K., Richter, O.M., Ludwig, B., Diederichs, K. & Welte, W. (1997). The structure of porin from *Paracoccus denitrificans* at 3.1 A resolution. *FEBS Lett,* ***404*** *(2-3):* 208-210.

Hoepelman, I.M. (1999). [Legionella epidemic in the Netherlands]. *Ned Tijdschr Geneeskd,* ***143*** *(23):* 1192-1196.

Hollifield, W.C., Jr., Fiss, E.H. & Neilands, J.B. (1978). Modification of a ferric enterobactin receptor protein from the outer membrane of *Escherichia coli*. *Biochem Biophys Res Commun,* ***83*** *(2):* 739-746.

Hwang, P.M., Choy, W.Y., Lo, E.I., Chen, L., Forman-Kay, J.D., Raetz, C.R., Prive, G.G., Bishop, R.E. & Kay, L.E. (2002). Solution structure and dynamics of the outer membrane enzyme PagP by NMR. *Proc Natl Acad Sci U S A,* ***99*** *(21):* 13560-13565.

Johnson, J.R., Oswald, E., O'bryan, T.T., Kuskowski, M.A. & Spanjaard, L. (2002). Phylogenetic distribution of virulence-associated genes among *Escherichia coli* isolates associated with neonatal bacterial meningitis in the Netherlands. *J Infect Dis,* ***185*** *(6):* 774-784.

Kaufmann, A., Stierhof, Y.D. & Henning, U. (1994). New outer membrane-associated protease of *Escherichia coli* K-12. *J Bacteriol,* ***176*** *(2):* 359-367.

Kienle, Z., Emody, L., Svanborg, C. & O'toole, P.W. (1992). Adhesive properties conferred by the plasminogen activator of *Yersinia pestis*. *J Gen Microbiol,* ***138*** *(Pt 8):* 1679-1687.

Kingma, R.L., Fragiathaki, M., Snijder, H.J., Dijkstra, B.W., Verheij, H.M., Dekker, N. & Egmond, M.R. (2000). Unusual catalytic triad of *Escherichia coli* outer membrane phospholipase A. *Biochemistry,* ***39*** *(33):* 10017-10022.

Klauser, T., Pohlner, J. & Meyer, T.F. (1992). Selective extracellular release of cholera toxin B subunit by *Escherichia coli*: dissection of Neisseria Iga beta-mediated outer membrane transport. *Embo J,* ***11*** *(6):* 2327-2335.

Koronakis, V., Sharff, A., Koronakis, E., Luisi, B. & Hughes, C. (2000). Crystal structure of the bacterial membrane protein TolC central to multidrug efflux and protein export. *Nature,* ***405*** *(6789):* 914-919.

Kramer, R.A., Brandenburg, K., Vandeputte-Rutten, L., Werkhoven, M., Gros, P., Dekker, N. & Egmond, M.R. (2002). Lipopolysaccharide regions involved in the activation of *Escherichia coli* outer membrane protease OmpT. *Eur J Biochem,* ***269*** *(6):* 1746-1752.

Kramer, R.A., Dekker, N. & Egmond, M.R. (2000a). Identification of active site serine and histidine residues in *Escherichia coli* outer membrane protease OmpT. *FEBS Lett,* ***468*** *(2-3):* 220-224.

Kramer, R.A., Zandwijken, D., Egmond, M.R. & Dekker, N. (2000b). In vitro folding, purification and characterization of *Escherichia coli* outer membrane protease OmpT. *Eur J Biochem,* ***267*** *(3):* 885-893.

Kreusch, A., Neubuser, A., Schiltz, E., Weckesser, J. & Schulz, G.E. (1994). Structure of the membrane channel porin from *Rhodopseudomonas blastica* at 2.0 A resolution. *Protein Sci,* ***3*** *(1):* 58-63.

Kuhn, P., Wilson, K., Patch, M.G. & Stevens, R.C. (2002). The genesis of high-throughput structure-based drug discovery using protein crystallography. *Curr Opin Chem Biol,* ***6*** *(5):* 704-710.

Lahteenmaki, K., Virkola, R., Saren, A., Emody, L. & Korhonen, T.K. (1998). Expression of plasminogen activator pla of *Yersinia pestis* enhances bacterial attachment to the mammalian extracellular matrix. *Infect Immun,* ***66*** *(12):* 5755-5762.

Leytus, S.P., Bowles, L.K., Konisky, J. & Mangel, W.F. (1981). Activation of plasminogen to plasmin by a protease associated with the outer membrane of *Escherichia coli*. *Proc Natl Acad Sci U S A,* ***78*** *(3):* 1485-1489.

Lundrigan, M.D. & Webb, R.M. (1992). Prevalence of ompT among *Escherichia coli* isolates of human origin. *FEMS Microbiol Lett,* ***76*** *(1-2):* 51-56.

Manning, P.A. & Reeves, P. (1976). Outer membrane of *Escherichia coli* K-12: demonstration of the temperature sensitivity of a mutant in one of the major outer membrane proteins. *Biochem Biophys Res Commun,* ***72*** *(2):* 694-700.

Martin, D., Cadieux, N., Hamel, J. & Brodeur, B.R. (1997). Highly conserved *Neisseria meningitidis*

surface protein confers protection against experimental infection. *J Exp Med,* ***185*** *(7):* 1173-1183.

Maurer, J., Jose, J. & Meyer, T.F. (1997). Autodisplay: one-component system for efficient surface display and release of soluble recombinant proteins from *Escherichia coli*. *J Bacteriol,* ***179*** *(3):* 794-804.

Meyer, J.E., Hofnung, M. & Schulz, G.E. (1997). Structure of maltoporin from *Salmonella typhimurium* ligated with a nitrophenyl-maltotrioside. *J Mol Biol,* ***266*** *(4):* 761-775.

Moe, G.R. & Granoff, D.M. (2001). Molecular mimetics of *Neisseria meningitidis* serogroup B polysaccharide. *Int Rev Immunol,* ***20*** *(2):* 201-220.

Moe, G.R., Tan, S. & Granoff, D.M. (1999). Differences in surface expression of NspA among *Neisseria meningitidis* group B strains. *Infect Immun,* ***67*** *(11):* 5664-5675.

Moe, G.R., Zuno-Mitchell, P., Hammond, S.N. & Granoff, D.M. (2002). Sequential immunization with vesicles prepared from heterologous *Neisseria meningitidis* strains elicits broadly protective serum antibodies to group B strains. *Infect Immun,* ***70*** *(11):* 6021-6031.

Moe, G.R., Zuno-Mitchell, P., Lee, S.S., Lucas, A.H. & Granoff, D.M. (2001). Functional activity of anti-Neisserial surface protein A monoclonal antibodies against strains of *Neisseria meningitidis* serogroup B. *Infect Immun,* ***69*** *(6):* 3762-3771.

Morley, S.L. & Pollard, A.J. (2001). Vaccine prevention of meningococcal disease, coming soon? *Vaccine,* ***20*** *(5-6):* 666-687.

Mulvey, M.A., Schilling, J.D., Martinez, J.J. & Hultgren, S.J. (2000). Bad bugs and beleaguered bladders: interplay between uropathogenic *Escherichia coli* and innate host defenses. *Proc Natl Acad Sci U S A,* ***97*** *(16):* 8829-8835.

Oomen, C.J., Hoogerhout, P., Bonvin, A.M., Kuipers, B., Brugghe, H., Timmermans, H., Haseley, S.R., Van Alphen, L. & Gros, P. (2003). Immunogenicity of Peptide-vaccine Candidates Predicted by Molecular Dynamics Simulations. *J Mol Biol,* ***328*** *(5):* 1083-1089.

Orskov, F. & Orskov, I. (1992). *Escherichia coli* serotyping and disease in man and animals. *Can J Microbiol,* ***38*** *(7):* 699-704.

Pautsch, A. & Schulz, G.E. (1998). Structure of the outer membrane protein A transmembrane domain. *Nat Struct Biol,* ***5*** *(11):* 1013-1017.

Peacock, E., Jacob, V.W. & Fallone, S.M. (2001). Escherichia coli O157:H7: etiology, clinical features, complications, and treatment. *Nephrol Nurs J,* ***28*** *(5):* 547-550, 553-545; quiz 556-547.

Peeters, C.C., Rumke, H.C., Sundermann, L.C., Rouppe Van Der Voort, E.M., Meulenbelt, J., Schuller, M., Kuipers, A.J., Van Der Ley, P. & Poolman, J.T. (1996). Phase I clinical trial with a hexavalent PorA containing meningococcal outer membrane vesicle vaccine. *Vaccine,* ***14*** *(10):* 1009-1015.

Plante, M., Cadieux, N., Rioux, C.R., Hamel, J., Brodeur, B.R. & Martin, D. (1999). Antigenic and molecular conservation of the gonococcal NspA protein. *Infect Immun,* ***67*** *(6):* 2855-2861.

Pollard, A.J. & Frasch, C. (2001). Development of natural immunity to *Neisseria meningitidis*. *Vaccine,* ***19*** *(11-12):* 1327-1346.

Popescu, A. & Doyle, R.J. (1996). The Gram stain after more than a century. *Biotech Histochem,* ***71*** *(3):* 145-151.

Prince, S.M., Achtman, M. & Derrick, J.P. (2002). Crystal structure of the OpcA integral membrane adhesin from Neisseria meningitidis. *Proc Natl Acad Sci U S A,* ***99*** *(6):* 3417-3421.

Ramakrishnan, V. (2002). Ribosome structure and the mechanism of translation. *Cell,* ***108*** *(4):* 557-572.

Rosenqvist, E., Hoiby, E.A., Wedege, E., Bryn, K., Kolberg, J., Klem, A., Ronnild, E., Bjune, G. & Nokleby, H. (1995). Human antibody responses to meningococcal outer membrane antigens after three doses of the Norwegian group B meningococcal vaccine. *Infect Immun,* ***63*** *(12):* 4642-4652.

Rupprecht, K.R., Gordon, G., Lundrigan, M., Gayda, R.C., Markovitz, A. & Earhart, C. (1983). omp T: *Escherichia coli* K-12 structural gene for protein a (3b). *J Bacteriol,* ***153*** *(2):* 1104-1106.

Schechter, I. & Berger, A. (1967). On the size of the active site in proteases. I. Papain. *Biochem Biophys Res Commun,* ***27*** *(2):* 157-162.

Schirmer, T., Keller, T.A., Wang, Y.F. & Rosenbusch, J.P. (1995). Structural basis for sugar translocation through maltoporin channels at 3.1 A resolution. *Science,* ***267*** *(5197):* 512-514.

Schulz, G.E. (2002). The structure of bacterial outer membrane proteins. *Biochim Biophys Acta,* ***1565*** *(2):* 308-317.

Shere, K.D., Sallustio, S., Manessis, A., D'aversa, T.G. & Goldberg, M.B. (1997). Disruption of IcsP, the major Shigella protease that cleaves IcsA, accelerates actin-based motility. *Mol Microbiol,* ***25*** *(3):* 451-462.

Snijder, H.J., Ubarretxena-Belandia, I., Blaauw, M., Kalk, K.H., Verheij, H.M., Egmond, M.R., Dekker, N. & Dijkstra, B.W. (1999). Structural evidence for dimerization-regulated activation of an integral membrane phospholipase. *Nature,* ***401*** *(6754):* 717-721.

Sodeinde, O.A. & Goguen, J.D. (1989). Nucleotide sequence of the plasminogen activator gene of *Yersinia pestis*: relationship to ompT of *Escherichia coli* and gene E of *Salmonella typhimurium*. *Infect Immun,* ***57*** *(5):* 1517-1523.

Sodeinde, O.A., Subrahmanyam, Y.V., Stark, K., Quan, T., Bao, Y. & Goguen, J.D. (1992). A surface protease and the invasive character of plague. *Science,* ***258*** *(5084):* 1004-1007.

Studier, F.W. & Moffatt, B.A. (1986). Use of bacteriophage T7 RNA polymerase to direct selective high-level expression of cloned genes. *J Mol Biol,* ***189*** *(1):* 113-130.

Stumpe, S., Schmid, R., Stephens, D.L., Georgiou, G. & Bakker, E.P. (1998). Identification of OmpT as the protease that hydrolyzes the antimicrobial peptide protamine before it enters growing cells of *Escherichia coli*. *J Bacteriol,* ***180*** *(15):* 4002-4006.

Sugimura, K. & Higashi, N. (1988). A novel outer-membrane-associated protease in *Escherichia coli*.

J Bacteriol, ***170*** *(8):* 3650-3654.

Sugimura, K. & Nishihara, T. (1988). Purification, characterization, and primary structure of *Escherichia coli* protease VII with specificity for paired basic residues: identity of protease VII and OmpT. *J Bacteriol,* ***170*** *(12):* 5625-5632.

Trent, M.S., Pabich, W., Raetz, C.R. & Miller, S.I. (2001). A PhoP/PhoQ-induced Lipase (PagL) that catalyzes 3-O-deacylation of lipid A precursors in membranes of *Salmonella typhimurium*. *J Biol Chem,* ***276*** *(12):* 9083-9092.

Vandeputte-Rutten, L., Bos, M.P., Tommassen, J. & Gros, P. (2003). Crystal structure of neisserial surface protein A (NspA), a conserved outer membrane protein with vaccine potential. *J Biol Chem,* ***26*** 26.

Vandeputte-Rutten, L., Kramer, R.A., Kroon, J., Dekker, N., Egmond, M.R. & Gros, P. (2001). Crystal structure of the outer membrane protease OmpT from *Escherichia coli* suggests a novel catalytic site. *Embo J,* ***20*** *(18):* 5033-5039.

Virji, M., Makepeace, K., Ferguson, D.J. & Watt, S.M. (1996). Carcinoembryonic antigens (CD66) on epithelial cells and neutrophils are receptors for Opa proteins of pathogenic neisseriae. *Mol Microbiol,* ***22*** *(5):* 941-950.

Virji, M., Makepeace, K. & Moxon, E.R. (1994). Distinct mechanisms of interactions of Opc-expressing meningococci at apical and basolateral surfaces of human endothelial cells; the role of integrins in apical interactions. *Mol Microbiol,* ***14*** *(1):* 173-184.

Vogt, J. & Schulz, G.E. (1999). The structure of the outer membrane protein OmpX from *Escherichia coli* reveals possible mechanisms of virulence. *Structure Fold Des,* **7** *(10):* 1301-1309.

Voulhoux, R., Bos, M.P., Geurtsen, J., Mols, M. & Tommassen, J. (2003). Role of a highly conserved bacterial protein in outer membrane protein assembly. *Science,* ***299*** *(5604):* 262-265.

Wade, R.C. (1997). 'Flu' and structure-based drug design. *Structure,* ***5*** *(9):* 1139-1145.

Webb, R.M. & Lundigran, M.D. (1996). OmpT in *Escherichia coli* correlates with severity of disease in urinary tract infections. *Med. Microbiol. Letters,* ***5*** 8-14.

Weiss, M.S., Wacker, T., Weckesser, J., Welte, W. & Schulz, G.E. (1990). The three-dimensional structure of porin from *Rhodobacter capsulatus* at 3 A resolution. *FEBS Lett,* ***267*** *(2):* 268-272.

White, C.B., Chen, Q., Kenyon, G.L. & Babbitt, P.C. (1995). A novel activity of OmpT. Proteolysis under extreme denaturing conditions. *J Biol Chem,* ***270*** *(22):* 12990-12994.

Wildes, S.S. & Tunkel, A.R. (2002). Meningococcal vaccines: a progress report. *BioDrugs,* ***16*** *(5):* 321-329.

Wlodawer, A. & Vondrasek, J. (1998). Inhibitors of HIV-1 protease: a major success of structure-assisted drug design. *Annu Rev Biophys Biomol Struct,* ***27*** 249-284.

Wright, J.C., Williams, J.N., Christodoulides, M. & Heckels, J.E. (2002). Immunization with the recombinant PorB outer membrane protein induces a bactericidal immune response against Neisseria meningitidis. *Infect Immun,* ***70*** *(8):* 4028-4034.

Yu, G.Q. & Hong, J.S. (1986). Identification and nucleotide sequence of the activator gene of the externally induced phosphoglycerate transport system of *Salmonella typhimurium*. *Gene,* ***45*** *(1):* 51-57.

Zeth, K., Diederichs, K., Welte, W. & Engelhardt, H. (2000). Crystal structure of Omp32, the anion-selective porin from *Comamonas acidovorans*, in complex with a periplasmic peptide at 2.1 A resolution. *Structure Fold Des,* ***8*** *(9):* 981-992.

Zhao, G.P. & Somerville, R.L. (1993). An amino acid switch (Gly281—>Arg) within the "hinge" region of the tryptophan synthase beta subunit creates a novel cleavage site for the OmpT protease and selectively diminishes affinity toward a specific monoclonal antibody. *J Biol Chem,* ***268*** *(20):* 14912-14920.

Zumia, A. & Grange, J.M. (2001). Multidrug-resistant tuberculosis—can the tide be turned? *Lancet Infect Dis,* ***1*** *(3):* 199-202.

2

Crystal structure of the outer membrane protease OmpT from *Escherichia coli* suggests a novel catalytic site

Lucy Vandeputte-Rutten, R. Arjen Kramer, Jan Kroon, Niek Dekker, Maarten R. Egmond and Piet Gros

EMBO J. (2001), **20**(18), 5033-5039

Abstract

OmpT from *Escherichia coli* belongs to a family of highly homologous outer membrane proteases, known as omptins, which are implicated in the virulence of several pathogenic Gram-negative bacteria. Here we present the crystal structure of OmpT, which shows a 10-stranded antiparallel β-barrel that protrudes far from the lipid bilayer into the extracellular space. We identified a putative binding site for lipopolysaccharide, a molecule that is essential for OmpT activity. The proteolytic site is located in a groove at the extracellular top of the vase-shaped β-barrel. Based on the constellation of active site residues, we propose a novel proteolytic mechanism, involving a His-Asp dyad and an Asp-Asp couple that activate a putative nucleophilic water molecule. The active site is fully conserved within the omptin family. Therefore, the structure described here provides a sound basis for the design of drugs against omptin-mediated bacterial pathogenesis. Coordinates are in the Protein Data Bank (accession No. 1I78).

Introduction

Omptins are outer membrane proteases found in several Gram-negative bacteria and include OmpT of *Escherichia coli* (Sugimura & Nishihara, 1988), PgtE of *Salmonella typhimurium* (mature part 49% identical to OmpT) (Yu & Hong, 1986), Pla of *Yersinia pestis* (50% identical) (Sodeinde & Goguen, 1989), SopA of *Shigella flexneri* (60% identical) (Egile *et al.*, 1997) and OmpP of *E. coli* (72% identical) (Kaufmann *et al.*, 1994). Several studies have implicated the omptin family in the pathogenicity of these bacteria (Stathopoulos, 1998). The presence of the *ompT* gene in clinical isolates of *E. coli* has been associated with complicated urinary tract disease (Webb & Lundigran, 1996), a notion supported by the observation that OmpT cleaves protamine, a highly basic antimicrobial peptide that is excreted by epithelial cells of the urinary tract (Stumpe *et al.*, 1998). Inactivation of the gene encoding Pla in *Y. pestis*, the causative agent of plague, increased the median lethal dose of the bacterium for mice by 10^6-fold (Sodeinde *et al.*, 1992). The role of Pla in pathogenicity might be related to its ability to activate plasminogen, a feature shared with OmpT (Lundrigan & Webb, 1992). SopA from *S. flexneri*, the causative agent of bacillary dysentery, cleaves the endogenous autotransporter IcsA that has an essential role in the formation of actin tails in host cells, and therefore SopA might be involved in actin-based motility inside infected cells (Egile *et al.*, 1997; Shere *et al.*, 1997). Thus, the proteolytic activity of the omptins is probably involved in a variety of ways in the pathogenicity of these bacteria, ranging from bacterial defence, plasmin-mediated tissue infiltration to motility inside infected cells.

OmpT is biochemically the best characterized member of the omptins. It preferentially cleaves substrates between two consecutive basic amino acids (Dekker *et al.*,

2001). The protease displays optimal activity at alkaline pH and it is dependent on lipopolysaccharide (LPS), showing no detectable enzymatic activity towards peptide substrates in the absence of LPS (Kramer *et al.*, 2000b). Hydrolysis of a fluorogenic peptide substrate by OmpT was characterized by a specificity constant k_{cat}/K_m of 10^8 $s^{-1}M^{-1}$, indicating a cleavage efficiency comparable with that of water soluble proteases such as chymotrypsin (Kramer *et al.*, 2000b). The enzyme does not contain any conserved active site sequence found in other known protease families. In addition, commonly used serine protease inhibitors have little or no effect on the activity of OmpT (Sugimura & Nishihara, 1988). However, because some serine protease inhibitors weakly affect OmpT activity, the omptins have been classified as novel serine proteases (family S18) (Rawlings & Barrett, 1994). Site-directed mutagenesis studies appeared to support this classification, since Ser99 and His212 have been found to be important for the activity of OmpT (Kramer *et al.*, 2000a).

Here we describe the first structure of an integral outer membrane protease, OmpT from *E. coli*, at 2.6 Å resolution. The crystallized protein contained three mutations to prevent autoproteolytic degradation. Based on the structure, we identified a putative LPS-binding site and provide support for the omptins constituting a novel class of proteases.

Materials and methods

Protein expression and purification

OmpT, containing the mutations S99A, G216K and K217G in order to abolish autoproteolysis (Kramer *et al.*, 2000b), was overexpressed without its signal sequence (of 20 residues) in *E. coli* and refolded as described previously (Kramer *et al.*, 2000b). For expression of seleno-methionine (Se-Met) containing OmpT, *E. coli* strain B834(DE3) (Met-auxotroph, Novagen) containing the plasmid that encodes OmpT (S99A, G216K, K217G) was grown in new minimal medium (Budisa *et al.*, 1995) supplemented with 0.3 mM L-Se-Met (Acros). Refolded native OmpT and Se-Met OmpT (~200 mg) were loaded onto a 100 mL Fast Flow S-Sepharose column (Amersham Pharmacia) equilibrated with buffer A [10 mM Zwittergent 3-12 (Fluka), 20 mM sodium acetate, pH 4.0]. The column was washed with buffer A and proteins were eluted with a linear gradient of NaCl to 1 M in buffer A. The native protein and the Se-Met derivative were concentrated to 25 mg/ml in buffer B (1% octyl-β-D-glucopyranoside (OG), 5 mM sodium acetate pH 4.0) using a second S-Sepharose column and centricon concentrators (Amicon). After dialysis, samples used for crystallization consisted of 20 mg/ml OmpT in buffer B containing 2.5 mM potassium chloride.

Crystallization

Crystallization conditions for native OmpT were screened using the hanging drop vapor diffusion method at 4 and 20°C. Droplets containing equal amounts (1 μl) of protein and mother liquor were equilibrated against 0.5 ml of reservoir solution. Sparse-matrix screens for initial trials were performed using Hampton research screen kits (Hampton research, CA). After 6 months, one small crystal with dimensions of 0.08 x 0.05 x 0.05 mm appeared at 4°C in 30% (v/v) 2-methyl-2,4-pentanediol (MPD, Fluka), 0.2 M ammonium acetate, 0.1 M sodium citrate pH 5.6. A narrower screening around this crystallization condition was performed: 28 % (v/v) MPD, 0.5 M NaCl and 0.1 M sodium citrate pH 5.5 yielded one small crystal per drop within a month. Se-Met OmpT was produced in order to obtain phases for structure determination. Se-Met OmpT appeared to crystallize faster and yielded larger crystals than the native protein. After 2 weeks, crystals occurred in 1% OG, 30% (v/v) MPD and 0.3 M sodium citrate pH 5.5. These crystals grew to maximum crystal dimensions of ~0.3 x 0.2 x 0.2 mm in 3 months.

X-ray diffraction analysis

Crystals were harvested from the droplets with cryo-loops and directly frozen into liquid nitrogen. X-ray data were collected at 100 K on a CCD detector at ID-14 EH4 beamline at the European Synchrotron Radiation Facility (ESRF) in Grenoble. Native data were collected to 2.6 Å, using an oscillation range of 0.2°. The crystal belongs to the trigonal space group $P3_221$, with unit cell parameters $a = b = 98.4$ Å, $c = 165.7$ Å, $\alpha = \beta = 90°$ and $\gamma = 120°$. Crystals have a solvent plus detergent content of 63% (v/v) and two OmpT molecules in the asymmetric unit. A dataset of a Se-Met OmpT crystal was collected at λ_{peak}=0.9790 Å to a resolution of 3.1 Å. Data were indexed using DENZO merged with SCALEPACK (Otwinowski & Minor, 1997) and processed further using TRUNCATE from the CCP4 suite (CCP4, 1994). A summary of the data collection and final processing statistics is provided in Table 2.1.

Structure determination and refinement

Using the peak dataset of Se-Met OmpT, all 10 selenium sites were found by direct methods with the DREAR/SnB package (Weeks & Miller, 1999). Phases subsequently were calculated using MLPHARE (Otwinowski, 1991) to 3.7 Å resolution. This yielded an R_{cullis} (ano) of 0.78 [R_{cullis} (ano)= $\Sigma(|\Delta PH_{obs}-\Delta PH_{calc}|\ /\ \Sigma|\Delta PH_{obs}|$ with $\Delta PH=F_{PH}(+)-F_{PH}(-)$]. With density modification in CNS (Brunger *et al.*, 1998), phases were extended to 3.1 Å resolution. The resulting electron density map allowed the placement of 80% of the residues using the program O (Jones *et al.*, 1991). The native dataset was used for refinement from 20 to 2.6 Å resolution. After a rigid body refinement, iterative model refinement was performed by model building in O, followed

Table 2.1 Summary of data and refinement statistics

	Native	**Se-Met**
Data set statistics		
resolution limits (outer shell) (Å)	20-2.6 (2.69-2.6)	40-3.1 (3.21-3.1)
space group	$P3_221$	$P3_221$
unit cell parameters (Å,°)	a = 98.39,	a = 97.79,
	b = 98.39,	b = 97.79,
	c = 165.70,	c = 165.86,
	$\alpha = 90, \beta = 90, \gamma = 120$	$\alpha = 90, \beta = 90, \gamma = 120$
mosaicity (°)	0.1	0.8
oscillation range (°)	0.2	0.5
total oscillation for data set (°)	25	100
total no. of reflections (outer shell)	43,471 (4,352)	107,336 (10,902)
no. of unique reflections (outer shell)[1]	27,400 (2,766)	17,252 (1,705)
redundancy	1.59 (1.57)	6.22 (6.39)
R_{merge} (%) (outer shell)[2]	7.4 (26.3)	9.7 (39.5)
completeness (%) (outer shell)	94.3 (97.7)	99.8 (100)
I/σ (I) (outer shell)	8.82 (2.54)	15.48 (4.56)
Refinement statistics		
resolution range (Å)	20-2.6	
total no. of non-hydrogen atoms	4,734	
no. of water molecules	29	
no. of β-OG molecules	4	
R_{work} (%)	23.7	
R_{free} (%)	28.0	
r.m.s.d. bond lengths (Å)	0.007	
r.m.s.d. bond angles (°)	1.35	
average B-factor (all protein atoms) (Å^2)	52.6	

[1] For the Se-Met dataset the Friedel mates have been counted separately.
[2] $R_{merge} = \Sigma(|I-\langle I\rangle|)/\Sigma(I)$

by simulated annealing and restrained individual *B*-factor refinement in CNS. The final model consists of all residues of OmpT in molecule A, residues 11-297 in molecule B, four OG molecules and 29 water molecules. For the side chains of residues Glu3, Thr4, Glu154, Glu167, Arg168, Lys216 and Tyr266 of molecule A and Glu33, Glu154, Lys216, and Tyr266 of molecule B, no electron density was observed. Therefore, these side chains were omitted from the model. The two monomers in the asymmetric unit pack in a perpendicular orientation to each other and interact through their hydrophobic transmembrane regions. Intermolecular

protein-protein interactions in the crystal are predominantly of a hydrophobic nature, with only one unique hydrogen bond (involving Arg100 in molecule A and the main chain oxygen of Ile160 in molecule B) and a salt bridge (involving Asp10 in molecule A and Lys277 in molecule B). In the Ramachandran plot, 85.4 % of the residues are in most favored regions, with 13.2 % in additionally allowed regions, 1 % in the generously allowed regions and one residue (Glu190) in a disallowed region. Nε of Arg188 is hydrogen bonded to the main chain oxygen of Glu190 generating a type II' β-turn, explaining the perturbed φ,ϕ-combination of Glu190. The overall temperature factor of the total structure is 53.2 $Å^2$, with the highest B-factors in the extracellular loops (Figure 2.3).

Results and Discussion

Structure determination

The OmpT structure was determined with the single-wavelength anomalous diffraction (SAD) phasing method using a Se-Met OmpT crystal, which diffracted to 3.1 Å resolution. The final structure was refined against data to 2.6 Å resolution using a crystal of OmpT containing natural methionines. The enzyme contained the mutations S99A, G216K and K217G, to abolish autoproteolytic activity. Additionally, crystals of a S99A mutant were obtained that diffracted to a lower resolution of 3.2 Å, yielding a map indicating an identical structure (unpublished results). OmpT was crystallized using 1% (w/v) OG, 30% (v/v) MPD and 0.3 M sodium citrate pH 5.5. It crystallized in the space group $P3_221$ with unit cell dimensions $a = b = 97.8$ Å and $c = 165.3$ Å. Two OmpT molecules are present in the asymmetric unit that show a high degree of structural similarity, with a root mean square deviation (r.m.s.d.) of 0.50 Å for main-chain atoms. The refined model consists of 584 amino acid residues, four OG and 29 water molecules, and has a crystallographic R-factor of 23.7% and an R_{free} of 28.0% for data in the 20-2.6 Å resolution range. Table 2.1 summarizes the statistics of the crystallographic data and the refinement. Coordinates and structure factors have been deposited in the Protein Data Bank with accession No. 1I78.

Overall structure

The overall structure of OmpT consists of an exceptionally long 10-stranded vase-shaped antiparallel β-barrel of ~70 Å in its longest dimension (Figure 2.1). The number, as well as the approximate position of the 10 β-strands, was predicted correctly by Kramer *et al.* (2000b). The β-strands have an average length of 23 residues, have a tilt angle of 37-45° with respect to the barrel axis and have a shear number of 12 (Figure 2.2). Like other outer membrane proteins (Buchanan *et al.*, 1999; Cowan *et al.*, 1992; Ferguson *et al.*,

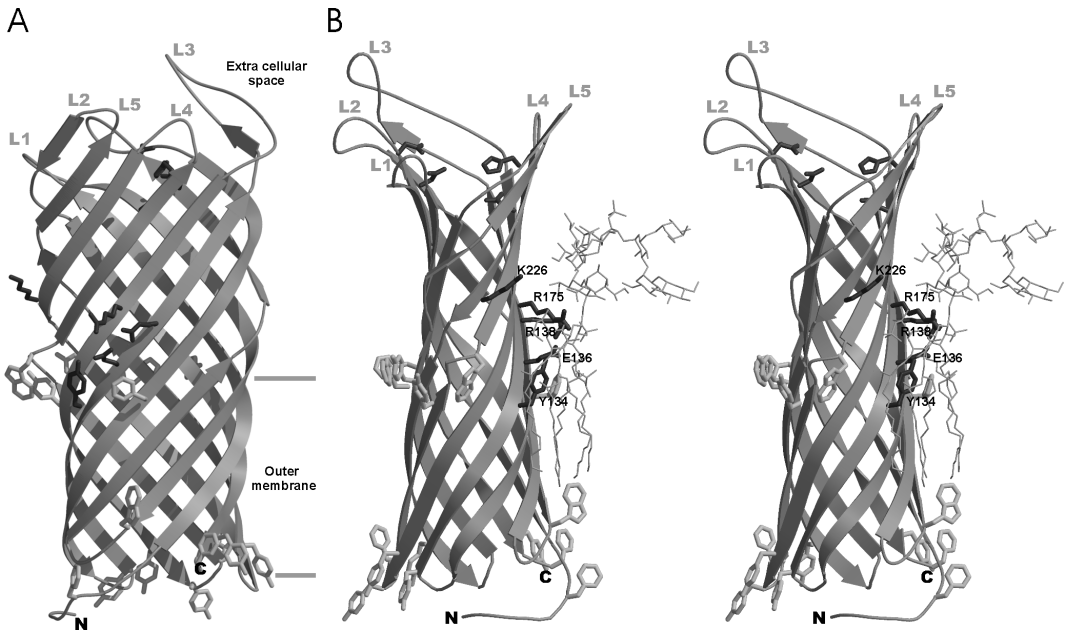

Figure 2.1 Overall structure of OmpT. (**A**) Ribbon representation of OmpT. The extracellular space is located at the top of the figure, and the periplasmic space is at the bottom. Extracellular loops are labeled L1-L5. The position of the membrane bilayer is delineated by horizontal lines. Aromatic residues that are located at the boundary of the hydrophobic and hydrophilic area on the molecular surface are colored light gray. The proposed catalytic residues are depicted in dark gray in the extracellular cleft, and the dark gray residues at the side of the barrel show the putative LPS-binding site. (**B**) Stereo representation of a modeled LPS molecule at the putative binding site. The orientation of the OmpT molecule is rotated 90° along the barrel axis, with respect to (A). The OmpT-LPS model was obtained by superimposing the putative LPS-binding site of OmpT onto the LPS-binding site of FhuA (Ferguson *et al.*, 2000). LPS (from the FhuA structure) is shown in thin gray lines. The putative LPS-binding residues in dark gray are labeled. This figure, Figures 2.5 and 2.7 were prepared using Bobscript (Esnouf, 1997) and Raster3D (Merritt *et al.*, 1997).

1998; Koronakis *et al.*, 2000; Kreusch *et al.*, 1994; Locher *et al.*, 1998; Pautsch & Schulz, 1998; Schirmer *et al.*, 1995; Snijder *et al.*, 1999; Vogt & Schulz, 1999; Weiss *et al.*, 1990), OmpT contains short turns at the periplasmic side of the barrel, long, more mobile loops (Figure 2.3) at the extracellular part and a hydrophobic band of 25 Å in height flanked by aromatic residues that determine the position of the molecule in the membrane. On the extracellular side, OmpT protrudes ~40 Å from the lipid bilayer with the outermost loops located just above the rim of the LPS core region. Near the top of OmpT, the β-

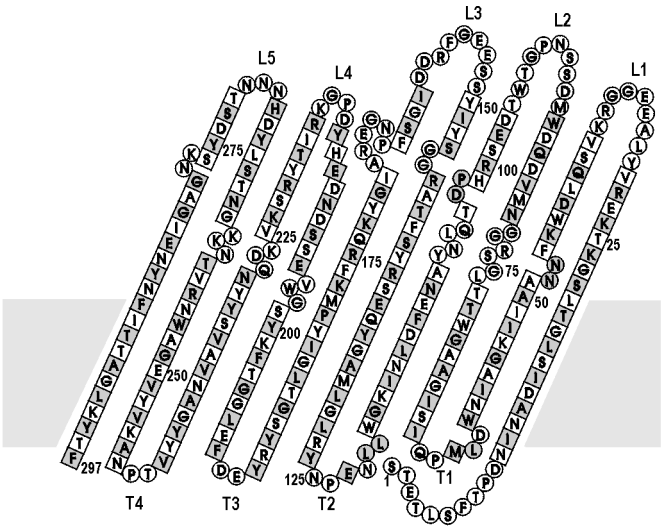

Figure 2.2 Topology model of the OmpT β-barrel. Amino acid residues are given in one-letter code. Squares represent residues that are present in the β-strands. Side chains of amino acids that are shaded gray point to the outside of the barrel. Extracellular loops are labeled L1-L5 and periplasmic turns are labeled T1-T4. Every 25th residue is marked with the corresponding residue number. The gray area indicates the approximate position of the outer membrane.

barrel has a circular diameter of ~32 Å, whereas in the central part the molecular cross-section is elliptical with dimensions of ~13 by ~26 Å, determined using the Cα positions.

Within the membrane region, the barrel is highly regular, hollow and positively charged on the inside (Figure 2.4). Above the membrane, the barrel is constricted and distorted in its hydrogen bonding pattern; seven side chains, i.e. Ser22, Thr73, Arg77, Gln228, Asn258, Lys259 and Lys260, form hydrogen bonds to main chain atoms in the β-barrel. This constricted area, consisting of a few layers of predominantly conserved aromatic residues, forms the floor of a negatively charged groove that harbors the active site (discussed below).

Putative LPS binding site

In vitro, OmpT displays enzymatic activity only in the presence of LPS (Kramer *et al.*, 2000b). It is as yet unclear how LPS contributes to OmpT activity, but preliminary experiments suggest that one LPS molecule per OmpT is sufficient for activity (unpublished results). Based on the structure of outer membrane protein FhuA from *E. coli* in complex with LPS, Ferguson *et al.* (1998, 2000) identified a structural motif for

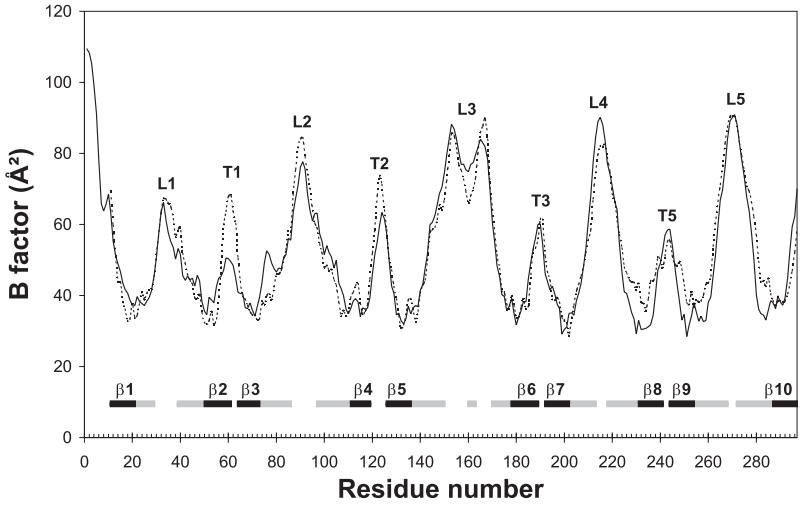

Figure 2.3 *B*-factors of the C^{α} atoms of the two OmpT molecules in the asymmetric unit, i.e. molecule A (solid line) and B (dashed line). β-Strands are shown by bars that are black within the membrane spanning region and gray outside this region. The positions of loops and turns are marked with L1-L5 and T1-T4, respectively.

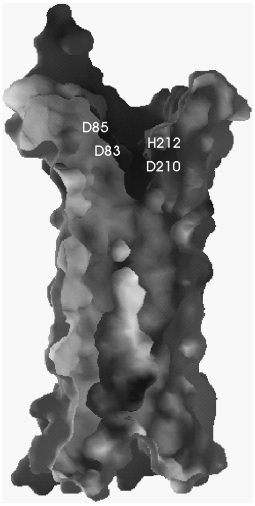

Figure 2.4 Surface of a cross-section of the β-barrel (orientation identical to Figure 2.1B). The extracellular cleft at the top of OmpT is negatively charged (dark gray), whereas the inside of the barrel at the membrane spanning region is positively charged (also dark gray). The positions of the proposed catalytic residues are labeled. This figure was produced by the program GRASP (Nicholls *et al.*, 1991).

LPS binding, consisting of four basic amino acids, which is conserved among pro- and eucaryotic LPS-binding proteins. Three of the four basic residues are found in a similar constellation in OmpT (Arg138, Arg175 and Lys226)(Figure 2.1B). The fourth conserved amino acid (Arg382 in FhuA) is lacking, possibly due to strong bending of OmpT at this

position. Two additional amino acids that bind LPS in FhuA (Glu304 and Phe302) also have counterparts in OmpT (Glu136 and Tyr134). The five similar residues in FhuA and OmpT are at the same height in the barrel and have a r.m.s.d. of 1.1 Å for all atoms. Based on these similarities, we propose that the above-mentioned residues constitute an LPS-binding site in OmpT. A model of OmpT with an LPS molecule at the proposed binding site is shown in Figure 2.1B. The structure of OmpT enables us to test, using mutagenesis studies, whether these residues are indeed responsible for LPS binding and if they contribute to OmpT activity.

Active site

OmpT exerts its proteolytic activity in the extracellular medium (Kramer *et al.*, 2000b). The extracellular part of the molecule contains a large negatively charged groove, which is consistent with the substrate specificity of OmpT for two consecutive basic residues (Figure 2.4). All 18 residues in this proposed active site groove are fully conserved within the omptin family (Figures 2.5 and 2.6). Substitution of serines, histidines and acidic residues by alanines have resulted in ~10-fold reduced activity for Glu27, Asp97, Asp208 or His101, ~500-fold reduced activity for Ser99, and ~10,000-fold reduced activity for Asp83, Asp85, Asp210 or His212 (Kramer *et al.*, 2000a).

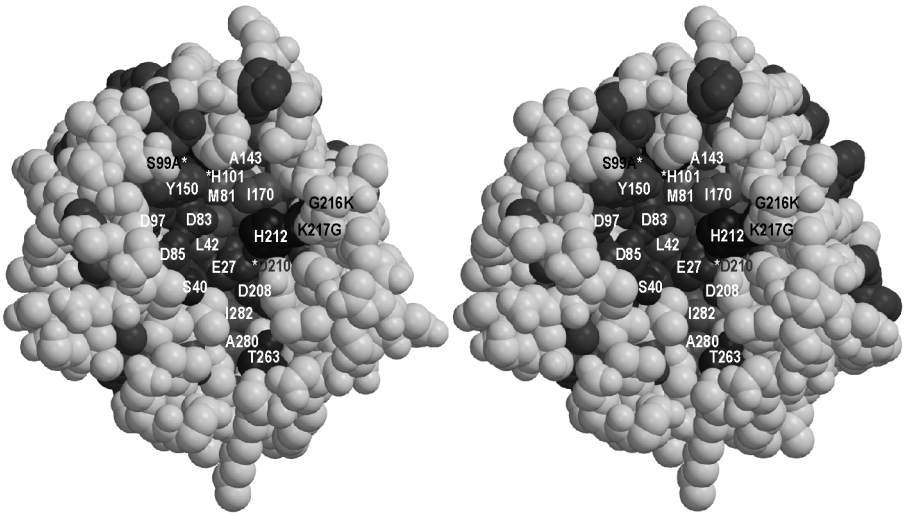

Figure 2.5 Stereo view of a space-filling representation of the active site groove of OmpT, viewed down the β-barrel axis. All conserved residues in the active site are colored dark gray and labeled. Residues S99, H101 and D210 are labeled with an asterisk, since they are hidden behind other residues. The three mutated residues S99A, G216K, K217G are labeled in black.

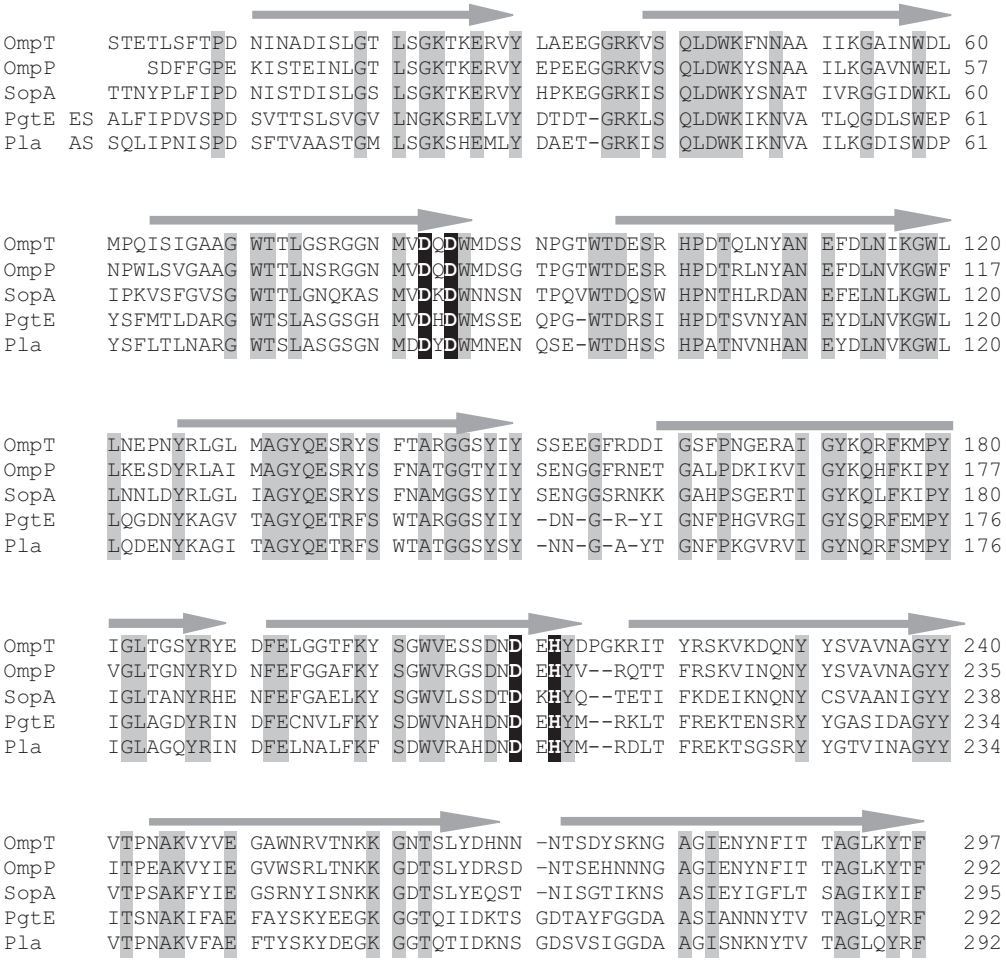

Figure 2.6 Sequence alignment of OmpT with other members of the omptin family, i.e. OmpP of *E. coli*, SopA of *S. flexneri,* PgtE of *S. typhimurium* and Pla of *Y. pestis*. All fully conserved residues are shaded gray. The four proposed catalytic residues are depicted with a black background. The approximate position of the 10 β-strands are indicated by arrows and the extracellular loops are labeled L1-L5.

The structure contradicts the classification of OmpT as a serine protease, since the previously proposed catalytic residues Ser99 (alanine in the crystal structure) and His212 are too far apart, with a distance of 9 Å between Cβ of Ser99 and $N\varepsilon_2$ of His212. Furthermore, the single histidine located close to Ser99, His101, is only moderately important for catalysis. The four residues most important for activity form pairs,

Asp83–Asp85 and His212–Asp210, which are located on opposite sides of the active site groove (Figure 2.7). The distance between the two couples is ~5 Å, determined by the closest distance between Asp83 and His212. The Asp83-Asp85 couple resembles the catalytic site of aspartic proteases. On the other hand, the His212-Asp210 couple resembles the His-Asp pair found in Ser-His-Asp triads of serine proteases. The observation that OmpT is active at high pH with a pK_a of 6.2 (Kramer *et al.*, 2000b) suggests the involvement of an active site histidine. However, a putative nucleophilic residue is not present near the His212-Asp210 couple. We propose a mechanism in which a water molecule (invisible in the electron density map at the current resolution), positioned between Asp83 and His212, is activated by the His212–Asp210 dyad and subsequently performs the nucleophilic attack on the scissile peptide bond. A schematic model of the peptide substrate in the active site is given in Figure 2.7B.

OmpT is highly specific for lysine and arginine at position P1 (nomenclature

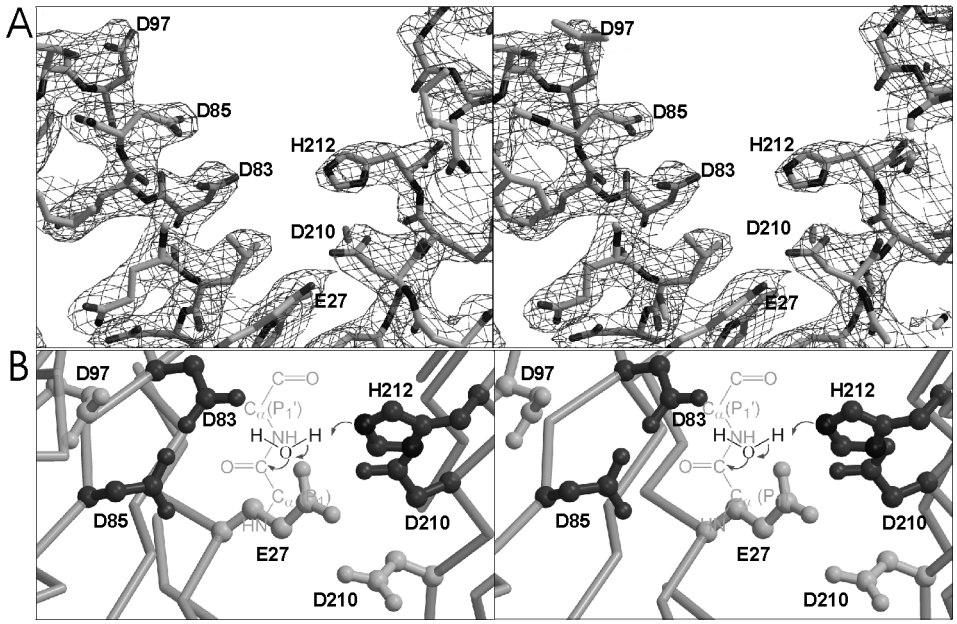

Figure 2.7 Stereo view of the proposed catalytic site. (**A**) The final $2F_o$-F_c electron density map, at 2.6 Å resolution and contoured at 1σ (orientation identical to Figure 2.1B). Residues are shown as sticks. (**B**) The catalytic site viewed from the top down the β-barrel axis. Active site residues are depicted by ball-and-sticks. Proposed catalytic residues are colored dark gray and the other residues that are probably involved in substrate binding are colored light gray. The proposed proteolytic mechanism, in which the His212-Asp210 couple abstracts a proton from a water molecule which then attacks the main chain carbon, is represented schematically. The putative water molecule is shown in dark gray and the main chain of a dipeptide substrate in light gray.

according to Schechter and Berger, 1967) and is less specific for residues at P1', with a decreasing preference for lysine, isoleucine, histidine and arginine (Dekker *et al.*, 2001). Furthermore, OmpT shows a high specificity for small hydrophobic residues (isoleucine, valine and alanine) at P2', and has a broad tolerance for residues at the P2 position (Dekker *et al.*, 2001). Given the high specificities for P1 and P2', we expect well-defined S1 and S2' subsites. A deep negative pocket containing Glu27 and Asp208 probably forms the S1 subsite, which determines the specificity for lysine and arginine at P1 (Figure 2.5). Approximately 7 Å away from this pocket, the groove is shallow and hydrophobic, with Met81 and Ile170 located at the bottom of the groove. This region may well form the S2' subsite, explaining the high specificity for small hydrophobic residues at P2'. Interactions between the substrate and the putative S1 and S2' subsites would position the scissile peptide bond between the Asp83-Asp85 and His212-Asp210 couples, in agreement with our proposed catalytic mechanism.

The current model implies a novel proteolytic mechanism, consistent with the observation that commonly used protease inhibitors do not or weakly affect the activity of OmpT. Solving the X-ray structure of OmpT in complex with a substrate analogue is needed to confirm our active site model and to provide more details on the catalytic mechanism. Since the active site is fully conserved among the omptins, the structure of OmpT may serve as a template to develop new types of antimicrobial compounds against omptin-mediated pathogenicity of Gram-negative bacteria.

Acknowledgements

We wish to thank Drs R.B.G. Ravelli, S. McSweeney and M.J. van Raaij for help with data collection at beamline ID14-EH4 at the ESRF in Grenoble. We also thank Dr D.A.A. Vandeputte for carefully reading the manuscript. This research has been supported financially by the council for Chemical Sciences of the Netherlands Organization for Scientific Research (NWO-CW).

References

Brunger, A.T., Adams, P.D., Clore, G.M., Delano, W.L., Gros, P., Grosse-Kunstleve, R.W., Jiang, J.S., Kuszewski, J., Nilges, M., Pannu, N.S., Read, R.J., Rice, L.M., Simonson, T. & Warren, G.L. (1998). Crystallography & NMR system: A new software suite for macromolecular structure determination. *Acta Crystallogr D Biol Crystallogr,* ***54*** *(Pt 5):* 905-921.

Buchanan, S.K., Smith, B.S., Venkatramani, L., Xia, D., Esser, L., Palnitkar, M., Chakraborty, R., Van Der Helm, D. & Deisenhofer, J. (1999). Crystal structure of the outer membrane active transporter FepA from *Escherichia coli*. *Nat Struct Biol,* ***6*** *(1):* 56-63.

Budisa, N., Steipe, B., Demange, P., Eckerskorn, C., Kellermann, J. & Huber, R. (1995). High-level biosynthetic substitution of methionine in proteins by its analogs 2-aminohexanoic acid, selenomethionine, telluromethionine and ethionine in *Escherichia coli*. *Eur J Biochem,* ***230*** *(2):* 788-796.

Cowan, S.W., Schirmer, T., Rummel, G., Steiert, M., Ghosh, R., Pauptit, R.A., Jansonius, J.N. & Rosenbusch, J.P. (1992). Crystal structures explain functional properties of two *E. coli* porins. *Nature,* ***358*** *(6389):* 727-733.

Dekker, N., Cox, R.C., Kramer, R.A. & Egmond, M.R. (2001). Substrate specificity of the integral membrane protease OmpT determined by spatially addressed peptide libraries. *Biochemistry,* ***40*** 1694-1701.

Egile, C., D'hauteville, H., Parsot, C. & Sansonetti, P.J. (1997). SopA, the outer membrane protease responsible for polar localization of IcsA in *Shigella flexneri*. *Mol Microbiol,* ***23*** *(5):* 1063-1073.

Esnouf, R.M. (1997). An extensively modified version of MolScript that includes greatly enhanced coloring capabilities. *J Mol Graph Model,* ***15*** *(2):* 132-134, 112-133.

Ferguson, A.D., Hofmann, E., Coulton, J.W., Diederichs, K. & Welte, W. (1998). Siderophore-mediated iron transport: crystal structure of FhuA with bound lipopolysaccharide. *Science,* ***282*** *(5397):* 2215-2220.

Ferguson, A.D., Welte, W., Hofmann, E., Lindner, B., Holst, O., Coulton, J.W. & Diederichs, K. (2000). A conserved structural motif for lipopolysaccharide recognition by procaryotic and eucaryotic proteins. *Structure Fold Des,* ***8*** *(6):* 585-592.

Jones, T.A., Zou, J.Y., Cowan, S.W. & Kjeldgaard (1991). Improved methods for binding protein models in electron density maps and the location of errors in these models. *Acta Crystallogr A,* ***47*** *(Pt 2):* 110-119.

Kaufmann, A., Stierhof, Y.D. & Henning, U. (1994). New outer membrane-associated protease of *Escherichia coli* K-12. *J Bacteriol,* ***176*** *(2):* 359-367.

Koronakis, V., Sharff, A., Koronakis, E., Luisi, B. & Hughes, C. (2000). Crystal structure of the bacterial membrane protein TolC central to multidrug efflux and protein export. *Nature,* ***405*** *(6789):* 914-919.

Kramer, R.A., Dekker, N. & Egmond, M.R. (2000a). Identification of active site serine and histidine residues in *Escherichia coli* outer membrane protease OmpT. *FEBS Lett,* ***468*** *(2-3):* 220-224.

Kramer, R.A., Zandwijken, D., Egmond, M.R. & Dekker, N. (2000b). In vitro folding, purification and characterization of *Escherichia coli* outer membrane protease OmpT. *Eur J Biochem,* ***267*** *(3):* 885-893.

Kreusch, A., Neubuser, A., Schiltz, E., Weckesser, J. & Schulz, G.E. (1994). Structure of the membrane channel porin from *Rhodopseudomonas blastica* at 2.0 A resolution. *Protein Sci,* ***3*** *(1):* 58-63.

Locher, K.P., Rees, B., Koebnik, R., Mitschler, A., Moulinier, L., Rosenbusch, J.P. & Moras, D.

(1998). Transmembrane signaling across the ligand-gated FhuA receptor: crystal structures of free and ferrichrome-bound states reveal allosteric changes. *Cell,* ***95*** *(6):* 771-778.

Lundrigan, M.D. & Webb, R.M. (1992). Prevalence of ompT among *Escherichia coli* isolates of human origin. *FEMS Microbiol Lett,* ***76*** *(1-2):* 51-56.

Merritt, Ethan, A., Bacon & David, J. (1997). Raster3D: Photorealistic Molecular Graphics. *Methods Enzymol,* ***277*** 505-524.

Nicholls, A., Sharp, K.A. & Honig, B. (1991). Protein folding and association: insights from the interfacial and thermodynamic properties of hydrocarbons. *Proteins,* ***11*** *(4):* 281-296.

Otwinowski, Z. (1991). Maximum likelyhood refinement of heavy atom parameters in Isomorphous Replacement and Anomalous Scattering. *Proceedings of the CCP4 study weekend 25-26 January 1991,*

Otwinowski, Z. & Minor, W. (1997). Processing of X-ray diffraction data collected in oscillation mode. *Methods Enzymol,* ***276*** 307-326.

Pautsch, A. & Schulz, G.E. (1998). Structure of the outer membrane protein A transmembrane domain. *Nat Struct Biol,* ***5*** *(11):* 1013-1017.

Rawlings, N.D. & Barrett, A.J. (1994). Families of serine peptidases. *Methods Enzymol,* ***244*** 19-61.

Schechter, N.D. and Berger, A. (1967) On the size of the active site in proteases. *Biochem Biophys Res Commun,* ***27***, 157-162

Schirmer, T., Keller, T.A., Wang, Y.F. & Rosenbusch, J.P. (1995). Structural basis for sugar translocation through maltoporin channels at 3.1 Å resolution. *Science,* ***267*** *(5197):* 512-514.

Shere, K.D., Sallustio, S., Manessis, A., D'aversa, T.G. & Goldberg, M.B. (1997). Disruption of IcsP, the major Shigella protease that cleaves IcsA, accelerates actin-based motility. *Mol Microbiol,* ***25*** *(3):* 451-462.

Snijder, H.J., Ubarretxena-Belandia, I., Blaauw, M., Kalk, K.H., Verheij, H.M., Egmond, M.R., Dekker, N. & Dijkstra, B.W. (1999). Structural evidence for dimerization-regulated activation of an integral membrane phospholipase. *Nature,* ***401*** *(6754):* 717-721.

Sodeinde, O.A. & Goguen, J.D. (1989). Nucleotide sequence of the plasminogen activator gene of *Yersinia pestis*: relationship to ompT of *Escherichia coli* and gene E of *Salmonella typhimurium*. *Infect Immun,* ***57*** *(5):* 1517-1523.

Sodeinde, O.A., Subrahmanyam, Y.V., Stark, K., Quan, T., Bao, Y. & Goguen, J.D. (1992). A surface protease and the invasive character of plague. *Science,* ***258*** *(5084):* 1004-1007.

Stathopoulos, C. (1998). Structural features, physiological roles, and biotechnological applications of the membrane proteases of the OmpT bacterial endopeptidase family: a micro-review. *Membr Cell Biol,* ***12*** *(1):* 1-8.

Stumpe, S., Schmid, R., Stephens, D.L., Georgiou, G. & Bakker, E.P. (1998). Identification of OmpT as the protease that hydrolyzes the antimicrobial peptide protamine before it enters growing cells of *Escherichia coli*. *J Bacteriol,* ***180*** *(15):* 4002-4006.

Sugimura, K. & Nishihara, T. (1988). Purification, characterization, and primary structure of *Escherichia coli* protease VII with specificity for paired basic residues: identity of protease VII and OmpT. *J Bacteriol,* ***170*** *(12):* 5625-5632.

Vogt, J. & Schulz, G.E. (1999). The structure of the outer membrane protein OmpX from *Escherichia coli* reveals possible mechanisms of virulence. *Structure Fold Des,* **7** *(10):* 1301-1309.

Webb, R.M. & Lundigran, M.D. (1996). OmpT in *Escherichia coli* correlates with severity of disease in urinary tract infections. *Med. Microbiol. Letters,* ***5*** 8-14.

Weeks, C.M. & Miller, R. (1999). Optimizing Shake-and-Bake for proteins. *Acta Crystallogr D Biol Crystallogr,* ***55*** *(Pt 2):* 492-500.

Weiss, M.S., Wacker, T., Weckesser, J., Welte, W. & Schulz, G.E. (1990). The three-dimensional structure of porin from *Rhodobacter capsulatus* at 3 A resolution. *FEBS Lett,* ***267*** *(2):* 268-272.

Yu, G.Q. & Hong, J.S. (1986). Identification and nucleotide sequence of the activator gene of the externally induced phosphoglycerate transport system of *Salmonella typhimurium*. *Gene,* ***45*** *(1):* 51-57.

3

Identification of essential acidic residues of outer membrane protease OmpT supports a novel active site

R. Arjen Kramer, Lucy Vandeputte-Rutten, Gerard Jan de Roon, Piet Gros, Niek Dekker and Maarten R. Egmond

FEBS Lett. (2001), **505**(3), 426-430

Abstract

Escherichia coli outer membrane protease OmpT has previously been classified as a serine protease with Ser99 and His212 as active site residues. The recently solved X-ray structure of the enzyme was inconsistent with this classification, and the involvement of a nucleophilic water molecule was proposed. Here, we substituted all conserved aspartate and glutamate residues by alanines and measured the residual enzymatic activities of the variants. Our results support the involvement of a nucleophilic water molecule that is activated by the Asp210/His212 catalytic dyad. Activity is also strongly dependent on Asp83 and Asp85. Both may function in binding of the water molecule and/or oxyanion stabilization. The proposed mechanism implies a novel proteolytic catalytic site.

Introduction

Escherichia coli OmpT (EC 3.4.21.87) is a 33.5 kDa outer membrane protease that cleaves peptides and proteins preferentially between two consecutive basic amino acids (Dekker *et al.*, 2001; Grodberg *et al.*, 1988; Kramer *et al.*, 2000b; Mangel *et al.*, 1994; Sugimura & Nishihara, 1988). The enzyme has been suggested to be involved in urinary tract disease (Webb & Lundigran, 1996), in DNA excision repair (Sedliakova *et al.*, 1997) and in the breakdown of antimicrobial peptides (Stumpe *et al.*, 1998), but its actual biological function remains to be elucidated. OmpT is a member of the omptin family that includes the proteases PgtE of *Salmonella typhimurium* (mature part 49% identical to OmpT) (Yu & Hong, 1986), Pla of *Yersinia pestis* (50% identical) (Sodeinde & Goguen, 1989), OmpP of *E. coli* (72% identical) (Kaufmann *et al.*, 1994) and SopA of *Shigella flexneri* (60% identical) (Egile *et al.*, 1997). As OmpT, Pla and OmpP lack cysteine residues, the omptins do not belong to the class of cysteine proteases. The omptin family appears to constitute a novel class of proteases, since the amino acids conserved within the omptins are not part of known active site consensus sequences found in serine proteases, aspartic proteases or metalloproteases (Barrett *et al.*, 1998). This is confirmed by the observation that OmpT activity is not or only slightly inhibited by commonly used class-specific protease inhibitors (Sugimura & Higashi, 1988; Sugimura & Nishihara, 1988; White *et al.*, 1995). Significant inhibition of OmpT activity has been observed only at high concentrations of the serine protease inhibitors diisopropylfluorophosphate (DFP) or phenylmethylsulfonyl fluoride (PMSF) (Sugimura & Nishihara, 1988). Members of the omptin family have been classified as serine proteases mainly based on these observations (Rawlings & Barrett, 1994), even though several experiments have been reported where DFP and PMSF did not affect the proteolytic activity of OmpT (Hollifield *et al.*, 1978; Sugimura & Higashi, 1988; White *et al.*, 1995).

In serine proteases, the scissile peptide bond is attacked by a nucleophilic hydroxyl of

the catalytic serine that is usually activated by a histidine residue (Barrett *et al.*, 1998). To identify the putative active site serine and histidine of OmpT, we previously substituted all conserved serines and histidines by site-directed mutagenesis and concluded that Ser99 and His212 are essential active site residues (Kramer *et al.*, 2000a). The activities of H212A, H212N and H212Q OmpT were reduced by four orders of magnitude. However, the mutation S99A in OmpT reduced activity only 500-fold, where at least a 10,000-fold reduced activity was expected (e.g. (Carter & Wells, 1988)). It was therefore emphasized that a role for Ser99 other than performing the nucleophilic attack should not be excluded. To further examine the active site mechanism, we wished to study the possible involvement of residues other than serine and histidine. In the classical serine protease triad, a negatively charged aspartate residue is thought to stabilize the transient positive charge on the histidine during catalysis (Barrett *et al.*, 1998). Recently, it was shown that a glutamate is able to perform this function as well (Hakansson *et al.*, 2000). Conserved acidic residues are thus obvious candidates for being an active site residue of OmpT. Furthermore, at least one aspartate or glutamate residue is expected to be involved in substrate binding, since OmpT specifically cleaves peptides between two positively charged amino acids (Dekker *et al.*, 2001). OmpT contains 36 acidic residues, of which six aspartates (at positions 43, 83, 85, 97, 208 and 210) and five glutamates (at positions 27, 111, 136, 193 and 250) are fully conserved within the omptin family (Figure 3.1). Using the same approach as described for the identification of Ser99 and His212 (Kramer *et al.*, 2000a), these 11 residues were replaced by alanines and the residual activities of the resulting variants were measured. In parallel with these mutagenesis studies, we solved the X-ray structure of OmpT, which revealed a putative active site cleft at the top of the extracellular region (Vandeputte-Rutten *et al.*, 2001). Ser99 and His212 are both located in this cleft, but they are separated by 9 Å. The concerted action of Ser99 and His212 was seriously questioned and an alternative mechanism was proposed, involving an Asp210/His212 catalytic dyad with a water molecule acting as nucleophile (Vandeputte-Rutten *et al.*, 2001).

Here, we present the mutagenesis data of the conserved aspartate and glutamate residues and discuss their importance for the proteolytic activity of OmpT. The results support the involvement of an Asp210/His212 catalytic dyad, suggesting that OmpT would be the first protease exhibiting this type of catalytic mechanism.

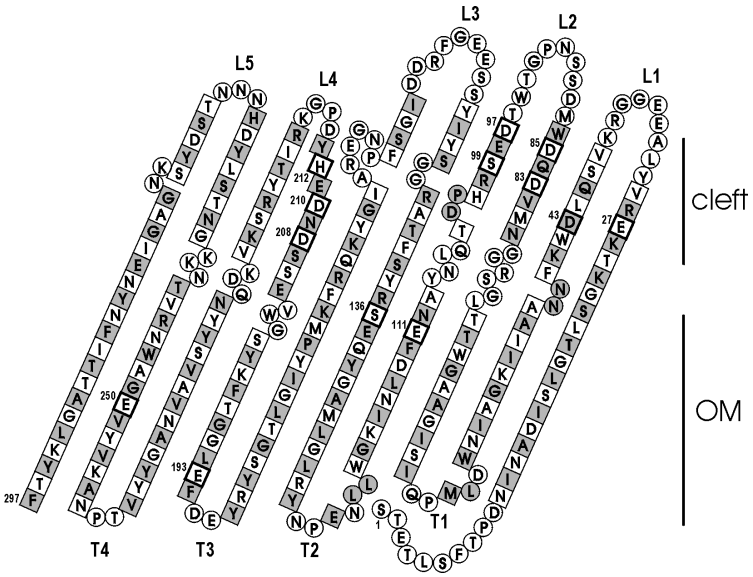

Figure 3.1 **Topology of OmpT (adapted from** (Vandeputte-Rutten *et al.*, 2001)**).** Numbers refer to amino acid positions in mature OmpT. Residues in β-strands are shown in squares; other residues are in circles. β-Strand residues pointing to the protein exterior are in shaded squares. Conserved acidic residues, as well as Ser99 and His212, are in squares with dark edges. The approximate positions of the outer membrane (OM) and the putative active site cleft of OmpT are indicated. The N-terminus and the short turns (T1-T4) are localized in the periplasm and the large loops (L1-L5) face the extracellular side of the membrane.

Materials and methods

Materials

DNA restriction enzymes were purchased from New England Biolabs. Oligonucleotides were bought from Amersham Pharmacia Biotech. Polyethyleneglycol tert-octylphenyl ether (Triton X-100) was obtained from Serva and polyoxyethylene sorbitanmonolaurate (Tween 20) was obtained from Bio-Rad. The fluorogenic peptide substrate Abz-Ala-Arg-Arg-Ala-Dap(dnp)-Gly (Abz = *o*-aminobenzoyl, Dap(dnp) = N-b-dinitrophenyl-L-diaminopropionic acid) was a kind gift of Mr. Ruud C. Cox (Utrecht University). Anti-OmpT monoclonal antibodies were obtained as described before (Kramer *et al.*, 2000a). Goat anti-mouse IgG alkaline phosphatase conjugate was purchased from Promega. All other chemicals were of analytical grade.

Bacterial strains and plasmids

E. coli K-12 strain DH5α (Hanahan, 1983) was used in the cloning procedures. *E. coli*

strain BL21(DE3) (Studier & Moffatt, 1986) lacks the *ompT* gene and was used for expression. Plasmids pND9 and pND10 (Kramer *et al.*, 2000b) are derivatives of pUC19 (Yanisch-Perron *et al.*, 1985), containing the *ompT* gene including its own promoter sequence oriented clockwise and counter-clockwise with the *lac* promoter, respectively.

All mutations were introduced using PCR according to the manufacturer's protocol provided with the QuikChange site-directed mutagenesis kit (Stratagene). The *ompT* gene contains only few unique restriction sites. Therefore, four additional unique restriction sites were introduced to facilitate subcloning of introduced mutations. The sites *Xho*I (at Ser89 of mature OmpT), *Sac*II (at Arg144), *Age*I (at Arg222) and *Eag*I (at Ala291) were introduced as silent mutations in plasmids pND10 and pND9, resulting in plasmids pRAK22 and pRAK23, respectively. Mutations resulting in the substitution of Asp or Glu by Ala were introduced individually into pRAK22. To facilitate the screening for introduced mutations, silent mutations resulting in the introduction or deletion of restriction sites were made concomitantly with the amino acid mutations. After verification of the correctly introduced mutations by DNA sequencing, all mutations were subcloned into pRAK23 using the newly introduced restriction sites. The sequences of the relevant parts of the constructed plasmids were checked by restriction enzyme analysis and DNA sequencing.

Expression, isolation and analysis of OmpT variants

After transformation by the various plasmids, BL21(DE3) cells were grown overnight in 10 ml LB medium (Sambrook *et al.*, 1989) with 50 μg/ml ampicillin at 37°C. Membrane fractions containing OmpT were isolated from the bacteria, as described before (Kramer *et al.*, 2000a), and solubilized in 200 μl buffer A (0.1% Triton X-100, 50 mM Tris, pH 7.5). The total amount of protein in the isolated membrane fractions was determined using the Bio-Rad protein assay with bovine serum albumin as a reference. Samples of membrane fractions corresponding to equal amounts of total protein were analyzed by Western blotting using anti-OmpT monoclonal antibodies, as described before (Kramer *et al.*, 2000a).

Enzymatic activity assays

Samples of membrane fractions were diluted in buffer A to appropriate concentrations (varying from 0.5 μg to 0.2 mg of total protein per ml) prior to OmpT activity measurements. The internally quenched fluorogenic substrate Abz-Ala-Arg-Arg-Ala-Dap(dnp)-Gly was used in a fluorimetric activity assay, as described previously (Kramer *et al.*, 2000b). Assay conditions were 5 μM substrate, 1 mM Tween 20, 5 mM EDTA, 10 mM Tris, pH 8.3. Activity was measured in a fluorimeter using excitation and emission wavelengths of 325 and 430 nm, respectively. After recording the initial linear increase in

fluorescence, 20 μg of trypsin was added to determine the fluorescence of completely hydrolyzed substrate, which enabled quantification of the inner filter effect and allowed for the calculation of the activity in enzymatic units (*U*=μmol substrate converted per min).

Results

Expression of OmpT

Single mutant proteins of OmpT were constructed with the conserved acidic residues replaced by alanines. BL21(DE3) cells expressing either these alanine variants or wild-type OmpT were grown in triplicate and membrane fractions were isolated. Cells lacking a plasmid with the gene for OmpT were used as a control. The fact that isolated membrane fractions were used instead of purified protein had two important consequences. An important advantage of using outer membrane fractions was that all samples contained endogenous lipopolysaccharide, which has been shown to be required for OmpT activity (Kramer *et al.*, 2000b). Unfortunately the concentration of OmpT in the samples could not be accurately determined. Therefore, concentrations of total protein were determined for each sample and used as a measure for the amount of OmpT. We previously validated this method for serine and histidine variants of OmpT by showing that the expression levels of these variants were comparable to that of wild-type OmpT (Kramer *et al.*, 2000a). To check whether this was also true for the aspartate and glutamate variants, SDS-PAGE and Western blot analysis were performed with all samples containing equal amounts of total protein. As expected, the expression levels of the variants and wild-type OmpT were comparable within a factor of three (data not shown). These differences are acceptable in our studies, since activities reduced by at least two orders of magnitude are expected when essential residues are replaced. SDS-PAGE and Western blotting were also used to check the correct folding of the variants. At room temperature, the presence of SDS is not sufficient to unfold the β-barrel conformation of OmpT. As a consequence, native OmpT has a more compact shape than the heat-denatured protein and runs faster on SDS-PAGE gel (Kramer *et al.*, 2000a; Kramer *et al.*, 2000b). This difference in migration rate between folded and unfolded protein is known as heat-modifiability, which is generally observed for outer membrane proteins (Heller, 1978). The Western blots showed that all of the 11 active site variants displayed this effect (data not shown), indicating their proper folding and assembly in the outer membrane.

Activity measurements of OmpT variants

The enzymatic activity of OmpT in the isolated membrane fractions was determined using a fluorimetric assay. For all variants, membrane fractions of three independent cell

cultures were measured. The average activities are shown in Figure 3.2. A large spread in the activities was observed for several variants, which was at least partially due to variations in expression levels as mentioned above. Variants E111A, E136A, E193A and E250A displayed enzymatic activities that were comparable to wild- type within a factor of two. In contrast, variant E27A, as well as all aspartate variants, showed significantly reduced activities compared to wild-type OmpT. Specific activities of the variants E27A, D43A, D97A and D208A were reduced 4-17-fold. The strongest decrease was observed for variants D83A, D85A and D210A, exhibiting at least 10,000-fold lower activity than wild-type OmpT.

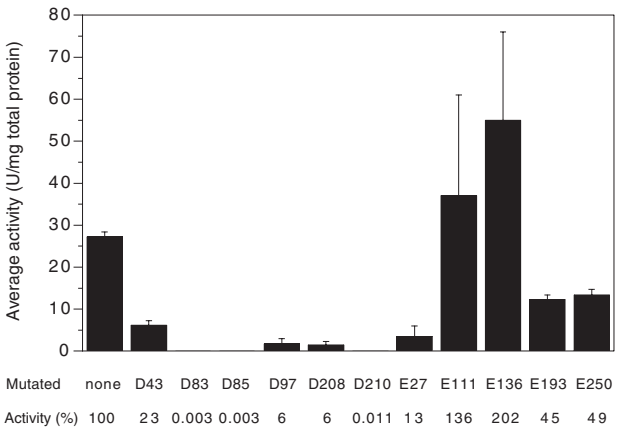

Figure 3.2 **Enzymatic activities of OmpT and its variants as measured in a fluorimetric assay.** Average absolute activities of three independent measurements (black bars) and the corresponding relative activities compared to wild-type OmpT (percentages) were determined for each variant. See the text for experimental details.

Discussion

The experimental basis for the current classification of OmpT as a serine protease is weak, as pointed out in the Introduction of this Chapter. To investigate the nature of the active site, we studied the involvement of acidic residues in substrate binding and/or hydrolysis by constructing single mutant proteins of OmpT. Substitution of the conserved residues Asp43, Glu111, Glu136, Glu193 or Glu250 by alanines did not lead to severe reductions in proteolytic activity (Figure 3.2). Not surprisingly, the side chain of none of these residues is located in the putative active site cleft (Figure 3.1) (Vandeputte-Rutten *et al.*, 2001). Deleting either of the remaining six conserved acidic residues, which are all located inside the highly negatively charged cleft (Figure 3.3) (Vandeputte-Rutten *et al.*,

Figure 3.3 **Active site cleft of OmpT** (adapted from (Vandeputte-Rutten *et al.*, 2001)). OmpT (ribbon presentation) is viewed parallel to the barrel axis from the extracellular side of the outer membrane. The conserved acidic residues Glu27, Asp83, Asp85, Asp97, Asp208 and Asp210, as well as Ser99 (Ala99 in the crystallized protein) and His212, are represented as stick model.

2001), resulted in at least seven-fold lower activity. OmpT preferentially cleaves peptides between two basic amino acids (Dekker *et al.*, 2001), therefore the anionic nature of the cleft is probably a major determinant of its substrate specificity. More specifically, we proposed earlier, based on the crystal structure of OmpT (Vandeputte-Rutten *et al.*, 2001), that Glu27 and Asp208 may define the high specificity of OmpT for arginine or lysine at P1 in the substrate (nomenclature as in reference (Schechter & Berger, 1967)). The mutagenesis data reported here are in good agreement with this proposal. For the P1' position, the specificity was less exclusive, but a positively charged amino acid was preferred there as well (Dekker *et al.*, 2001), likely due to interaction with an anionic residue of OmpT. Assuming that the substrate has an extended conformation and that the P1 side chain points towards Glu27 and Asp208, the P1' chain would be located close to Asp97. D97A OmpT displayed only 6% residual activity, therefore we propose that Asp97 is responsible for the observed P1' specificity. A schematic model of a peptide in the active site is shown in Figure 3.4.

Substituting the aspartate at position 83, 85 or 210 reduced activity at least 10,000-fold, suggesting that these residues may participate directly in enzymatic catalysis. The absolute requirement for more than one aspartate is reminiscent of the aspartic proteases, in which two aspartates activate a nucleophilic water molecule (Barrett *et al.*, 1998). The relative orientation of Asp83 and Asp85 is in fact similar to that in aspartic proteases (Vandeputte-Rutten *et al.*, 2001). However, OmpT does not contain the D(T/S)G consensus sequence of aspartic proteases and it is not active at acidic pH (Kramer *et al.*, 2000b), while the overall fold is very different from aspartic proteases (Barrett *et al.*, 1998). A possible role for the Asp83/Asp85 couple is discussed below. The X-ray structure

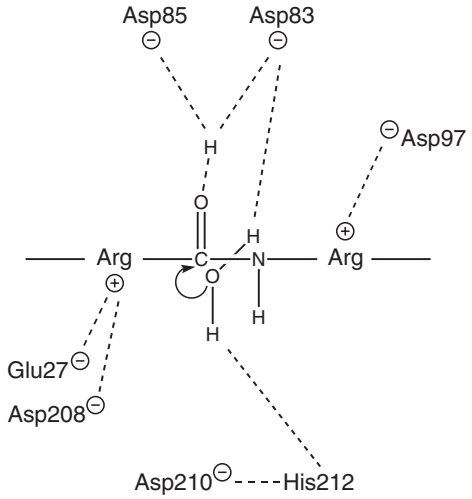

Figure 3.4 **Schematic two-dimensional model of a peptide in the active site of OmpT.** Hydrogen bonds and ionic interactions are indicated by dashed lines. The curved arrow represents the nucleophilic attack on the carbonyl carbon of the scissile peptide bond.

of OmpT showed that the relative orientation of Asp210 and His212 is similar to that in the classical Ser/His/Asp triad and that there is no density at the position where a serine would be expected (Figure 3.3) (Vandeputte-Rutten *et al.*, 2001). Based on this information, we recently postulated that OmpT has an Asp210/His212 catalytic dyad with a water molecule acting as nucleophile (Vandeputte-Rutten *et al.*, 2001). The observation that Asp210 is indeed essential for activity supports this hypothesis. The existence of an Asp/His catalytic dyad has been proposed for several enzymes catalyzing hydrolytic reactions, including phospholipase A2 (Yuan & Tsai, 1999), phosphoesterases (Knofel & Strater, 1999), endonucleases (Gorman *et al.*, 1997), endocellulases (Russell, 1998) and haloalkane dehalogenase (Pries *et al.*, 1995). Interestingly, it has never been observed in proteases, implying that OmpT would be the first example of a protease using this type of catalytic mechanism. As amide bonds are relatively stable, other factors are expected to facilitate peptide cleavage by activated water. Presumably the Asp83/Asp85 couple plays a role in the catalytic mechanism, for example by coordinating the nucleophilic water molecule as proposed before (Vandeputte-Rutten *et al.*, 2001). In this way, Asp83 and Asp85 would be indirectly involved in activation of the water molecule, a mechanism that is different from the direct activation of water by aspartates in aspartic proteases. Alternatively or in addition, a proton shared by the carboxyl moieties of Asp83 and Asp85 might stabilize the oxyanion intermediate during the reaction. In agreement with these hypotheses, the mutagenesis experiments show that both amino acids are required for activity. Further insight in the role of the essential residues Asp83, Asp85 and Asp210 might be obtained by determining the kinetic parameters k_{cat} and K_M of the corresponding OmpT variants. Unfortunately though, the residual activities of

variants D83A, D85A and D210A OmpT were very close to the detection limit of our assay, making it impossible to obtain reliable Michaelis-Menten curves for these variants. The preferred route to detailed elucidation of the active site mechanism would be to determine the X-ray structure of OmpT in the presence of a peptide substrate. Attempts to crystallize OmpT in complex with a substrate analogue are currently under way.

Prior to submission of this paper, we became aware of a very recent publication on omptin Pla of *Y. pestis* by Kukkonen *et al.* (Kukkonen *et al.*, 2001), who observed proteolytic importance for Pla residues corresponding to Ser99, His101, His212, Asp83, Asp85 and Asp210 in OmpT. They could not settle the exact roles of these residues, but hypothesized that Pla may contain a Ser99/His212/Asp210 triad (OmpT numbering), whereas Asp83, Asp85 and His101 were proposed to be involved in substrate interaction (Kukkonen *et al.*, 2001). Now that we have solved the crystal structure of OmpT and generated mutagenesis data on all conserved Ser, His, Asp and Glu residues in OmpT, we have a sound basis for our novel active site model, which does not involve a nucleophilic serine. The fact that the proposed catalytic residues Asp83, Asp85, Asp210 and His212 of OmpT have proteolytically important counterparts in Pla, indicates that all omptins likely use the same catalytic mechanism

Acknowledgements

The authors wish to thank Mr. Ruud C. Cox for synthesis of the fluorogenic substrate. This research has been financially supported by the Council for Chemical Sciences of the Netherlands Organization for Scientific Research (CW-NWO).

References

Barrett, A.J., Rawlings, N.D. & Woessner, J.F. (1998). *Handbook of Proteolytic Enzymes,* Academic Press, San Diego.

Carter, P. & Wells, J.A. (1988). Dissecting the catalytic triad of a serine protease. *Nature, 332 (6164):* 564-568.

Dekker, N., Cox, R.C., Kramer, R.A. & Egmond, M.R. (2001). Substrate specificity of the integral membrane protease OmpT determined by spatially addressed peptide libraries. *Biochemistry, 40* 1694-1701.

Egile, C., D'hauteville, H., Parsot, C. & Sansonetti, P.J. (1997). SopA, the outer membrane protease responsible for polar localization of IcsA in *Shigella flexneri*. *Mol Microbiol, 23 (5):* 1063-1073.

Gorman, M.A., Morera, S., Rothwell, D.G., De La Fortelle, E., Mol, C.D., Tainer, J.A., Hickson, I.D. & Freemont, P.S. (1997). The crystal structure of the human DNA repair endonuclease

HAP1 suggests the recognition of extra-helical deoxyribose at DNA abasic sites. *Embo J, 16 (21):* 6548-6558.

Grodberg, J., Lundrigan, M.D., Toledo, D.L., Mangel, W.F. & Dunn, J.J. (1988). Complete nucleotide sequence and deduced amino acid sequence of the ompT gene of *Escherichia coli* K-12. *Nucleic Acids Res, 16 (3):* 1209.

Hakansson, K., Wang, A.H. & Miller, C.G. (2000). The structure of aspartyl dipeptidase reveals a unique fold with a Ser- His-Glu catalytic triad. *Proc Natl Acad Sci U S A, 97 (26):* 14097-14102.

Hanahan, D. (1983). Studies on transformation of *Escherichia coli* with plasmids. *J Mol Biol, 166 (4):* 557-580.

Heller, K.B. (1978). Apparent molecular weights of a heat-modifiable protein from the outer membrane of *Escherichia coli* in gels with different acrylamide concentrations. *J Bacteriol, 134 (3):* 1181-1183.

Hollifield, W.C., Jr., Fiss, E.H. & Neilands, J.B. (1978). Modification of a ferric enterobactin receptor protein from the outer membrane of *Escherichia coli*. *Biochem Biophys Res Commun, 83 (2):* 739-746.

Kaufmann, A., Stierhof, Y.D. & Henning, U. (1994). New outer membrane-associated protease of *Escherichia coli* K-12. *J Bacteriol, 176 (2):* 359-367.

Knofel, T. & Strater, N. (1999). X-ray structure of the *Escherichia coli* periplasmic 5'-nucleotidase containing a dimetal catalytic site. *Nat Struct Biol, 6 (5):* 448-453.

Kramer, R.A., Dekker, N. & Egmond, M.R. (2000a). Identification of active site serine and histidine residues in *Escherichia coli* outer membrane protease OmpT. *FEBS Lett, 468 (2-3):* 220-224.

Kramer, R.A., Zandwijken, D., Egmond, M.R. & Dekker, N. (2000b). In vitro folding, purification and characterization of *Escherichia coli* outer membrane protease ompT. *Eur J Biochem, 267 (3):* 885-893.

Kukkonen, M., Lahteenmaki, K., Suomalainen, M., Kalkkinen, N., Emody, L., Lang, H. & Korhonen, T.K. (2001). Protein regions important for plasminogen activation and inactivation of alpha2-antiplasmin in the surface protease Pla of *Yersinia pestis*. *Mol Microbiol, 40 (5):* 1097-1111.

Mangel, W.F., Toledo, D.L., Brown, M.T., Worzalla, K., Lee, M. & Dunn, J.J. (1994). Omptin: an *Escherichia coli* outer membrane proteinase that activates plasminogen. *Methods Enzymol, 244* 384-399.

Pries, F., Kingma, J., Krooshof, G.H., Jeronimus-Stratingh, C.M., Bruins, A.P. & Janssen, D.B. (1995). Histidine 289 is essential for hydrolysis of the alkyl-enzyme intermediate of haloalkane dehalogenase. *J Biol Chem, 270 (18):* 10405-10411.

Rawlings, N.D. & Barrett, A.J. (1994). Families of serine peptidases. *Methods Enzymol, 244* 19-61.

Russell, R.B. (1998). Detection of protein three-dimensional side-chain patterns: new examples of convergent evolution. *J Mol Biol, 279 (5):* 1211-1227.

Sambrook, J., Fritsch, E.F. & Maniatis, T. (1989). *Molecular Cloning: A Laboratory Manual,* Cold Spring Harbor Laboratory Press, Cold Spring Harbor, NY.

Schechter, I. & Berger, A. (1967). On the size of the active site in proteases. I. Papain. *Biochem Biophys Res Commun, 27 (2):* 157-162.

Sedliakova, M., Masek, F., Slezarikova, V. & Pirsel, M. (1997). The effect of the OmpT protease on excision repair in UV-irradiated *Escherichia coli*. *J Photochem Photobiol B, 41 (3):* 245-248.

Sodeinde, O.A. & Goguen, J.D. (1989). Nucleotide sequence of the plasminogen activator gene of Yersinia pestis: relationship to ompT of *Escherichia coli* and gene E of *Salmonella typhimurium*. *Infect Immun, 57 (5):* 1517-1523.

Studier, F.W. & Moffatt, B.A. (1986). Use of bacteriophage T7 RNA polymerase to direct selective high-level expression of cloned genes. *J Mol Biol, 189 (1):* 113-130.

Stumpe, S., Schmid, R., Stephens, D.L., Georgiou, G. & Bakker, E.P. (1998). Identification of OmpT as the protease that hydrolyzes the antimicrobial peptide protamine before it enters growing cells of Escherichia coli. *J Bacteriol, 180 (15):* 4002-4006.

Sugimura, K. & Higashi, N. (1988). A novel outer-membrane-associated protease in *Escherichia coli*. *J Bacteriol, 170 (8):* 3650-3654.

Sugimura, K. & Nishihara, T. (1988). Purification, characterization, and primary structure of *Escherichia coli* protease VII with specificity for paired basic residues: identity of protease VII and OmpT. *J Bacteriol, 170 (12):* 5625-5632.

Vandeputte-Rutten, L., Kramer, R.A., Kroon, J., Dekker, N., Egmond, M.R. & Gros, P. (2001). Crystal structure of the outer membrane protease OmpT from *Escherichia coli* suggests a novel catalytic site. *Embo J, 20 (18):* 5033-5039.

Webb, R.M. & Lundigran, M.D. (1996). OmpT in *Escherichia coli* correlates with severity of disease in urinary tract infections. *Med. Microbiol. Letters, 5* 8-14.

White, C.B., Chen, Q., Kenyon, G.L. & Babbitt, P.C. (1995). A novel activity of OmpT. Proteolysis under extreme denaturing conditions. *J Biol Chem, 270 (22):* 12990-12994.

Yanisch-Perron, C., Vieira, J. & Messing, J. (1985). Improved M13 phage cloning vectors and host strains: nucleotide sequences of the M13mp18 and pUC19 vectors. *Gene, 33 (1):* 103-119.

Yu, G.Q. & Hong, J.S. (1986). Identification and nucleotide sequence of the activator gene of the externally induced phosphoglycerate transport system of *Salmonella typhimurium*. *Gene, 45 (1):* 51-57.

Yuan, C. & Tsai, M. (1999). Pancreatic phospholipase A(2): new views on old issues. *Biochim Biophys Acta, 1441 (2-3):* 215-222.

4

Structural analysis of the outer membrane protease OmpT from *Escherichia coli* inhibited by zinc

Lucy Vandeputte-Rutten, Niek Dekker, Arjen Kramer,
Maarten Egmond and Piet Gros

manuscript in preparation

Abstract

Escherichia coli outer membrane protease OmpT is not inhibited by commonly used protease inhibitors. It is known, however, that zinc has an inhibitory effect on the catalytic activity. To gain more insight into the catalytic mechanism and the effect of zinc on the structure of OmpT, we determined the crystal structure of OmpT in complex with Zn^{2+}. The structure shows that OmpT contains two Zn^{2+}-binding sites, which are present in the active site. These binding sites are however different in the two molecules in the asymmetric unit. Interestingly, the structure reveals that in both molecules Zn^{2+} induces large, and comparable, conformational changes of the extracellular part of the molecule, which harbours the active site, resulting in a twist of the β-barrel and disorder of the extra-cellular loops. Furthermore, the finding of a well-coordinated Zn^{2+} supports the catalytic mechanism previously proposed for OmpT.

Introduction

OmpT from *Escherichia coli* is a well-studied member of a family of highly homologous outer membrane proteases, called omptins. Omptins are implicated as virulence factors in several Gram-negative bacteria. Important members of the omptin family include PgtE from *Salmonella typhimurium* (Yu & Hong, 1986), Pla from *Yersinia pestis* (Sodeinde & Goguen, 1989), SopA from *Shigella flexneri* (Egile *et al.*, 1997) and OmpP from *Escherichia coli* (Kaufmann *et al.*, 1994). OmpT itself is implicated in complicated urinary tract disease (Webb & Lundigran, 1996), and in neonatal meningitis (Johnson *et al.*, 2002). The activity of OmpT is dependent on the presence of lipopoplysaccharide (LPS), an abundant component in the outer leaflet of the outer membrane of Gram-negative bacteria. OmpT shows specific catalytic activity towards two consecutive basic residues (Dekker *et al.*, 2001), and was classified earlier as a serine protease (Rawlings & Barrett, 2000). However, known protease inhibitors, such as diisopropylfluorophosphate (DFP) and phenylmethylsulfonyl fluoride (PMSF), fail to inhibit the catalytic activity of OmpT (Kramer *et al.*, 2002; Kramer *et al.*, 2000). Moreover, we recently solved the crystal structure of OmpT (Vandeputte-Rutten *et al.*, 2001), showing an arrangement of the catalytic site residues that is incompatible with OmpT being a serine protease. We therefore proposed a novel catalytic mechanism involving His212, Asp210, Asp83 and Asp85 and a water molecule. In many instances, a crystal structure of an enzyme with its inhibitor has provided valuable information on the catalytic mechanism used by the enzyme. It is known that the divalent metal ion Zn^{2+} inhibits the catalytic activity of OmpT in an uncompetitive manner, with an inhibition constant of 9.9 μM at pH 7.4 (Mangel *et al.*, 1994). Here we present the structure of OmpT in complex with Zn^{2+} to gain more insight into the catalytic mechanism of OmpT.

Materials and Methods

OmpT expression and purification

For crystallization purposes OmpT, without the 20-amino-acid signal sequence, containing the mutations S99A, G216K and K217G and selenomethionines was over produced in *Escherichia coli* strain BL21(DE3), refolded and purified as described previously (Kramer *et al.*, 2000; Vandeputte-Rutten *et al.*, 2001).

Crystallization and data collection

OmpT crystals were obtained as described before (Vandeputte-Rutten *et al.*, 2001), in 1% (w/v) octyl-β-D-glucopyranoside (BOG), 300 mM sodium citrate pH 5.5 and 30% (v/v) 2-methyl-2,4-pentanediol (MPD). In one drop containing a crystal, the mother liquor was gradually exchanged in five steps to 1% (w/v) BOG, 20 mM Tris-HCl pH 8.0 and 32% (v/v) MPD, in order to obtain a condition optimal for zinc binding. Subsequently, the crystal was transferred to a drop containing 2 mM of $ZnCl_2$, 1% (w/v) BOG, 20 mM Tris-HCl pH 8.0 and 32% (v/v) MPD. After one hour of soaking the crystal was harvested from the droplet using a cryo-loop and directly flash-cooled into liquid nitrogen. X-ray data were collected at the ID14-EH2 beamline at the European Synchrotron Radiation Facility (ESRF) in Grenoble at 100K, and with $\lambda = 0.93$ Å. The crystal diffracted to a resolution of 2.55 Å. The space group was $P3_221$ with lattice constants $a = b = 93.2$ Å and $c = 156.1$ Å. For a crystal soaked in 1% (w/v) BOG, 20 mM Tris-HCl pH 8.0 and 32% (v/v) MPD, without $ZnCl_2$, lattice constant were also determined. Data were processed using DENZO (Otwinowski & Minor, 1997), SCALEPACK (Otwinowski & Minor, 1997) and TRUNCATE (Collaborative Computational Project, 1994). A summary of the statistics of datacollection, processing and refinement is provided in table 4.1.

Structure determination

Attempts to scale the data, obtained for the OmpT/Zn^{2+} complex with the previously obtained native data failed. Even when the *a* and *b* axis were interchanged, the data did not scale. As a consequence the crystal structure had to be solved using molecular replacement. CNS (Brunger *et al.*, 1998) was used to perform the rotation and translation search using one OmpT molecule including residues A11 to A297 (PDB access code 1I78). The structure was subsequently built using O and refined using REFMAC (Murshudov *et al.*, 1999).

Table 4.1

Summary of data and refinement statistics

Data set statistics	
Resolution limits (outer shell) (Å)	40-2.55 (2.64-2.55)
Space group	$P3_221$
Unit cell parameters (Å,°)	$a = b = 93.15$, $c = 156.11$, $\alpha = \beta = 90$, $\gamma = 120$
Mosaicity (°)	0.12
Oscillation (°)	0.5
Total oscillation for data set (°)	60
Total no. of reflections (outer shell)	95866 (6463)
No. of unique reflections (outer shell)	26150 (2352)
Redundancy (outer shell)	3.67 (2.75)
R_{merge} (%) (outer shell)	6.6 (31.1)
Completeness (%) (outer shell)	98.3 (90.3)
$I/\sigma(I)$ (outer shell)	13.99 (3.28)
Refinement statistics	
Resolution range (Å)	40-2.55
Total no. of non-hydrogen atoms	3449
No.of water molecules	15
No.of BOG molecules	2
R_{work} (%)	23.9
R_{free} (%)	26.0
r.m.s.d. bond lengths (Å)	0.013
r.m.s.d. bond angles (º)	1.459
Average *B*-factor (all protein atoms) (Å^2)	25.5

Results and Discussion

Structure determination

To gain more insight into the structural basis of Zn^{2+} inhibition, we determined the structure of an OmpT/Zn^{2+} complex. For this purpose, an OmpT crystal was soaked in 2 mM $ZnCl_2$. Data collection and processing statistics are summarized in table 4.1. The OmpT/Zn^{2+} complex crystal diffracted to 2.55 Å resolution, which is higher than obtained for native crystals. Cell dimensions in the crystal from the OmpT/Zn^{2+} complex are $a = b = 93.2$ Å and $c = 156.1$ Å ($P3_221$), whereas in native crystals *a* and *b* are approximately 98 Å and *c* is approximately 166 Å, with no more than 1 Å deviation. This means that the cell dimensions are 5.6% shorter for *a* and *b* axis and 6.2% shorter for *c* axis compared to the native crystals. This remarkable change in cell dimensions is

not caused by the buffer, in which a OmpT crystal was soaked prior to soaking with $ZnCl_2$, because the cell dimensions of a native crystal soaked in 20 mM Tris pH 8.0, 32% MPD and 1% BOG, were not altered (data not shown).

Presumably due to changed cell dimensions, coordinates from the native OmpT structure could not directly be used in structure elucidation of the OmpT/Zn^{2+} complex. Firstly, the dataset from the OmpT/Zn^{2+} complex could not be scaled to the native dataset, in either *a*, *b*, *c* or *b*, *a*, *c* cell axis orientations. Secondly, rigid body refinement starting from the coordinates of the native structure yielded *R*-factors of over 55%. Because structure determination in this way was not successful, molecular replacement was performed. Like in the native crystals, two monomers, A and B, were present in the asymmetric unit in the OmpT/Zn^{2+} crystals. Rigid body refinement resulted in an *R*-factor of 44.0%, which dropped to 41.1% after individual *B*-factor refinement, with an R_{free} of 41.2%.

Inspection of the σ_A-weighted $2F_{obs}$-F_{calc} electron density-map revealed that much of the electron density was missing for the extracellular loops of both molecules in the asymmetric unit, whereas the membrane embedded parts of the native OmpT model fitted well in the electron-density. Figure 4.1 shows molecule A of the OmpT/Zn^{2+} complex structure with molecule A of the native structure super-positioned on top of it with a σ_A-weighted $2F_{obs}$-F_{calc} electron density-map calculated with the OmpT/Zn^{2+} model found with molecular replacement. Due to electron density missing for the extracellular loops as well as slightly altered electron density in the active site of the OmpT/Zn^{2+} complex, the map was difficult to interpret around the active site of OmpT. We therefore calculated an anomalous difference map, which revealed eight high peaks that could be assigned to the seleniums in Met61, Met81, Met131 and Met178 of both OmpT molecules. A peak expected for the selenium in Met87 was not detected, because Met87 is located in loop 2, which is disordered. Met81 has substantially shifted from its original position in the native protein. The selenium from Met81 shifted 4.2 Å in molecule A and 3.7 Å in molecule B towards the periplasmic side of the β-barrel, while the Cα shifted only 0.9 Å in molecule A and 0.5 Å in molecule B in the same direction. At the wavelength we used for data collection a selenium atom emits 3.5 electrons, and a Zn^{2+} ion 2.3 electrons. Therefore, the five lower peaks observed in the anomalous difference map, likely represent the presence of Zn^{2+} ions. By including the Zn^{2+} ions and rebuilding the OmpT/Zn2+ structure the *R*-factor dropped drastically to 27.8% and the R_{free} to 31.2%. The final structure has an *R*-factor of 23.9%, an R_{free} of 26.0% and contains two OmpT molecules, 2 BOG's, 1 citrate and 5 zinc ions. No electron density was observed for the extracellular loops (residues A30-A38, A85-A100, A147-A170, A213-A219, A258-A280, B32-B38, B87-B95, B145-B149, B158-B168, B210-B226, B259-B283), which were therefore omitted from the structure.

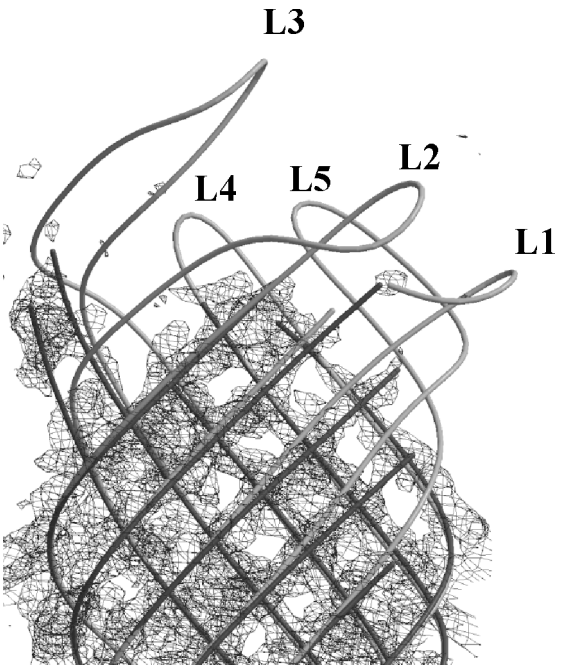

Figure 4.1 A representation of coils of the OmpT/Zn^{2+} complex structure shown in dark grey and the native structure shown in light grey. Around the molecular replacement molecule consisting of all residues from the native structure, the σ_A-weighted $2F_{obs}$-F_{calc} electron density map calculated after molecular replacement and rigid body refinement is shown. This figure was prepared using BOBSCRIPT (Esnouf, 1999).

Crystal packing

In agreement with its decreased cell dimensions, the OmpT/Zn^{2+} complex crystal has a more compact crystal packing than the native crystals. The OmpT/Zn^{2+} crystal packing and the native crystal packing can be superimposed as in Figure 4.2, in which the molecules are assigned A, B, A' and B'. A striking difference between the crystal packing of the OmpT/Zn^{2+} complex crystal and the native crystal, is the increase of the distance between the two-fold symmetry related molecules A and A'. This may be due to the bending of the extra cellular part of the structure of molecule A of the OmpT/Zn^{2+} complex with respect to the native structure. Likely the bending is directly caused by binding of Zn^{2+} in the active site. Related to the bended structure of molecule A, molecule B is moved closer to molecule A (Figure 4.2). Due to increased distance between the two-fold symmetry related molecules A and A', the four BOG molecule which are located between them (Figure 4.3A) are also shifted from their original

positions (Figure 4.3B). In the native crystal form these detergent molecules are nicely arranged in one plane, whereas in the OmpT/Zn^{2+} complex crystal the sugar parts of the two detergent molecules closest to the two-fold rotation axis are stacked on top of each other. In the native crystal only two hydrophilic interactions were made between proteins A and B, one hydrogen bond and one salt bridge, which was present between the loops of molecule A and B (area encircled in Figure 4.2). In the OmpT/Zn^{2+} complex, however, many hydrophilic contacts are made between the extracellular loops of molecule A and those of molecule B.

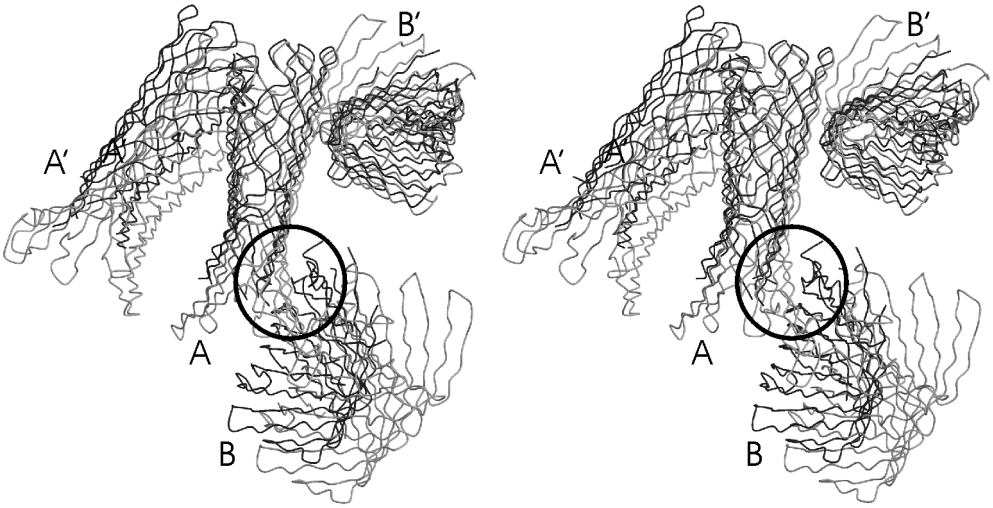

Figure 4.2 Crystal packing of the native crystal shown in light grey and the OmpT/Zn^{2+} complex crystal shown in dark grey super-positioned by a origin shift. Molecules are shown as Cα traces and assigned A, A', B, B'. The circle shows the position where hydrophilic crystal contacts are present.

Zinc binding sites

Both OmpT molecules in the asymmetric unit were found to bind two Zn^{2+} ions in the active site. Interestingly, in both molecules the Zn^{2+} binding sites are different (Figure 4.4). In molecule A, one Zn^{2+} ion is bound between Asp208 and Gln174. For the side chain of Glu27, which would be in the position to bind to the Zn^{2+} ion, no electron density was observed. The second Zn^{2+} ion is positioned between Asp83, Asp210 and His212. In molecule B, one Zn^{2+} ion is present between Glu27 and Asp208. The second

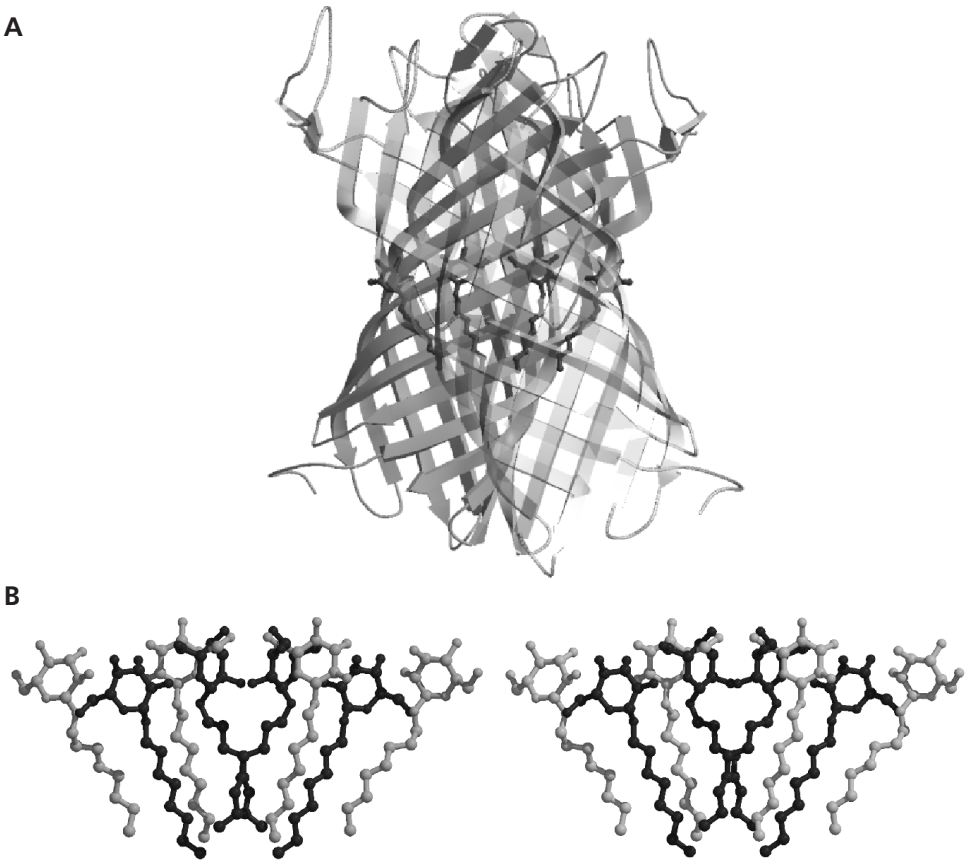

Figure 4.3 β-octyl-glucoside molecules bound between the two symmetry related OmpT molecules A and A'. A) Ribbon representation of the native OmpT molecule A (behind) with its two fold symmetry related molecule A' shown opaque (in front). In dark grey four β-octyl-glucoside molecules are shown as ball-and-stick. B) A stereo figure of a ball-and-stick representation of the four β-octyl-glucoside molecules in the native structure shown in light grey and the four β-octyl-glucoside molecules in the OmpT/Zn^{2+} complex structure shown in dark grey.

Zn^{2+} is located between Asp83 and Asp85. The different binding of Zn^{2+} in molecules A and B could be the result of different crystal contacts made by these two molecules.

A remarkable feature of Zn^{2+} with respect to most other class II divalent cations is that it can be coordinated by four, five or six ligands, whereas for example Hg^{2+} and Co^{2+} are usually coordinated by six ligands. Due to this feature, Zn^{2+} is often involved in catalysis. According to Harding et. al. (Harding, 2001) an atom can be defined as a ligand

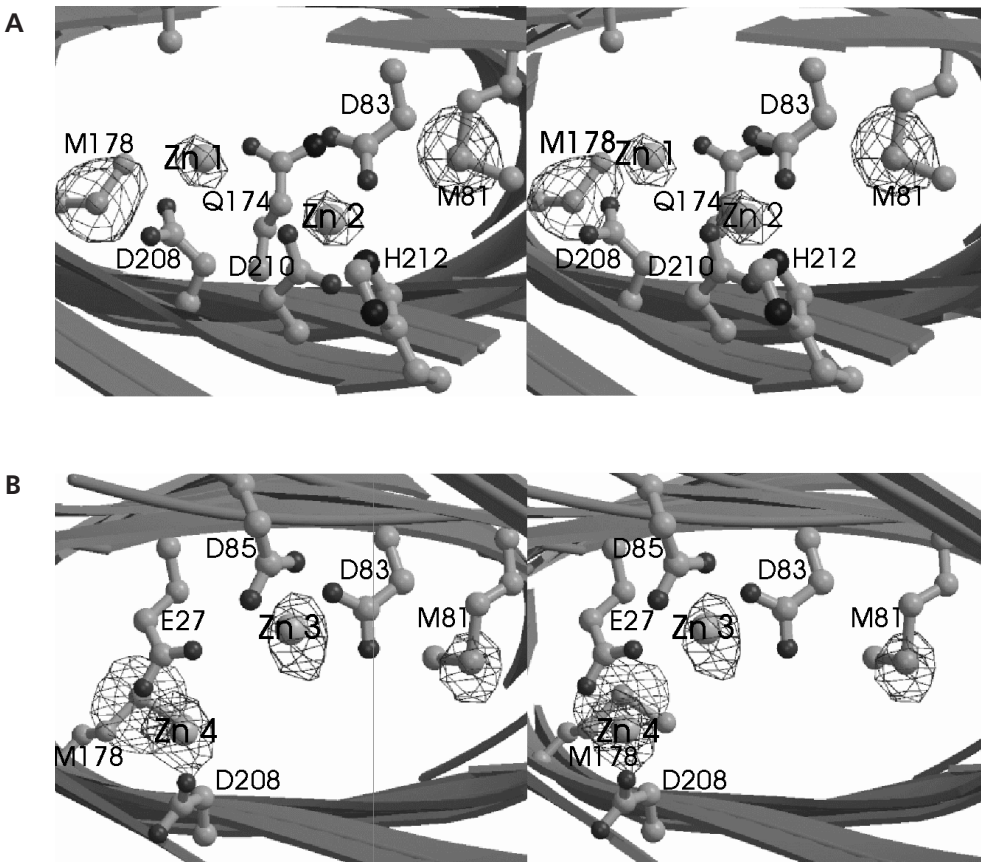

Figure 4.4 Stereo representation of the active site of the two OmpT molecules in the asymmetric unit containing the zinc ions. The anomalous map shown at 6σ, shows the positions of the seleniums and zinc ions. Methionines containing the seleniums and residues that are involved in binding Zn^{2+} are shown in ball-and-stick and labelled with one letter codes. The β-barrel is shown as ribbons. The view is from the top (extracellular side) of the OmpT molecule. A) molecule A and B) molecule B in the asymmetric unit.

when its distance from the metal atom is within target distance + 0.75 Å. Target chelating distances to Zn^{2+} are 2.00 Å for N of His, 2.04 Å for monodentate Asp or Glu, 2.09 Å for O of H_2O and 2.15 Å for bidentate Asp or Glu. In table 4.2 chelating distances between the Zn^{2+} ions and the ligands in OmpT are given. According to this table, the H_2O molecules that we inferred from the electron density map, are too distant from the Zn^{2+} ions to participate in coordination. However, due to the poor electron density in

this area, we cannot exclude that additional H_2O molecules are present close to the Zn^{2+} ions. In addition, the moderate resolution of 2.55 Å of the OmpT/Zn^{2+} complex crystal structure, does not allow the accurate determination of chelating distances for the ligands as listed in table 4.2. In the Protein Data Bank many structures are deposited which contain Zn^{2+} ions. In most cases Zn^{2+} is coordinated by one or more histidines. Some proteins, of which thermolysin is a well-known example, require Zn^{2+} for catalysis. In thermolysin, a Zn^{2+} is coordinated by two histidines, one glutamic acid (in a bidentate manner) and a H_2O molecule. This kind of coordination represents one of the most common coordination types for Zn^{2+}. In the crystal structure of the OmpT/Zn^{2+} complex three of the four zinc ions only have an aspartic, a glutamic, or a glutamine residue as a ligand, whereas only one Zn^{2+} coordination involves a histidine as well.

Table 4.2

Zn^{2+} ligands

		Ligand			
Zn^{2+}	OmpT Molecule	No.	Type	Atom	Distance (Å)
Zn^{2+} 1	A	174	Asn	Oδ1	2.25
	A	208	Asp	Oδ2	2.81
Zn^{2+} 2	A	83	Asp	Oδ2	1.94
	A	210	Asp	Oδ2	2.29
	A	210	Asp	Oδ1	2.53
	A	212	His	Nε2	2.32
			H_2O	O	3.24
Zn^{2+} 3	B	83	Asp	Oδ1	2.13
	B	83	Asp	Oδ2	2.97
	B	85	Asp	Oδ1	2.44
	B	85	Asp	Oδ2	2.88
			H_2O	O	3.00
Zn^{2+} 4	B	27	Glu	Oε1	2.05
	B	27	Glu	Oε2	2.72
	B	208	Asp	Oδ1	1.91
			H_2O	O	3.09

It may not seem surprising that Zn^{2+} binds in the active site of OmpT and inhibits its activity, because the active site of OmpT contains acidic residues and therefore has affinity for positively charged ligands. However, if binding of Zn^{2+} in the substrate binding pockets on itself is sufficient to cause an inhibitory effect, the inhibition should be competitive, whereas Mangel *et al*. previously demonstrated that Zn^{2+} inhibits OmpT

non-competitively (Mangel *et al.*, 1994). This implies that the Zn^{2+} binds strongly to the catalytic residues, instead of to the substrate binding residues. In the OmpT/Zn^{2+} complex we observe indeed one Zn^{2+} ion in both monomers in the asymmetric unit (Zn^{2+} 2 and Zn^{2+} 3 in Figure 4.2) liganded to a few of the proposed catalytic residues i.e. Asp210, His212, Asp83 and Asp85 (Kramer *et al.*, 2001; Vandeputte-Rutten *et al.*, 2001). Zn^{2+} 2 is liganded to Asp83, Asp210 and His212, whereas Zn^{2+} 3 is liganded to Asp83 and Asp85. Taking in account that the inhibition is non-competitive and that Asp210, His212, Asp83 and Asp85 are the most likely catalytic site residues we can assume that the Zn^{2+} 2 or the Zn^{2+} 3 coordination causes the large inhibitory effect of Zn^{2+}. Furthermore, it is tempting to speculate that Zn^{2+} 2 has the highest affinity to OmpT of all four Zn^{2+} ions present in the active site, because it has a histidine as a ligand and the highest coordination number, which is five, consisting of the monodentate carboxylate of Asp83, the bidentate carboxylate of Asp210, the Nε2 nitrogen of histine (His212), and a water molecule. The observation that Zn^{2+} 2 and Zn^{2+} 3 both have Asp83 as a ligand, strongly suggests that Asp83 is indeed a catalytic residue as was proposed earlier (Kramer *et al.*, 2001; Vandeputte-Rutten *et al.*, 2001).

Structural changes induced by zinc binding

In the native crystals of OmpT, the two monomers in the asymmetric unit have a root-mean-square deviation (r.m.s.d.) of only 0.5 Å, and even the loops superimpose without large deviations (Figure 4.5A), indicating that the structure of OmpT is well ordered in a certain conformation in the absence of a substrate or lipopolysaccharide (LPS) (Vandeputte-Rutten *et al.*, 2001). The OmpT/Zn^{2+} complex crystal structure clearly shows that the apparent rigid structure becomes disordered, upon Zn^{2+} binding.

Although the Zn^{2+} binding sites in both molecules in the asymmetric unit of the OmpT/Zn^{2+} complex differ from one another, the structural changes caused by Zn^{2+} binding show similarities (Figures 4.5B and 4.5C). The β-barrel regions, starting from residues Phe176 and Tyr185 towards the periplasmic side of the barrel do not change much with respect to the native structure. The r.m.s.d. between all built Cα atoms of molecule A of the OmpT/Zn^{2+} complex and the corresponding Cα atoms in the native structure was 1.1 Å. In the case of molecule B the r.m.s.d. was 1.8 Å. The extracellular parts of the barrels are skewed with respect to the native structure and the active sites have become narrower. In molecule A, the Cα atoms of the proposed catalytic residues Asp83 and His212 have become 2.3 Å closer to one another in the OmpT/Zn^{2+} complex structure with respect to the native structure. The distance between the Oδ1 of Asp83 and the Nε2 of His212 shifted from 5.2 Å to 3.4 Å. In molecule B, for residue His212 no electron density was observed. Electron density was also absent for the proposed catalytic residue Asp210, whereas Asp208 was visible. Therefore, to determine the

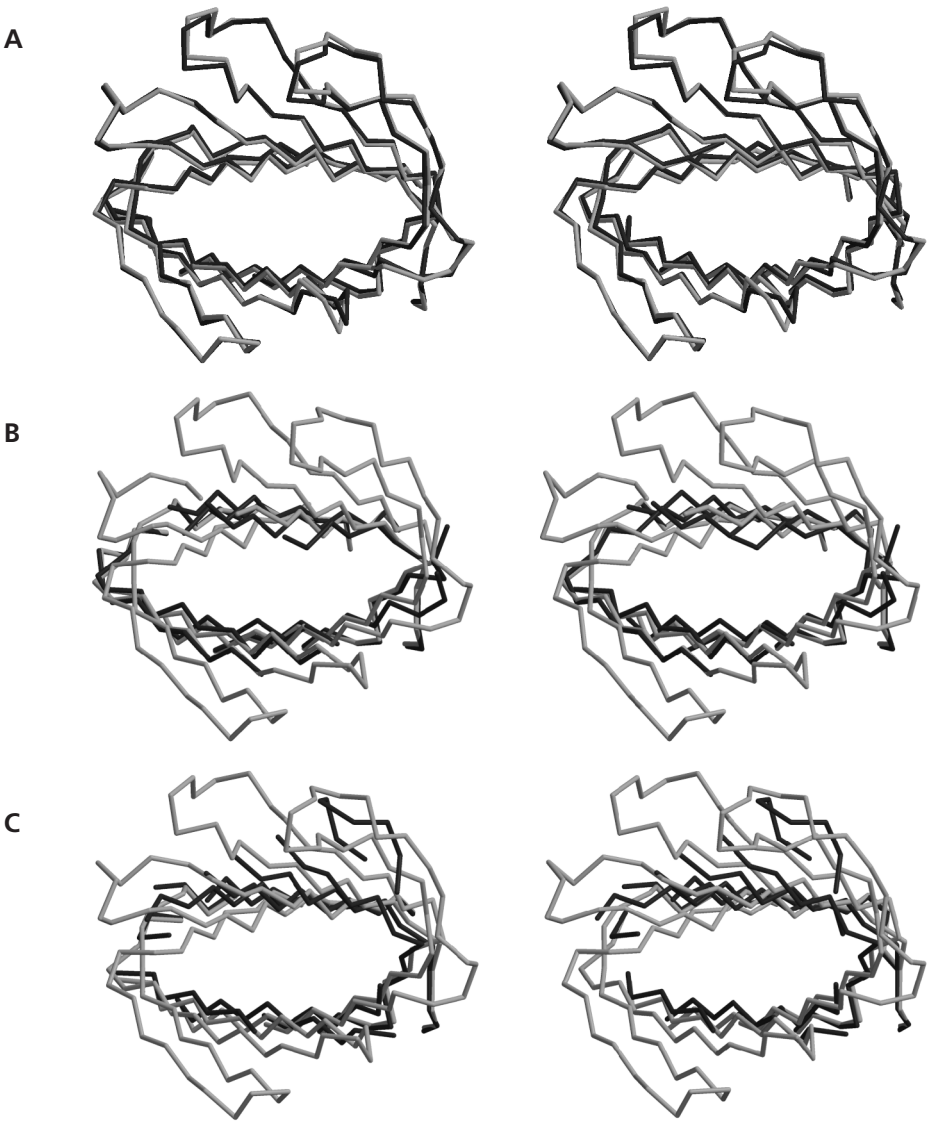

Figure 4.5 Stereo representations of super-positioned Cα traces of OmpT viewed from the extracellular side. A) Structure of the native molecule A, shown in light grey, and molecule B, shown in dark grey, overlaid. B) Molecule A of the native structure, shown in light grey, super positioned on top of molecule A in the OmpT/Zn^{2+} structure. C) Molecule B of the native structure, shown in light grey, super positioned on top of molecule B in the OmpT/Zn^{2+} structure.

difference of the width of the active site in molecule B, we measured the distance between the Cα atoms of Asp83 and Asp208. In molecule B this distance was 14.2 Å in the OmpT/Zn^{2+} complex and 16.3 Å in the native structure. For molecule A these distances were 12.4 Å versus 15.9 Å. Besides the observation that the active site becomes narrower, some changes in side-chain orientations in the proposed P2' binding pocket occurred. For both Trp44 and the earlier described Se-Met81 the side chain is oriented downwards with respect to the native structure. These observations imply that OmpT has a certain degree of flexibility.

In summary, the structure of Zn^{2+}-inhibited OmpT reveals large conformational changes and a high degree of disorder, when compared to the native structure of OmpT. Flexibility in the extracellular part of the β-barrel structure, which forms the active site, likely plays a role in substrate binding and possibly enzyme catalysis. Possibly, LPS binding affects this flexibility, but the mechanism of activation of OmpT by LPS remains unclear.

Acknowledgements

We wish to thank the staff at the European Synchrotron Radiation Facility (ESRF) in Grenoble for assistance with data collection at beamline ID14-EH2. This research has been supported financially by the council for Chemical Sciences of the Netherlands Organization for Scientific Research (NWO-CW).

References

Brunger, A.T., Adams, P.D., Clore, G.M., Delano, W.L., Gros, P., Grosse-Kunstleve, R.W., Jiang, J.S., Kuszewski, J., Nilges, M., Pannu, N.S., Read, R.J., Rice, L.M., Simonson, T. & Warren, G.L. (1998). Crystallography & NMR system: A new software suite for macromolecular structure determination. *Acta Crystallogr D Biol Crystallogr,* ***54*** *(Pt 5):* 905-921.

Collaborative Computational Project, N. (1994). The CCP4 Suite: Programs for Protein Crystallography. *Acta Crystallogr D Biol Crystallogr,* ***50*** 760-763.

Dekker, N., Cox, R.C., Kramer, R.A. & Egmond, M.R. (2001). Substrate specificity of the integral membrane protease OmpT determined by spatially addressed peptide libraries. *Biochemistry,* ***40*** 1694-1701.

Egile, C., D'hauteville, H., Parsot, C. & Sansonetti, P.J. (1997). SopA, the outer membrane protease responsible for polar localization of IcsA in *Shigella flexneri*. *Mol Microbiol,* ***23*** *(5):* 1063-1073.

Esnouf, R.M. (1999). Further additions to MolScript version 1.4, including reading and contouring of electron-density maps. *Acta Crystallogr D Biol Crystallogr,* ***55*** *(Pt 4):* 938-940.

Harding, M.M. (2001). Geometry of metal-ligand interactions in proteins. *Acta Crystallogr D Biol Crystallogr,* ***57*** *(Pt 3):* 401-411.

Johnson, J.R., Oswald, E., O'bryan, T.T., Kuskowski, M.A. & Spanjaard, L. (2002). Phylogenetic distribution of virulence-associated genes among *Escherichia coli* isolates associated with neonatal bacterial meningitis in the Netherlands. *J Infect Dis,* ***185*** *(6):* 774-784.

Kaufmann, A., Stierhof, Y.D. & Henning, U. (1994). New outer membrane-associated protease of *Escherichia coli* K-12. *J Bacteriol,* ***176*** *(2):* 359-367.

Kramer, R.A., Brandenburg, K., Vandeputte-Rutten, L., Werkhoven, M., Gros, P., Dekker, N. & Egmond, M.R. (2002). Lipopolysaccharide regions involved in the activation of *Escherichia coli* outer membrane protease OmpT. *Eur J Biochem,* ***269*** *(6):* 1746-1752.

Kramer, R.A., Vandeputte-Rutten, L., De Roon, G.J., Gros, P., Dekker, N. & Egmond, M.R. (2001). Identification of essential acidic residues of outer membrane protease OmpT supports a novel active site. *FEBS Lett,* ***505*** *(3):* 426-430.

Kramer, R.A., Zandwijken, D., Egmond, M.R. & Dekker, N. (2000). In vitro folding, purification and characterization of *Escherichia coli* outer membrane protease ompT. *Eur J Biochem,* ***267*** *(3):* 885-893.

Mangel, W.F., Toledo, D.L., Brown, M.T., Worzalla, K., Lee, M. & Dunn, J.J. (1994). Omptin: an *Escherichia coli* outer membrane proteinase that activates plasminogen. *Methods Enzymol,* ***244*** 384-399.

Murshudov, G.N., Vagin, A.A., Lebedev, A., Wilson, K.S. & Dodson, E.J. (1999). Efficient anisotropic refinement of macromolecular structures using FFT. *Acta Crystallogr D Biol Crystallogr,* ***55*** *(Pt 1):* 247-255.

Otwinowski, Z. & Minor, W. (1997). Processing of X-ray diffraction data collected in oscillation mode. *Methods Enzymol,* ***276*** 307-326.

Rawlings, N.D. & Barrett, A.J. (2000). MEROPS: the peptidase database. *Nucleic Acids Res,* ***28*** *(1):* 323-325.

Sodeinde, O.A. & Goguen, J.D. (1989). Nucleotide sequence of the plasminogen activator gene of *Yersinia pestis*: relationship to *ompT* of *Escherichia coli* and gene E of *Salmonella typhimurium*. *Infect Immun,* ***57*** *(5):* 1517-1523.

Vandeputte-Rutten, L., Kramer, R.A., Kroon, J., Dekker, N., Egmond, M.R. & Gros, P. (2001). Crystal structure of the outer membrane protease OmpT from *Escherichia coli* suggests a novel catalytic site. *Embo J,* ***20*** *(18):* 5033-5039.

Webb, R.M. & Lundigran, M.D. (1996). OmpT in *Escherichia coli* correlates with severity of disease in urinary tract infections. *Med. Microbiol. Letters,* ***5*** 8-14.

Yu, G.Q. & Hong, J.S. (1986). Identification and nucleotide sequence of the activator gene of the externally induced phosphoglycerate transport system of *Salmonella typhimurium*. *Gene,* ***45*** *(1):* 51-57.

5

Crystal Structure of Neisserial Surface Protein A (NspA), a Conserved Outer Membrane Protein with Vaccine Potential

Lucy Vandeputte-Rutten, Martine P. Bos, Jan Tommassen, and Piet Gros

J. Biol. Chem. (2003), **278**(27),24825-24830

Abstract

The neisserial surface protein A (NspA) from *Neisseria meningitidis* is a promising vaccine candidate because it is highly conserved among meningococcal strains and induces bactericidal antibodies. NspA is a homologue of the Opa proteins, which mediate adhesion to host cells. Here, we present the crystal structure of NspA, determined to 2.55-Å resolution. NspA forms an eight-stranded antiparallel β-barrel. The four loops at the extracellular side of the NspA molecule form a long cleft, which contains mainly hydrophobic residues and harbours a detergent molecule, suggesting that the protein might function in the binding of hydrophobic ligands, such as lipids. In addition, the structure provides a starting point for structure-based vaccine design. The atomic coordinates and structure factors have been deposited in the Protein Data Bank (accession No. 1P4T)

Introduction

The Gram-negative bacterium *Neisseria meningitidis* causes life-threatening meningitis and septicaemia in humans. Based on the immunological characteristics of the capsular polysaccharides, *N. meningitidis* strains are divided in 12 serogroups. Strains of serogroups A, B and C are the predominant cause of meningococcal disease (Frasch, 1989). Effective vaccines, which consist of capsular polysaccharide conjugated to tetanus toxoid protein to generate sufficient immunological memory, are now available against serogroups A and C (Anderson *et al.*, 1994; Costantino *et al.*, 1992). Unfortunately however, the capsular polysaccharide of serogroup B is poorly immunogenic, making this type of vaccine ineffective (Mandrell & Zollinger, 1982; Zollinger & Mandrell, 1983). Therefore, attention has shifted towards the possibility of using outer membrane proteins (OMPs) as targets for vaccine development (Poolman & Berthet, 2001). OMPs perform a variety of functions including the following: (*a*) they may form channels in the outer membrane for uptake of nutrients or the secretion of proteins; (*b*) they may be enzymes involved in, for example, the modification of lipopolysaccharides or in proteolysis; or (*c*) they may function as adhesins mediating the interaction of the bacterium to host cells. Despite these different functions, they appear to share a common fold, i.e. they form transmembrane β-barrels consisting of antiparallel amphipathic β-strands. The number of β-strands in the OMPs, of which the structure has been solved, varies and ranges from 8 to 22 (Schulz, 2002). The best-studied OMPs for vaccine development against *N. meningitidis* are the porins PorA and PorB and the adhesin OpcA, which elicit bactericidal and protective antibody responses (Saukkonen *et al.*, 1987). However, due to the antigenic heterogeneity of these proteins (Rosenqvist *et al.*, 1993a) or phase-variable expression of their genes (Rosenqvist *et al.*, 1993b), they are unable to provide protection against all or

most of the serogroup B strains. Recently, the 18-kDa OMP NspA (Neisserial surface protein A) has been identified (Martin *et al.*, 1997), which is remarkably conserved among *N. meningitidis* and *Neisseria gonorrhoeae* isolates (Cadieux *et al.*, 1999; Martin *et al.*, 1997; Moe *et al.*, 1999; Moe *et al.*, 2001; Plante *et al.*, 1999). The function of NspA is unknown, but it shows considerable sequence similarity with members of the Opa family of OMPs (Martin *et al.*, 1997), which are important adhesins involved in the entry of neisseriae into epithelial cells by interacting, for example, with the human carcinoembryonic antigen cell adhesion molecule (CEACAM) receptors (Chen & Gotschlich, 1996; Virji *et al.*, 1996). Several studies have shown that NspA can elicit antibodies that are protective and bactericidal against a wide range of *N. meningitidis* serogroup B strains, making NspA an attractive vaccine candidate (Cadieux *et al.*, 1999; Martin *et al.*, 1997; Moe *et al.*, 1999; Moe *et al.*, 2001; Plante *et al.*, 1999). Recently, Moe *et al.* (Moe *et al.*, 2002) showed that sequential immunization using vesicles derived from different meningococcal strains, thus containing different PorA, PorB and lipopolysaccharide types, resulted in a protective antibody response against NspA, underscoring the importance of NspA as a possible vaccine candidate.

To date the crystal structure of only one OMP of *N. meningitidis* has been solved, i.e. that of OpcA (Prince *et al.*, 2002), which forms a closed 10-stranded β-barrel. Structural studies can not only provide insight into the function of OMPs, but they can also reveal the conformation of epitopes that are recognized by bactericidal antibodies, thus being helpful for the design of vaccines. Here, we describe the crystal structure of NspA, at 2.55-Å resolution, which shows an eight-stranded antiparallel β-barrel structure with a hydrophobic groove at the extracellular side harbouring a detergent molecule.

Materials and Methods

Cloning of the nspA gene and expression of the recombinant protein

Genomic DNA of *N. meningitidis* strain H44/76 was prepared using the Qiagen genomic preparation kit. The part of the *nspA* gene encoding the mature domain of the protein, i.e. without the 19-amino-acid signal peptide, was PCR-amplified with the primer pair 5'-gctacatatggaaggcgcatccggcttttacg-3' and 5'-gctaggatcctcagaatttgacgcgcacaccgg-3'. The PCR product was cloned into pCRII-TOPO (Invitrogen), digested with *Nde*I and *Bam*HI, and ligated into pET11a (Novagen), yielding pET11a-NspA. Five-liter cultures of *Escherichia coli* strain BL21(DE3) (Novagen), containing pET11a-NspA, were grown at 37 °C in L-broth (Tommassen *et al.*, 1983) containing 100 μg/ml ampicillin. At an optical density at 600 nm of 0.6, 0.1 mM of isopropyl-thio-β-D-galactopyranoside was added to induce expression of the recombinant gene. After another 4 h of incubation

at 37°C, cells were harvested and washed with 600 ml of 0.9% (w/v) NaCl. NspA was present in inclusion bodies, which were isolated according to Dekker *et al.* (Dekker *et al.*, 1995) and solubilized in 8 M urea containing 10 mM glycine, pH 8.0. Residual insoluble material and membranes were removed by ultracentrifugation (100,000 g for 1 h).

Refolding and purification of NspA

Urea-solubilized NspA protein was folded *in vitro* by 5-fold dilution into 20 mM ethanolamine, pH 11, containing 1% (w/v) 3-dimethyldodecylammoniopropane-sulfonate (DodMe2NprSO3, Fluka) and left overnight at room temperature while stirring. Refolding was evaluated by SDS-PAGE on gels containing 14% acrylamide under "semi-native" conditions, *i.e.* with no SDS in the gel and only 0.03% instead of 3% SDS in the 3-fold sample-buffer (additionally containing 0.1 M Tris-HCl, pH 6.8, 15.4% (v/v) glycerol, 7.7% (v/v) β-mercaptoethanol, and 0.008% (w/v) bromophenol blue) and without heating before electrophoresis. For denaturation, the sample was boiled for 5 minutes with 1% (w/v) SDS. The gels were stained with Coomassie Brilliant Blue for visualization of the protein bands. To purify the folded NspA, the mixture was loaded onto a 1-ml mono S column (Amersham Biosciences), pre-equilibrated with 10 mM DodMe2NprSO3, 20 mM Tris-HCl, pH 8.5 (buffer A). Prior to loading, the pH of the protein sample was adjusted to pH 8.5 using 1 M HCl. The column was washed with buffer A, and proteins were eluted with a linear gradient of 0-500 mM NaCl in buffer A, total volume 50 ml. Fractions containing folded NspA were pooled, diluted 10-fold in buffer A, and again loaded on a mono S column. The column was washed with buffer B (20 mM Tris-HCl, pH 7.5, 0.06% (v/v) n-decylpentaoxyethylene ($C_{10}E_5$; Bachem P-1005)). The protein was eluted with 500 mM NaCl in buffer B and concentrated to 6 mg/ml using Centricon concentrators with molecular mass cutoff of 10 kDa (Amicon). The protein was dialyzed three times against 10 ml of 0.06% $C_{10}E_5$ prior to crystallization.

Chemical cross-linking

A 200-µl sample of NspA was incubated at 0.2 mg/ml in 20 mM buffer (either sodium acetate pH 4.5 or Tris-HCl pH 8.5) containing 1% (v/v) *n*-octyl-poly-oxyethylene (O-POE, Alexis), and 5 µl of a 1% stock solution of glutaraldehyde in 1% (v/v) O-POE was added. The cross-linking reaction was allowed to proceed for 4 h at room temperature. Subsequently, 100 µl of SDS-PAGE sample buffer was added, and 20 µl of this solution was analyzed by SDS-PAGE.

Analytical ultracentrifugation

Protein molecular weights were determined by sedimentation equilibrium

centrifugation experiments, using a Beckman Optima XL-A analytical Ultracentrifuge with absorbance monitoring. Cells contained double-sector charcoal-filled epon centerpieces and had column lengths of ~8 mm and depths of 3 mm. A protein sample of 50 μl was used. The sedimentation equilibrium experiments were run at 18,000 rpm at 20 °C using a loading concentration of ~1.0 mg/ml corresponding to a measured absorption at 280 nm (A_{280}) of ~0.3 in the cell. Optima XL-A data analysis software running under the program Microcal Origin version 3.78 (MicroCal Software, Inc.) was used to calculate the molecular weight. Data were fitted to single component and monomer/dimer models. A density of 1 g/cm^3 was assumed for the solvent plus detergent, which was 1% (v/v) O-POE and 20 mM Tris-HCl pH 8.5.

Crystallization of NspA and data collection

NspA at a concentration of 6 mg/ml in 0.06% (w/v) $C_{10}E_5$ was crystallized at 4 °C by the hanging drop vapour diffusion method against a reservoir solution of 12% (w/v) polyethylene glycol 3000, 0.1 M lithium sulfate, 0.1 M N-(2-acetamido)iminodiacetic acid (Fluka), pH 6.6, and 2% (v/v) isopropanol. The crystallization drops contained equal volumes (0.5 μl) of reservoir solution and purified NspA. Crystals were hexagonal and grew to a size of up to 0.5x0.5x0.1 mm^3 in a few days. Crystals were soaked in a cryo solution containing the reservoir solution, 0.06% (w/v) $C_{10}E_5$, and 20% (v/v) glycerol and directly cooled in liquid nitrogen. X-ray data were collected at 100 K on a charge-coupled device (CCD) detector at the ID14 EH1 beamline at the European Synchrotron Radiation Facility (ESRF). Native data were collected to 2.55 Å resolution using a wavelength of 0.933 Å and an oscillation range of 1°. The space group of the crystal was R32 (for the native data set, $a = b = 97.37$ Å, $c = 171.94$ Å in the trigonal setting). Due to the position of the crystal in the loop, which caused the long 3-fold axis to be perpendicular to the plane of the loop, we measured over 125° to obtain a complete data set. This resulted in a high redundancy of ~9. Derivative data were collected at 100 K on the EMBL beamline X11 at DESY (Hamburg). The wavelength was 0.811 Å. Crystals contained one monomer in the asymmetric unit and had a V_m of 4.74 Å^3/Da, corresponding to a solvent plus detergent content of 74% (v/v). All diffraction data were processed using DENZO (Otwinowski & Minor, 1997), SCALEPACK (Otwinowski & Minor, 1997) and TRUNCATE (Collaborative Computational Project, 1994).

Heavy atom derivatives and phasing

The structure was finally solved using the single-wavelength anomalous dispersion phasing method. Initially, molecular replacement was tried because NspA shares sequence similarity with OmpA and, to a lesser extent, with OmpX. The core β-barrel of OmpA (Protein Data Bank code 1qjp) was used for molecular replacement. Most residues were

Table 1. Summary of data and refinement statistics

Native	**$KAu(CN)_2$**	
Data set statistics		
Resolution limits (outer shell) (Å)	40-2.55 (2.64-2.55)	40-3.95 (4.09-3.95)
Space group	R32	R32
Unit cell parameters (Å,°)	a=97.37, b=97.37, c=171.94, α=90, β=90, γ=120	a=97.83, b=97.83, c=171.87 α=90, β=90, γ=120
Mosaicity (°)	0.32	0.49
Oscillation range (°) / Total oscillation (°)	1 / 125	1 / 370
Total no. of reflections (outer shell)	125566 (8944)	98783 (3304)
No. of unique reflections (outer shell)[1]	10350 (1029)	5388 (549)
R_{merge} (%) (outer shell)[2]	7.0 (37.5)	5.0 (12.2)
Completeness (%) (outer shell)	98.6 (99.7)	99.9 (100)
I/σ (I) (outer shell)	19.0 (5.2)	23.5 (16.7)
Refinement statistics		
Resolution range (Å)	30-2.55	
Total no. of non-hydrogen atoms	1278	
Rwork (%)	22.2	
Rfree (%)	25.8	
r.m.s.d. bond lengths (Å)	0.016	
r.m.s.d. bond angles (°)	1.77	

[1] For the $KAu(CN)_2$ dataset the Friedel mates have been counted separately.

[2] $R_{merge} = \Sigma(|I-<I>|)/\Sigma(I)$

replaced by alanines. The structure could not be refined properly, and therefore, a heavy atom derivative was prepared. A crystal was soaked for 1 h in 2 μl of reservoir solution containing 0.06% $C_{10}E_5$ and 10 mM of the heavy atom compound. Anomalous signals were calculated using SCALEPACK. The $KAu(CN)_2$ data set showed the highest anomalous signal with a total χ^2 of 4.5 (10 in the lowest resolution shell and 1.5 in the highest resolution shell). For convenience and due to the presence of ice rings, the data were processed to only 3.95 Å resolution. Shake and Bake (DREAR/SnB package) (Weeks & Miller, 1999) was used to find the gold atom positions. Two sites were found; one $Au(CN)_2^-$ was close (~3 Å) to Phe27, which is located close to the trimer axis. The distances between three gold peaks was ~6.8Å. The second peak was found close to the backbone of Ser144. Phases were subsequently calculated using MLPHARE (Collaborative Computational Project, 1994) to 4.0 Å resolution. This yielded an R-cullis of 0.79. With density modification in CNS (Brunger *et al.*, 1998), phases were extended to 2.55 Å resolution using the native dataset. Model building was performed using the program O (Jones *et al.*, 1991), and the structure was refined using simulated annealing and individual *B*-factor refinement using REFMAC5 (Murshudov *et al.*, 1999).

Results

Refolding and quaternary structure of NspA

NspA was overproduced without its signal sequence in *E. coli*, which resulted in the formation of NspA protein aggregates (inclusion bodies). After solubilization of these inclusion bodies, NspA was refolded in a buffer containing the detergent DodMe2NprSO3. Folding was monitored by semi-native SDS-PAGE. OMPs are generally heat-modifiable, *i.e.* folded monomers run faster in SDS-PAGE gels than heat-denatured proteins. In contrast, we observed that NspA migrated slower in the gel after refolding. The denatured protein migrated at a mass of ~18 kDa, whereas the folded protein migrated at 22 kDa, which agrees well with the electrophoretic mobility of native NspA isolated from neisserial membranes (Moe *et al.*, 1999). To investigate whether the reduced electrophoretic mobility of folded NspA is due to dimerization, we performed analytical ultracentrifugation experiments as well as chemical cross-linking. Both methods (data not shown) as well as the crystal structure (see below) strongly indicated that NspA is a monomer in a detergent-containing solution.

Structure solution

The NspA structure was solved with the single-wavelength anomalous dispersion phasing method using $KAu(CN)_2$. The refined model contained one monomer (155

amino acids), five partial $C_{10}E_5$ molecules, one sulfate ion, one ethanolamine, and nine water molecules in the asymmetric unit and had a crystallographic R-factor of 22.2% and an R_{free} of 25.8% for data in the 30-2.55 Å resolution range. For the side chains Glu1, Lys53 and Lys79, no electron density was observed and therefore these were omitted from the Protein Databank Bank file. The Ramachandran plot shows 92.4% of the φ/ϕ combinations in the most favoured regions, 6.1% in the additionally allowed regions and 0.8% (residue Asn38 and Thr138, which are present in T1 and L4, respectively) in the disallowed regions. The overall temperature factor is 40 $Å^2$. Table 1 summarizes the statistics of the crystallographic data and refinement. The crystal packing consisted of crystallographic trimers, which were packed in alternating directions, in such a way that the upper part of the molecule that faced up made contacts with the upper part of a symmetry-related molecule that faced down.

Overall structure

NspA (Figure 5.1A) consists of an eight-stranded antiparallel β-barrel with a height of ~50 Å and a main chain diameter of ~20 Å. It has a shear number of 10 with β-strands

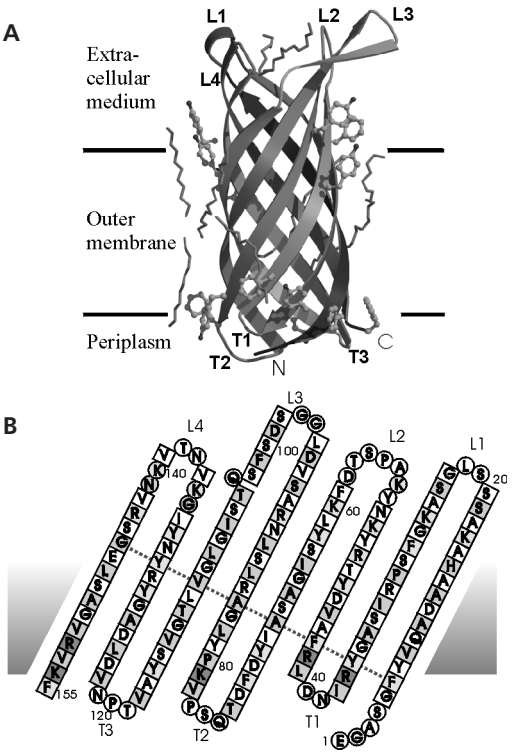

Figure 5.1 **Overall structure of NspA.** A, a ribbon representation of NspA. Aromatic residues located at the membrane boundaries are drawn by *ball-and-stick* model. Parts of the $C_{10}E_5$ molecules for which electron density was observed are shown in light *grey bonds*. Membrane boundaries are indicated by the *black lines*. B, topology plot of NspA. Amino acids are shown in one-letter code. Residues present in β-strands are shown as *squares*. Other residues are presented as *circles*. Side chains of residues that are shaded *light grey* point to the outside of the barrel. Extracellular loops are labelled *L1* to *L4* and the periplasmic turns *T1* to *T3*. The *dashed line* indicates the hydrogen-bonding register within the β-barrel. Panel A from this figure and figure 2C and figure 3 were prepared using Bobscript (Esnouf, 1999) and Raster3D (Merrit & Murphy, 1994).

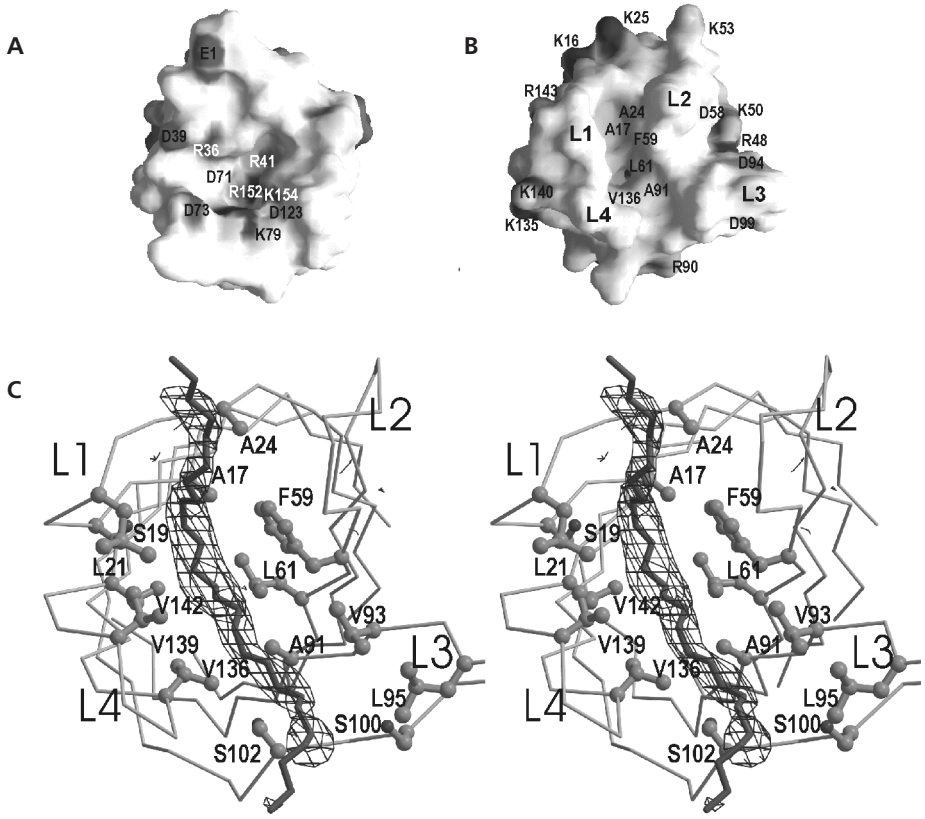

Figure 5.2 **NspA viewed from the periplasmic side and the extracellular side.** A, bottom view (periplasmic side) and B, top view (extracellular side), showing the molecular surface. A, the centre is positively charge and B, the centre contains a hydrophibic groove. Loops are indicated with *L1* to *L4*. Some residue positions are indicated by one-letter code. C, stereo representation of the NspA β-barrel as Cα-trace, in *light grey*, viewed from the top. Residues that are within a distance of 4.5 Å to the detergent molecule in the crystal structure are shown in *ball-and-stick* model and are labelled by one-letter code. A complete $C_{10}E_5$ detergent molecule is shown in *dark grey*, and the electron density observed in the $2F_o - F_c$ map is shown as *chicken wire* around the detergent molecule. Figures 2A and 2B were prepared using GRASP (Nicholls *et al.*, 1991).

having an angle of ~40° with respect to the barrel axis. In general, OMPs contain short turns at the periplasmic side of the protein and longer loops at the extracellular side with the N and C termini located at the periplasmic side (see, for example, Refs. (Koronakis *et al.*, 2001; Prince *et al.*, 2002; Vandeputte-Rutten *et al.*, 2001)). The four long loops of NspA are therefore likely to be located at the extracellular side of the membrane. Like other OMPs, NspA contains two rings of aromatic residues (Figure 5.1A) that flank both

sides of the membrane and may stabilize the position of the barrel in the membrane (Schulz, 2000). The lower ring contains 7 aromatic residues, whereas the upper ring is less well defined. Located on top of the upper aromatic ring is a rim of mainly basic residues that contains 7 lysines and 3 arginines (Figure 5.1B), a feature also found in other OMPs (Zeth *et al.*, 2000). Four detergent ($C_{10}E_5$) molecules are present at the sides of the barrel (Figure 5.1A). Two of them are present at the interfaces of the crystallographic trimer, which indicates that NspA is probably not a trimer in solution. The inside of the β-barrel harbours an extensive hydrogen-bonding network as well as cavities, but there is no pore through which ions or other molecules could be transported. The periplasmic side of NspA is mainly basic in the centre with 5 positively charged residues residing in the middle and some aspartates further away from the β-barrel axis (Figure 5.2A). The four extracellular loops of NspA form a long groove at the top of the molecule, which is highly hydrophobic (Figure 5.2B). Interestingly, we observed additional electron density at the location of this hydrophobic groove, in the $2F_o$ - F_c and F_o - F_c omit-electron density maps of NspA, which probably corresponds to part of a $C_{10}E_5$ detergent molecule (Figure 5.2C).

Loop structures

NspA contains four long extracellular loops, which are well conserved among the different neisserial strains. The loops have relatively low temperature factors, allowing for accurate determination of their conformations. Loops 2 and 4 show some uncommon features compared to the more standard β-hairpin loops seen in β-sheet structures. In the case of loop 2, this could be the result of crystal contacts with the same loop from five other symmetry-related NspA molecules (Figure 5.3A). However, the presence of a conformation-restraining proline in the middle of the extremity of the loop might indicate that loop 2 indeed has an uncommon conformation in the native NspA structure. In loop 4, adjacent residues, Gly134 and Lys135 in strand 7 and Lys140 and Asn141 in strand 8, are directed outwards from the barrel. Loops 1 and 3 both adopt a 2:4 tight β-hairpin conformation. Loop 3 (Figure 5.3A) contains 2 glycine residues, which have a large degree of freedom for backbone angles, at its extremity. The conformation of the loop seems to be stabilized by a hydrogen bond between a side chain oxygen of Asp94 and the backbone nitrogen of Gly97. Due to the presence of two well exposed aspartates, Asp94 and Asp99, the loop is negatively charged. This is in contrast with the overall positive charge of NspA, which has a theoretical isoelectric point of 9.64.

Homology of NspA to other outer membrane proteins

Three other OMP structures that contain eight β-strands have been solved before, *i.e.* the crystal structures of OmpA (Pautsch & Schulz, 1998) and OmpX (Vogt & Schulz,

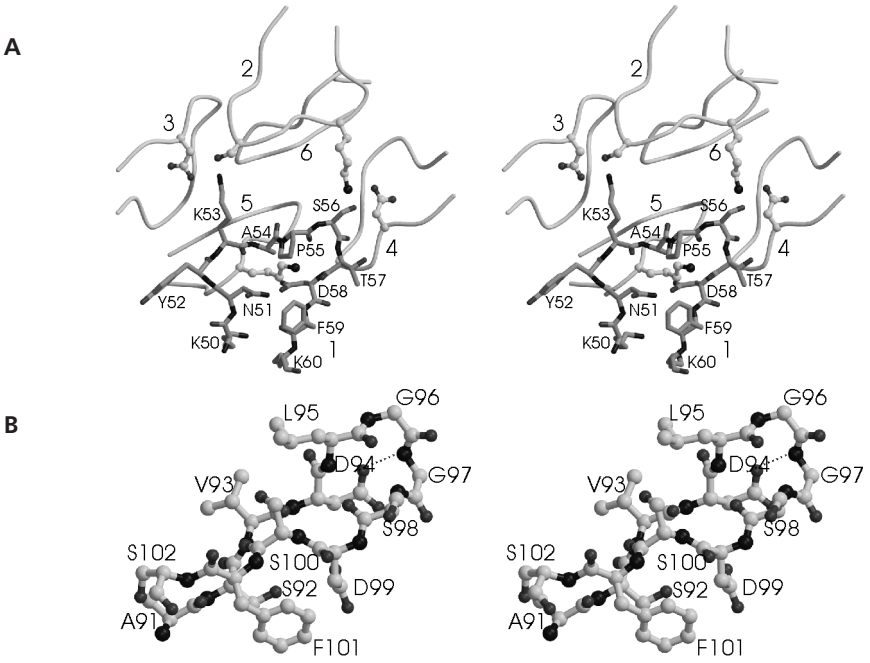

Figure 5.3 **Structure of loops 2 and 3.** A, loop 2 in *grey sticks* and with labels shown together with five symmetry-related loop 2s, which are shown as *coils*. Residues in the symmetry-related loops (labelled *2-6*) that make hydrogen bonds to residues in the original (labelled *1*) are shown by *ball-and-stick*. B, stereo representation of a *ball-and-stick* model of a part of the immunodominant loop 3. Residues are labelled, and one of the hydrogen bonds is indicated by a *dotted line*.

1999) and the solution structure of PagP (Hwang *et al.*, 2002), all from *E. coli*. We searched for more structural homologs of NspA in the Protein Data Bank using the program DALI (Holm & Sander, 1993). This search revealed OmpA and OmpX with the highest z scores of 17.8 and 12.9, respectively, and 144 and 139 Cα-atoms of NspA overlay with the Cα-atoms of OmpA and OmpX with root-mean-square deviations of 2.5 Å and 3.4 Å, respectively. The structure of NspA resembles that of OmpA most, probably because the OmpA β-barrel also has a shear number of 10, whereas the shear number of OmpX is 8. The third protein found by the DALI search was a soluble bacterial protein, quinohemoprotein amine dehydrogenase from *Paracoccus denitrificans* (Datta *et al.*, 2001), a part of which forms of an eight-stranded β-barrel. Using the DALI program, we also found that 126 Cα-atoms of NspA can be superpositioned on OpcA (Prince *et al.*, 2002),

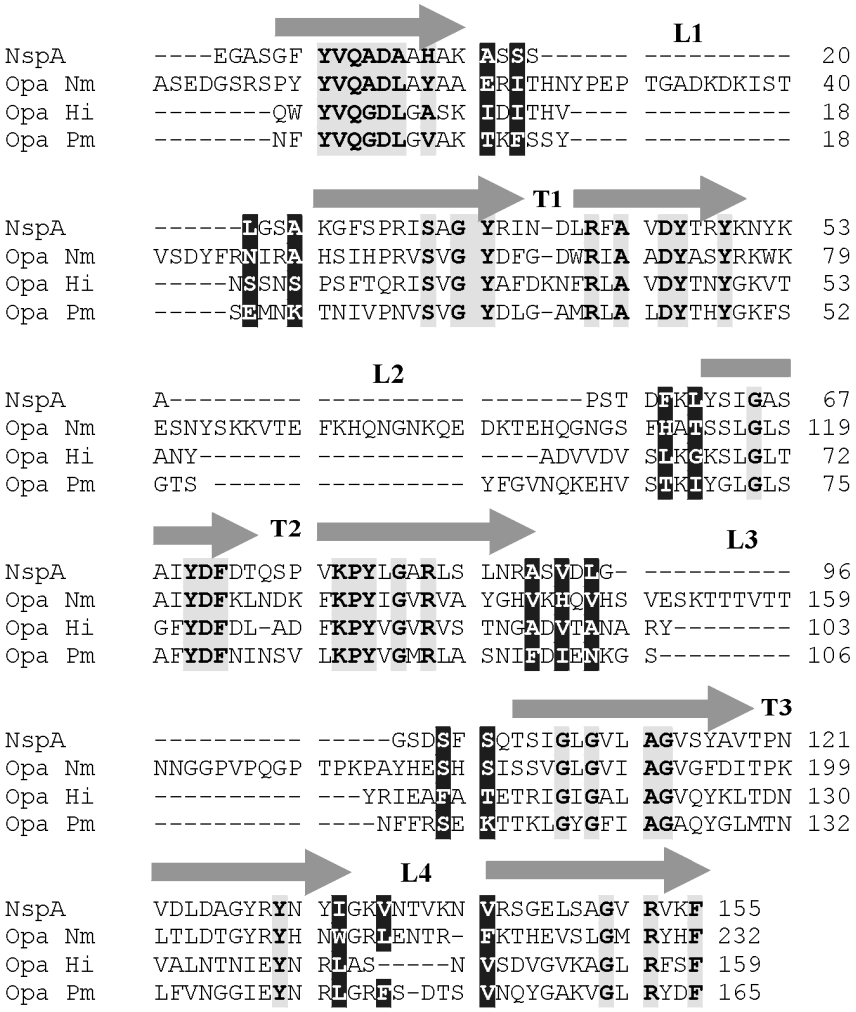

Figure 5.4 **Sequence alignment.** Alignment of NspA from strain H44/76 with an Opa protein from *N. meningitidis* serogroup A strain B494 (Opa Nm, Genbank™ accession number AAC45976), with a homologous OMP from *H. influenzae* (Opa Hi, Genbank™ accession number AAC23104) and with an OMP from *P. multocida* (Opa Pm, Genbank™ accession number AAK03109). Fully conserved residues are shown with a *light grey* background. Residues that make contact to the detergent molecule in the groove at the top of NspA are shown in *white letters* with a *dark grey background*. *Arrows* indicate the β-strands in NspA.`

a 10-stranded β-barrel from *N. meningitidis*, with an root-mean-square deviation of only 3.0 Å and a z score of 9.3. Similarly, another 10-stranded β-barrel, OmpT from *E. coli* (Vandeputte-Rutten *et al.*, 2001), superpositions on NspA with 122 residues with an root-mean-square deviation of 3.8 Å and a z score of 9.4. Although these scores reflect the overall similarities between these 8- and 10-stranded β-barrels, no further remarkable similarities between NspA on the one hand and OpcA or OmpT on the other hand could be detected.

NspA shares the highest sequence homology (~38.7% identity) to the members of the neisserial Opa protein family of adhesins (Figure 5.4). No three-dimensional structure has been solved for these important molecules, but Marlorny *et al.* (Malorny *et al.*, 1998) predicted the topology of Opa. Residues that are present in the membrane-spanning β-strands of NspA are highly conserved between NspA and Opa, particularly the residues that are located on the inside of the β-barrel. It is therefore likely that the structures of Opa and NspA are highly similar in the membrane-spanning region. A major difference between NspA and Opa is the length of the extracellular loops, which are much longer in Opa proteins. Using the sequence similarity between Opa and NspA, we refined the previously predicted Opa topology model (Figure 5.4). In the previous topology model, turn 2 was exceptionally long. In the crystal structure of NspA, this turn is almost as short as the other two turns. Based on the sequence homology between Opa and NspA, it is likely that the fourth strand in the previously predicted topology model has to be shifted toward the extracellular side by 8 residues.

NspA has, in addition, high sequence similarity (~35% identity) with two non-characterized Opa proteins from *Haemophilus influenzae* and *Pasteurella multocida* (Figure 5.4). The loops from the *H. influenzae* and *P. multocida* proteins are more comparable in length with the loops in NspA than to those of the neisserial Opa proteins. Since the hydrophobic groove harbouring a detergent molecule is a remarkable feature of the NspA structure, we examined specifically whether the hydrophobic residues contacting the detergent molecule are conserved in the *H. influenzae* and *P. multocida* proteins. Although none of them was fully conserved, most of the substitutions involved replacements by other hydrophobic residues, especially in the cases of the residues that are located most centrally.

Discussion

There is an obvious need for a vaccine that offers protection against diverse group B meningococcal strains. As described in the Introduction of this chapter, this vaccine should consist of non-capsular components, such as the OMPs present in outer membrane vesicles (OMVs). The major hurdle in development of such a vaccine has been

the fact that the meningococcus possesses a huge capacity to change its outer surface by phase and antigenic variation of many of its OMPs. For this reason, the OMV vaccines tested so far were very effective against their homologous strains but offered far less protection against heterologous strains. Therefore, novel vaccine candidates that are conserved among strains and will likely confer broad protection need to be identified. One very promising vaccine candidate is NspA, which is remarkably conserved among neisserial strains. The relatively low amount of NspA generally present in OMVs may prevent a sufficiently high immune response against this protein in vaccines. However, Moe *et al.* (Moe *et al.*, 2002) have recently shown that sequential immunization with OMVs that were heterologous for the major immunodominant OMPs, but all contained NspA, resulted in protective immunity that was at least partly mediated by bactericidal anti-NspA antibodies. Thus, given in the correct formulation, NspA could be a very important novel vaccine component. Our present study aids in the further development of NspA-based vaccines. For example, we developed efficient procedures to produce NspA and to refold it *in vitro* into its native conformation. This refolded NspA can be used in vaccine formulations. As an alternative strategy, the use of peptide vaccines can be considered. In general, bactericidal antibodies are directed to conformational epitopes, which are, in OMPs, typically located in the extracellular loops. In a previous study, we described that bactericidal antibodies could not be elicited in mice with a linear peptide derived from an epitope from PorA. However, based on the crystal structure of a peptide containing a sequence derived from a PorA epitope in complex with a Fab fragment of a bactericidal antibody, a conformationally restrained peptide was designed. With this peptide, a specific bactericidal immune response could be elicited, demonstrating the value of structural information (Oomen *et al.*, 2003). In NspA, loop 3 is the longest of the four loops and is probably, as in the crystal structure, most exposed *in vivo*. Hou *et al.* (Hou *et al.*, 2002) have shown that loop 3 is an important target for bactericidal antibodies directed against recombinant NspA. The structure of the extracellular loops, particularly loop 3, may greatly aid in the design of peptide vaccines.

The function of NspA is not known yet, although experiments performed by Moe *et al.* (Moe *et al.*, 2001) suggest that NspA is at least not necessary for causing bacteremia in infant rats. Nevertheless, the observation that NspA is highly conserved and is expressed in all neisserial strains tested so far suggests that its function is important. Based on the sequence similarity of NspA to Opa proteins, which are adhesins facilitating colonization of the human naso-pharynx, it could be possible that NspA is an adhesin as well. However, preliminary experiments, in which we measured the adherence of an *E. coli* strain overexpressing NspA to primary human corneal cells, do not support this idea. Either NspA is not adhesin or its adhesive function is blocked on the surface of *E. coli*, possibly due to the long lipopolysaccharides. It is interesting that the structure of NspA

contains a remarkable hydrophobic groove at the top of the molecule, which harbours a detergent molecule. Among the crystal structures of the closed OMPs, *i.e.* OmpA, OmpX, PagP, OmpT, OpcA and OMPLA (Snijder & Dijkstra, 2000), only OmpX also contains a central hydrophobic patch at the extracellular side of the molecule, but it does not form such an extended groove as in NspA. Possibly, NspA could bind a lipid-like molecule, such as a membrane lipid, *in vivo*, thereby possibly playing a role in the invasion of *N. meningitidis* into host cells by interacting with the lipid bilayer of these cells. Future studies, which can now be guided by the elucidated structure of NspA, will bring more insight into the function of NspA.

Acknowledgements

We are grateful for measument time at beamline ID14-EH1 at the European Synchrotron Radiation facility (ESRF) in Grenoble, where the native data set has been measured. We also thank Andrea Schmith for helping at X11 at the European Molecular Biology Laboratory (EMBL) Outstation at Deutsches Elektronen Synchrotron (DESY) in Hamburg. This research has been supported financially by the council for Chemical Sciences of the Netherlands Organization for Scientific Research (NWO-CW) and by the EC project MenB vaccine QLRT-1999-CT-00359.

References

Anderson, E.L., Bowers, T., Mink, C.M., Kennedy, D.J., Belshe, R.B., Harakeh, H., Pais, L., Holder, P. & Carlone, G.M. (1994). Safety and immunogenicity of meningococcal A and C polysaccharide conjugate vaccine in adults. *Infect Immun,* ***62*** *(8):* 3391-3395.

Brunger, A.T., Adams, P.D., Clore, G.M., Delano, W.L., Gros, P., Grosse-Kunstleve, R.W., Jiang, J.S., Kuszewski, J., Nilges, M., Pannu, N.S., Read, R.J., Rice, L.M., Simonson, T. & Warren, G.L. (1998). Crystallography & NMR system: A new software suite for macromolecular structure determination. *Acta Crystallogr D Biol Crystallogr,* ***54*** *(Pt 5):* 905-921.

Cadieux, N., Plante, M., Rioux, C.R., Hamel, J., Brodeur, B.R. & Martin, D. (1999). Bactericidal and cross-protective activities of a monoclonal antibody directed against Neisseria meningitidis NspA outer membrane protein. *Infect Immun,* ***67*** *(9):* 4955-4959.

Chen, T. & Gotschlich, E.C. (1996). CGM1a antigen of neutrophils, a receptor of gonococcal opacity proteins. *Proc Natl Acad Sci U S A,* ***93*** *(25):* 14851-14856.

Collaborative Computational Project, N. (1994). The CCP4 Suite: Programs for Protein Crystallography. *Acta Crystallogr D Biol Crystallogr,* ***50*** 760-763.

Costantino, P., Viti, S., Podda, A., Velmonte, M.A., Nencioni, L. & Rappuoli, R. (1992). Development and phase 1 clinical testing of a conjugate vaccine against meningococcus A and C. *Vaccine,* ***10*** *(10):* 691-698.

Datta, S., Mori, Y., Takagi, K., Kawaguchi, K., Chen, Z.W., Okajima, T., Kuroda, S., Ikeda, T., Kano, K., Tanizawa, K. & Mathews, F.S. (2001). Structure of a quinohemoprotein amine dehydrogenase with an uncommon redox cofactor and highly unusual crosslinking. *Proc Natl Acad Sci U S A,* ***98*** *(25):* 14268-14273.

Dekker, N., Merck, K., Tommassen, J. & Verheij, H.M. (1995). In vitro folding of Escherichia coli outer-membrane phospholipase A. *Eur J Biochem,* ***232*** *(1):* 214-219.

Esnouf, R.M. (1999). Further additions to MolScript version 1.4, including reading and contouring of electron-density maps. *Acta Crystallogr D Biol Crystallogr,* ***55*** *(Pt 4):* 938-940.

Frasch, C.E. (1989). Vaccines for prevention of meningococcal disease. *Clin Microbiol Rev,* ***2 Suppl*** S134-138.

Holm, L. & Sander, C. (1993). Protein structure comparison by alignment of distance matrices. *J Mol Biol,* ***233*** 123-138

Hou, V.C., Raad, Z., Moe, G.R., Dave, A., & Granoff, D.M. (2002) *13th International Pathogenic Neisseria Conference*, *September 1-6, 2002*, p. 127 (abstr.), Norwegian Institute of Public Health, Oslo, Norway

Hwang, P.M., Choy, W.Y., Lo, E.I., Chen, L., Forman-Kay, J.D., Raetz, C.R., Prive, G.G., Bishop, R.E. & Kay, L.E. (2002). Solution structure and dynamics of the outer membrane enzyme PagP by NMR. *Proc Natl Acad Sci U S A,* ***99*** *(21):* 13560-13565.

Jones, T.A., Zou, J.Y., Cowan, S.W. & Kjeldgaard (1991). Improved methods for building protein models in electron density maps and the location of errors in these models. *Acta Crystallogr A,* ***47*** *(Pt 2):* 110-119.

Koronakis, V., Andersen, C. & Hughes, C. (2001). Channel-tunnels. *Curr Opin Struct Biol,* ***11*** *(4):* 403-407.

Malorny, B., Morelli, G., Kusecek, B., Kolberg, J. & Achtman, M. (1998). Sequence diversity, predicted two-dimensional protein structure, and epitope mapping of neisserial Opa proteins. *J Bacteriol,* ***180*** *(5):* 1323-1330.

Mandrell, R.E. & Zollinger, W.D. (1982). Measurement of antibodies to meningococcal group B polysaccharide: low avidity binding and equilibrium binding constants. *J Immunol,* ***129*** *(5):* 2172-2178.

Martin, D., Cadieux, N., Hamel, J. & Brodeur, B.R. (1997). Highly conserved Neisseria meningitidis surface protein confers protection against experimental infection. *J Exp Med,* ***185*** *(7):* 1173-1183.

Merrit, E.A. & Murphy, M.E.P. (1994). Raster3D Version 2.0 - A program for photorealistic molecular graphics. *Acta Crystallogr D Biol Crystallogr,* ***50*** 869-873.

Moe, G.R., Tan, S. & Granoff, D.M. (1999). Differences in surface expression of NspA among Neisseria meningitidis group B strains. *Infect Immun,* ***67*** *(11):* 5664-5675.

Moe, G.R., Zuno-Mitchell, P., Hammond, S.N. & Granoff, D.M. (2002). Sequential Immunization with Vesicles Prepared from Heterologous Neisseria meningitidis Strains Elicits Broadly

Protective Serum Antibodies to Group B Strains. *Infect Immun,* ***70*** *(11):* 6021-6031.

Moe, G.R., Zuno-Mitchell, P., Lee, S.S., Lucas, A.H. & Granoff, D.M. (2001). Functional activity of anti-Neisserial surface protein A monoclonal antibodies against strains of Neisseria meningitidis serogroup B. *Infect Immun,* ***69*** *(6):* 3762-3771.

Murshudov, G.N., Vagin, A.A., Lebedev, A., Wilson, K.S. & Dodson, E.J. (1999). Efficient anisotropic refinement of macromolecular structures using FFT. *Acta Crystallogr D Biol Crystallogr,* ***55*** *(Pt 1):* 247-255.

Nicholls, A., Sharp, K.A. & Honig, B. (1991). Protein folding and association: insights from the interfacial and thermodynamic properties of hydrocarbons. *Proteins,* ***11*** *(4):* 281-296.

Oomen, C.J., Hoogerhout, P., Bonvin, A.M., Kuipers, B., Brugghe, H., Timmermans, H., Haseley, S.R., Van Alphen, L. & Gros, P. (2003). Immunogenicity of Peptide-vaccine Candidates Predicted by Molecular Dynamics Simulations. *J Mol Biol,* ***328*** *(5):* 1083-1089.

Otwinowski, Z. & Minor, W. (1997). Processing of X-ray diffraction data collected in oscillation mode. *Meth in Enzym,* ***276*** *(Macromolecular Crystallography, part A):* 307-326.

Pautsch, A. & Schulz, G.E. (1998). Structure of the outer membrane protein A transmembrane domain. *Nat Struct Biol,* ***5*** *(11):* 1013-1017.

Plante, M., Cadieux, N., Rioux, C.R., Hamel, J., Brodeur, B.R. & Martin, D. (1999). Antigenic and molecular conservation of the gonococcal NspA protein. *Infect Immun,* ***67*** *(6):* 2855-2861.

Poolman, J. & Berthet, F.X. (2001). Alternative vaccine strategies to prevent serogroup B meningococcal diseases. *Vaccine,* ***20 Suppl 1*** S24-26.

Prince, S.M., Achtman, M. & Derrick, J.P. (2002). Crystal structure of the OpcA integral membrane adhesin from Neisseria meningitidis. *Proc Natl Acad Sci U S A,* ***99*** *(6):* 3417-3421.

Rosenqvist, E., Hoiby, E.A., Wedege, E., Caugant, D.A., Froholm, L.O., Mcguinness, B.T., Brooks, J., Lambden, P.R. & Heckels, J.E. (1993a). A new variant of serosubtype P1.16 in Neisseria meningitidis from Norway, associated with increased resistance to bactericidal antibodies induced by a serogroup B outer membrane protein vaccine. *Microb Pathog,* ***15*** *(3):* 197-205.

Rosenqvist, E., Hoiby, E.A., Wedege, E., Kusecek, B. & Achtman, M. (1993b). The 5C protein of Neisseria meningitidis is highly immunogenic in humans and induces bactericidal antibodies. *J Infect Dis,* ***167*** *(5):* 1065-1073.

Saukkonen, K., Abdillahi, H., Poolman, J.T. & Leinonen, M. (1987). Protective efficacy of monoclonal antibodies to class 1 and class 3 outer membrane proteins of Neisseria meningitidis B:15:P1.16 in infant rat infection model: new prospects for vaccine development. *Microb Pathog,* ***3*** *(4):* 261-267.

Schulz, G.E. (2000). beta-Barrel membrane proteins. *Curr Opin Struct Biol,* ***10*** *(4):* 443-447.

Schulz, G.E. (2002). The structure of bacterial outer membrane proteins. *Biochim Biophys Acta,* ***1565*** *(2):* 308-317.

Snijder, H.J. & Dijkstra, B.W. (2000). Bacterial phospholipase A: structure and function of an

integral membrane phospholipase. *Biochim Biophys Acta,* ***1488*** *(1-2):* 91-101.

Tommassen, J., Van Tol, H. & Lugtenberg, B. (1983). The ultimate localization of an outer membrane protein of Escherichia coli K-12 is not determined by the signal sequence. *Embo J,* ***2*** *(8):* 1275-1279.

Vandeputte-Rutten, L., Kramer, R.A., Kroon, J., Dekker, N., Egmond, M.R. & Gros, P. (2001). Crystal structure of the outer membrane protease OmpT from Escherichia coli suggests a novel catalytic site. *Embo J,* ***20*** *(18):* 5033-5039.

Virji, M., Makepeace, K., Ferguson, D.J. & Watt, S.M. (1996). Carcinoembryonic antigens (CD66) on epithelial cells and neutrophils are receptors for Opa proteins of pathogenic neisseriae. *Mol Microbiol,* ***22*** *(5):* 941-950.

Vogt, J. & Schulz, G.E. (1999). The structure of the outer membrane protein OmpX from Escherichia coli reveals possible mechanisms of virulence. *Structure Fold Des,* **7** *(10):* 1301-1309.

Weeks, C.M. & Miller, R. (1999). Optimizing Shake-and-Bake for proteins. *Acta Crystallogr D Biol Crystallogr,* ***55*** *(Pt 2):* 492-500.

Zeth, K., Diederichs, K., Welte, W. & Engelhardt, H. (2000). Crystal structure of Omp32, the anion-selective porin from Comamonas acidovorans, in complex with a periplasmic peptide at 2.1 A resolution. *Structure Fold Des,* ***8*** *(9):* 981-992.

Zollinger, W.D. & Mandrell, R.E. (1983). Importance of complement source in bactericidal activity of human antibody and murine monoclonal antibody to meningococcal group B polysaccharide. *Infect Immun,* ***40*** *(1):* 257-264.

Summary

The proteins found in the outer membrane of Gram-negative bacteria perform a wide variety of functions. Some of these OMPs function as adhesins that mediate adhesion to receptors on host cells facilitating entry of the bacterium into the host. Others function as pores that transport substances varying from ions to whole proteins. Only a small number of OMPs are enzymes that are involved in processes such as the degradation of phospholipids or cleavage of proteins. Despite their different functions, OMPs possess a general structure. They consist of β-strands, that are arranged into a barrel-like structure, referred to as β-barrel, and in addition contain long loops at the extracellular side and short turns at the periplasmic side. OMPs are particularly interesting for biomedical purposes: (1) OMPs are found in the outer membranes of pathogenic Gram-negative bacteria and are often implicated as virulence factors. (2) They are surface-exposed and therefore suitable for vaccine development. Structural information obtained techniques such as with crystallography or NMR is important to gain insight into the function of OMPs and in addition provides detailed information on regions that may be targeted for drug or vaccine design.

In this thesis the crystal structures of the OMPs, OmpT from *Escherichia coli* and NspA from *Neisseria meningitidis,* are described. OmpT serves as a paradigm for the omptin family of outer membrane proteases. A number of omptin members are implicated as virulence factors. One example is Pla from *Yersinia pestis*, which increases the virulence of this bacterium, leading to bubonic plague. NspA from *N. meningitidis* is a promising vaccine candidate, as it is conserved among different strains of *N. meningitidis* and *Neisseria gonorrhoeae*. NspA shares significant sequence homology with Opa proteins, which are important adhesins of *N. meningitidis.*

OmpT cleaves substrates between two consecutive basic amino acids. Its activity is dependent on the presence of lipopolysaccharide (LPS). OmpT has traditionally been classified as a novel member of the serine protease family. The observations that OmpT contains no cysteines, that its activity has a high pH optimum and cannot be inhibited by EDTA, suggest that OmpT is not a cysteine protease, aspartic protease or metalloprotease. The classification of OmpT as a serine protease is, however, controversial. Indeed, site directed mutagenesis studies showed that mutation of Ser99 and His212, which are part of the putative catalytic triad led to a significant reduction of catalytic activity. In contrast, commonly used serine protease inhibitors fail to inhibit OmpT activity significantly.

Chapter 2 describes the crystal structure of OmpT at 2.6 Å resolution. It is the first structure of an outer membrane protease. OmpT forms a 10-stranded β-barrel, which protrudes far into the extra-cellular space, comparable with FhuA. The barrel is

constricted above the membrane spanning region. The structure is informative in two respects. It shows that, indeed, OmpT has an unusual catalytic site and it reveals a putative LPS binding site. The catalytic site is located in a large, negatively charged groove, at the extracellular side of the molecule. In this active site Ser99 and His212 are located more than 8 Å apart, making it unlikely that they participate in one catalytic triad. Instead, based on the structure we propose a novel catalytic site. In **chapter 3**, site directed mutagenesis studies of the conserved acidic residues are described. Mutation of any of the three aspartic acid residues, Asp83, Asp85 and Asp210, resulted in a reduction of activity comparable to the His212Ala mutant (~10,000 fold). Furthermore, mutation of Glu27, Asp97 and Asp208 resulted in significant reduction in activity by ~10 fold. Asp83 and Asp85 are located in close proximity to each other in the crystal structure, forming a couple at one side of the active site groove, and face Asp210 and His212, which form a couple on the other side of the groove. Therefore, based on the structure as well as the mutagenesis data, we propose a novel catalytic site for OmpT, consiting of Asp83, Asp85, Asp210 and His212. In the putative mechanism a water molecule, held in place by Asp83, is activated by the His212-Asp210 dyad, similar to activation of the catalytic serine in serine proteases. The Asp83-Asp85 couple forms the oxyanion hole in a similar fashion as is proposed for aspartic proteases, in which the aspartic couple donates a proton to the oxyanion in the tetrahedral transition state.

The confirmation of our hypothesis awaits the elucidation of a crystal structure of OmpT in complex with a substrate analogue or inhibitor. Attempts to solve a structure of OmpT in complex with a substrate analogue have thus far failed. However, we were able to solve a crystal structure of OmpT in complex with zinc, which is a strong inhibitor of OmpT activity. The results are described in **chapter 4**. In order to obtain an OmpT/Zn^{2+} complex structure, we soaked an OmpT crystal with $ZnCl_2$. In both OmpT molecules in the asymmetric unit, two Zn^{2+} ions bound in the catalytic site, occupying in total four different binding sites. Binding of Zn^{2+} induces conformational changes in the active site, bringing the Asp83-Asp85 and Asp210-His212 couples more than 2 Å closer to each other. Additionally, binding of Zn^{2+} results in high disorder of the extracellular loops. The four Zn^{2+} ions in the asymmetric unit are coordinated differently. Interestingly, the two Zn^{2+} ions that have the highest coordination numbers are both liganded to Asp83. Zinc acts as a non-competitive inhibitor, which means that a substrate can bind but catalysis is inhibited. Therefore, it is likely that Asp83 is not important for substrate binding, but is involved in the catalytic process, like we propose.

The constellation of the active site observed in the crystal structure, in which the proposed four catalytic residues lay in close proximity to each other, seems to be compatible with activity. It is possible however, that the crystal structure of OmpT described in **chapter 2** represents an inactive form of OmpT. Catalytic activity of

OmpT is dependent on the presence of LPS, whereas this molecule is lacking in the structure. A consensus three-dimensional LPS binding motif, consisting of four basic amino acids, was recently proposed, based on the crystal structure of the OMP FhuA in complex with LPS. The structure of OmpT reveals a similar binding site for LPS, consisting of three basic amino acids. The location of this site, at a considerable distance from the active site, close to the membrane-spanning region, suggests that LPS does not participate directly in the catalytic process. This is supported by observation that LPS molecules lacking core sugars are sufficient to allow catalysis by OmpT. Possibly, binding of LPS to OmpT results in a slight conformational change of the barrel, which affects the structure of the catalytic site. The OmpT/ Zn^{2+} complex structure supports the viewpoint that conformational changes likely occur near the active site of OmpT.

Chapter 5 describes the crystal structure of neisserial surface protein A (NspA), an outer membrane protein from *N. meningitidis.* NspA is a potential vaccine candidate against *N. meningitidis*, because it is highly conserved among meningococcal strains and it induces bactericidal antibodies. These antibodies are directed towards the extracellular loops of NspA, especially against loop 3. The function of NspA is unknown, but because it is highly conserved, it is thought to be important. The structure of NspA, which forms an eight-stranded β-barrel, revealed two interesting features. Firstly, the structure shows the exact conformation of the loop 3, which is the longest loop and which forms an epitope against which bactericidal antibodies are directed. This conformation may form the basis of a rational structure-based design of cyclic peptides that mimic the structure of the loop and can potentially be used as peptide vaccines against *N. meningitidis* strains, including serogroup B, for which no vaccine is available yet. A second remarkable feature of the NspA structure is the presence of a long hydrophobic groove at the extracellular side of NspA, in which a detergent molecule is bound. This suggests that NspA can bind hydrophobic ligands, such as lipids. Although NspA is not involved in causing bacteremia in the blood in infant rats, NspA might be important in another life stage of the meningococcus. NspA could be involved in adhesion to or invasion into human epithelial cells by binding to hydrophobic ligands, such as the membrane lipids of host cells.

In summary, the structures of the two outer membrane proteins, OmpT and NspA described in this thesis, provide valuable information on their functions and provide starting points for the design of drugs and vaccines, respectively.

Samenvatting

Eiwitten die aanwezig zijn in de buitenmembraan van Gram-negatieve bacteriën hebben een variëteit aan functies. Een aantal van deze eiwitten functioneert als "adhesinen", welke zorgen voor de aanhechting aan receptoren van gastheercellen, zodat de bacterie kan binnendringen in de gastheer. Anderen vormen poriën die zorgen voor het transport van ionen, eiwitten, etc. Een klein aantal buitenmembraan eiwitten zijn enzymen die betrokken zijn bij processen, bijvoorbeeld de afbraak van fosfolipiden of eiwitten. Ondanks de verschillende functies van buitenmembraan eiwitten, bezitten deze eiwitten toch een gemeenschappelijke structuur. Ze bestaan uit β-strands, die zo gerangschikt liggen dat ze een ton-achtige structuur vormen. Deze structuren worden "β-barrels" genoemd, en hebben lange loops aan de extracellulaire zijde and korte turns aan de periplasmatische zijde. Buitenmembraan eiwitten zijn bijzonder interessant voor biomedische doeleinden: (1) Ze zijn aanwezig in de buitenmembraan van ziekte-verwekkende Gram-negatieve bacteriën en zijn vaak betrokken bij ziekte verwekking. (2) Ze zijn blootgesteld aan de omgeving buiten de bacterie en zijn daarom geschikt voor vaccin ontwikkeling. Structurele informatie verkregen met technieken zoals kristallografie en NMR is belangrijk om meer inzicht te verkrijgen in het functioneren van buitenmembraan eiwitten and geeft bovendien gedetailleerde informatie over de delen die gebruikt zouden kunnen worden voor het ontwikkelen van medicijnen of vaccins.

In dit proefschrift worden de structuren van twee buitenmembraan eiwitten, OmpT van *Escherichia coli* en NspA van *Neisseria meningitidis* beschreven. *Escherichia coli* is een bacterie die normaal in de darmen van de mens voorkomt. In sommige gevallen kan deze bacterie blaasontsteking veroorzaken. *Neisseria meningitidis* is een bacterie die hersenvliesontsteking kan veroorzaken. OmpT fungeert als paradigma voor een familie van buitenmembraan proteases, omptins genoemd. Een aantal leden van deze familie is betrokken bij ziekteverwekking. Een goed voorbeeld is Pla van *Yersinia pestis*, welke de virulentie verhoogt van deze bacterie die de pest veroorzaakt. NspA van *N. meningitidis* is een veel belovende vaccinkandidaat, omdat het een eiwit is dat geconserveerd is tussen verschillende Neisseria stammen. NspA vertoont ook gelijkenis met Opa eiwitten, welke belangrijk zijn voor de aanhechting van *N. meningitidis* aan menselijke cellen.

OmpT knipt substraten tussen twee opeenvolgende positief geladen aminozuren. De activiteit van OmpT is afhankelijk van de aanwezigheid van lipopolysaccharide (LPS), een belangrijke component van de buitenmembraan. OmpT was oorspronkelijk geclassificeerd als een nieuw lid van de serine protease familie. Het feit dat OmpT geen cysteines bezit, dat het actief is bij hoge pH en dat de activiteit niet geremd kan worden

door EDTA, suggereert dat OmpT geen cysteine protease, aspartaat protease of metalloprotease is. De classificatie van OmpT als serine protease is nog steeds onderwerp van discussie. Aan de ene kant hebben mutagenese studies laten zien dat mutaties van serine 99 en histidine 212, welke deel uit maken van de mogelijk katalytische triade, zoals verwacht tot een significante daling van activiteit leiden. Aan de andere kant kunnen veel gebruikte serine protease remmers de activiteit van OmpT niet of nauwelijks remmen.

Hoofdstuk 2 beschrijft de kristalstructuur van OmpT, opgelost tot 2.6 Å resolutie (=oplossend vermogen), de eerste structuur van een buitenmembraan protease. OmpT vormt een β-barrel met tien β-strands, die ver naar buiten uitsteekt. De β-barrel is gesloten boven het gedeelte dat in de membraan zit. De structuur geeft informatie in twee opzichten. Hij laat zien dat OmpT inderdaad een ongewoon katalytisch centrum heeft, en onthult een mogelijke LPS bindingsplaats. Het katalytisch centrum ligt in een grote, negatief geladen groeve, aan de buitenzijde van het molecuul. In dit actieve centrum liggen Ser99 en His212 meer dan 8 Å van elkaar vandaan, wat het onwaarschijnlijk maakt dat ze deel uitmaken van één en dezelfde katalytische triade. In **hoofdstuk 3**, worden mutagenese studies aan de geconserveerde zure residuen beschreven. Mutatie van elk van de drie aspartaten, Asp83, Asp85 en Asp210, resulteert in een verlaging van de activiteit met zo'n 10.000 keer. Verder resulteert de mutatie van Glu27, Asp97 en Asp208 in een tienvoudige verlaging van activiteit. Asp83 en Asp85 liggen dicht bij elkaar in de kristalstructuur en vormen een koppel aan de ene kant van het actieve centrum. Aan de andere kant van het centrum, vormen Asp210 en His212 een koppel. Gebaseerd op de kristalstructuur en de mutagenese data, stellen we een nieuw katalytische centrum voor OmpT voor, die bestaat uit Asp83, Asp85, Asp210 en His212. In het voorgestelde mechanisme wordt een watermolecuul, dat op zijn plaats wordt gehouden door Asp83, geactiveerd door het His212-Asp210 koppel, zoals bij activatie van de katalytische serine in serine proteases. Het Asp83-Asp85 koppel vormt de "oxyanion" holte, zoals voorgesteld voor aspartaat proteases, waarin het aspartaat koppel een proton doneert aan het oxyanion in het tetrahedrale transitie stadium.

Om onze hypothese te bevestigen is het nodig om de kristalstructuur van OmpT in complex met een substraatanaloog of remmer te bepalen. Pogingen om zo'n structuur te bepalen zijn tot nu toe niet succesvol geweest. We hebben echter wel de kristalstructuur van OmpT in complex met zink, een sterke remmer van OmpT activiteit, kunnen bepalen. De resultaten van deze structuur zijn beschreven in **hoofdstuk 4**. Om een structuur van een OmpT/Zn^{2+} complex te verkrijgen hebben we een OmpT kristal gedrenkt in $ZnCl_2$. In de asymmetrische eenheid bevinden zich twee OmpT moleculen die beide twee Zn^{2+} ionen hebben gebonden in het katalytisch centrum. Deze Zn^{2+} ionen bezetten in totaal vier verschillende binding plaatsen. Het binden van Zn^{2+} door OmpT veroorzaakt aanzienlijke veranderingen in de structuur in en rond het actieve

centrum, waardoor de Asp83-Asp85 en Asp210-His212 koppels meer dan 2 Å dichter bij elkaar komen. Verder veroorzaakt binding van Zn^{2+} wanorde in de extracellulaire loops. De vier Zn^{2+} ionen in de asymmetrische eenheid zijn verschillend gecoördineerd. De twee Zn^{2+} ionen die het hoogste coördinatie nummer hebben zijn beide gebonden aan Asp83. Zink is een non-competitieve remmer, wat betekent dat een substraat weliswaar kan binden, maar dat katalyse wordt geremd. Daarom is het waarschijnlijk dat Asp83 niet belangrijk is voor substraatbinding, maar betrokken is bij het katalytisch proces, zoals wij voorstellen.

De rangschikking van de aminozuren in het actieve centrum zoals waargenomen in de kristalstructuur, waarin de katalytische residuen dicht bij elkaar liggen, lijkt compatibel met activiteit. Het is echter mogelijk dat de kristalstructuur zoals beschreven in hoofdstuk 2 een inactieve vorm van OmpT weergeeft. De katalytische activiteit is afhankelijk van de aanwezigheid van LPS, terwijl dat molecuul niet aanwezig is in de structuur. Op basis van de structuur van het buitenmembraan eiwit FhuA in complex met LPS, is een "consensus" drie-dimensionaal LPS bindingsmotief, dat bestaat uit vier positief geladen aminozuren, voorgesteld. De structuur van OmpT suggereert een soortgelijke bindingsplaats voor LPS, die bestaat uit drie positief geladen aminozuren. De locatie van deze bindingsplaats, een aanzienlijke afstand van het actieve centrum verwijderd, suggereert dat LPS niet direct deel neemt aan het katalytisch proces. Dit wordt nog versterkt door de observatie dat LPS moleculen die "core" suikers missen nog steeds OmpT activeren. Het is mogelijk dat binding van LPS aan OmpT resulteert in een geringe structurele verandering, die de structuur van het katalytisch centrum beïnvloed. De OmpT/Zn2+ complex structuur versterkt het idee dat structurele veranderingen mogelijk optreden dichtbij het actieve centrum van OmpT.

Hoofdstuk 5 beschrijft de kristalstructuur van neisserial surface protein A (NpsA), een buitenmembraan eiwit van *Neisseria meningitidis*. NspA is een goede vaccin kandidaat tegen verschillende Neisseria stammen omdat het goed geconserveerd is tussen Neisseria stammen en omdat het bacteriedodende antilichamen opwekt. Deze antilichamen zijn gericht tegen de extracellulaire loops van NspA, in het bijzonder tegen loop 3. De functie van NspA is onbekend, maar omdat het eiwit zo goed geconserveerd is, is de functie waarschijnlijk belangrijk. De structuur van NpsA, welke een β-barrel met acht β-strands vormt, onthult twee belangrijke eigenschappen. Ten eerste, de structuur onthult de exacte structuur van loop 3, de langste loop. Deze structuur kan gebruikt worden voor het ontwerpen van cyclische peptiden die gebruikt zouden kunnen worden als peptide vaccins tegen *N. meningitidis* stammen, waaronder serogroep B, waartegen nog geen vaccin beschikbaar is. Een tweede bijzondere eigenschap van NspA is de aanwezigheid van een lange hydrofobe groeve aan de extracellulaire zijde van NspA, waar in de structuur een detergent molecuul in gebonden zit. Dit suggereert dat NspA hydrofobe

liganden kan binden, bijvoorbeeld lipiden. Hoewel NspA niet betrokken is bij het vermenigvuldigen van de meningococ in het bloed van jonge ratten, is NspA mogelijk belangrijk in een ander stadium in het leven van de meningococ. NspA kan bijvoorbeeld betrokken zijn bij adhesie of bij invasie in menselijke epitheel cellen door te binden aan hydrofobe liganden, zoals membraan lipiden van de gastheer cellen.

Samengevat, de structuren van de twee buitenmembraan eiwitten, OmpT en NspA beschreven in dit proefschrift, geven veel informatie over hun functies en vormen een goed begin voor het ontwerpen van medicijnen en vaccins, respectievelijk.

Dankwoord

Hoewel mijn naam als enige op de voorkant van dit boekje staat, hebben vele mensen bijgedragen aan de totstandkoming van dit proefschrift. Ten eerste wil ik Prof. Dr. J. Kroon, die spijtig genoeg veel te vroeg is gestorven, en Prof. Dr. P. Gros vanaf deze plaats hartelijk bedanken. Beste Jan, met jou als mijn promotor kon ik helaas niet lang genoeg van jouw brede ervaring genieten. Bedankt voor het vertrouwen dat je in me stelde. Beste Piet, bedankt voor de kans die je me hebt gegeven om eerst als hoofdvakstudent en later als onderzoeker in opleiding (OIO) bij de afdeling Kristal- en Structuurchemie interessant onderzoek te doen naar het functioneren van buitenmembraaneiwitten door middel van structuur opheldering. Ik heb ik een erg leuke tijd gehad.

Zonder de goede samenwerkingsverbanden met de secties "Enzymology en Protein Engeneering" (EPE) en "Moleculaire Microbiologie" was dit proefschrift nooit tot stand gekomen. Prof. Dr. M. Egmond (EPE), beste Maarten bedankt dat je mijn tweede promotor wilt zijn en dat ik altijd ideeën met je kon uitwisselen. Beste Niek (EPE), jammer dat je zo snel vertrok naar AstraZeneca, maar zeker hier en ook nog steeds op een lange afstand heb je me veel geholpen. Arjen (EPE), bedankt voor de "bakken" zuiver eiwit. Wat een ordelijkheid legde jij aan de dag.

Alhoewel het meeste in dit boekje uit de samenwerking met de sectie EPE is gekomen, werkte ik tijdens mijn promotie in eerste instantie samen met Moleculaire Microbiologie. Carmen (beide) bedankt voor de hulp bij de zuiveringen van PorA. Helaas is de structuur daarvan nog steeds niet opgehelderd, maar zal dat in de toekomst hopelijk nog eens gebeuren. Gelukkig had ik ook de eer om de structuur van NspA (een nog betere vaccinkandidaat dan PorA) te mogen ophelderen. Martine, bedankt voor je inzet en het werk aan NspA. Prof. Dr. J. Tommassen, beste Jan, bedankt voor de goede mogelijkheden en je enthousiasme en ideeën. Hopelijk blijft het, ook in toekomst, een vruchtbare samenwerking.

Naar Grenoble of Hamburg gaan om kristallen te meten was een belangrijke bezigheid tijdens mijn promotie. Naast diegene van het lab die mij vergezelden tijdens de reizen, dank ik ook de stafleden van het EMBL die hebben geholpen bij de metingen. Raimond en Maaike, heel veel dank voor de heerlijke avonden bij jullie in Grenoble. Raimond, nog bedankt voor je kostbare tijd (een hele nacht lang) om Arie en mij te helpen. Ook heb jij mij geholpen met de meest cruciale stap in de structuurbepaling, het bepalen van de fasen.

Sjors en Clasien, jullie begonnen hier omstreeks dezelfde periode met jullie promoties. Met jullie heb ik dus ook de meeste leuke (en soms minder leuke) tijden meegemaakt. De congressen in York en Krakau waren naast hun informatieve waarde, door jullie aanwezigheid extra leuk. Clasien, leuk dat we elkaars paranimfen zijn.

Jean bedankt voor de begeleiding tijdens mijn hoofdvak. Door jou was ik al goed ingewerkt toen ik hier als OIO begon. Verder wil ik mijn andere collega's ook bedanken voor alle hulp en gezelligheid op de sectie. Arie, Eric, Bert, Fin, Hans, Huub, Jenny, Loes, Marjan (wat een administratie komt er bij kijken, gelukkig dat jij er was), Martin L., Nicole, Rob, Roland, Shizuko, Toine en Ton S., en ex-collega's Ab, Anne, Annika, Allison, Barend, Bauke, Bogos, Carien, Dianne, Jeroen, Martin W., Roeland, Stephane, Ton L. en Wijnand, allen bedankt voor de leuke tijd met jullie. Ik heb ook een groot aantal hoofdvak studenten mee mogen maken, waarvan ik er zelf drie heb mogen begeleiden. Patrick, Stan en Ad, bedankt voor jullie inzet en enthousiasme.

Jan, Aloys en Ingrid (Audio Visuele dienst) bedankt voor de opmaak van dit boekje (in het bijzonder de kaft, die er misschien niet zo bijzonder uit ziet, jullie en ik weten beter) en de mooie posters die jullie voor mij hebben gemaakt. Door jullie kon ik mijn werk altijd goed presenteren.

Verder wil ik al mijn familie en vrienden buiten het lab heel hartelijk bedanken voor de ontspanning buiten het werk om. Mama bedankt voor je hulp in het begin met het onder de knie krijgen van de kristallografie. Wat een geluk heb ik met zo'n lieve moeder die ook nog eens in de kristallografie werkte. Mitja, bedankt voor alles, maar dan ook alles.

Lucy

Curriculum vitae

De schrijfster van dit proefschrift werd op 5 augustus 1974 geboren te Leiden. In 1991 behaalde zij haar Havo-diploma en in 1993 haar Vwo-diploma aan het "Bonaventura College" te Leiden. Vanaf hetzelfde jaar tot mei 1998 studeerde zij Biomedische Wetenschappen aan de Rijksuniversiteit Leiden. Tijdens de doctoraal fase heeft zij in Leiden stages gevolgd bij afdeling Stralings Genetica en Chemische Mutagenese (o.l.v. Drs. R. Kooistra, Prof. Dr. A. Pastink), afdeling Medische Biochemie (Drs. P. Keblusek, Dr. A. Zantema, Prof. Dr. van der Eb), afdeling Metabolische ziekten en endocrinology (Drs. E.H. van Essen, H.H. Lemkes). Verder werd een stage gevolgd bij de afdeling "Biochemistry" aan de Univeristeit van Oxford (o.l.v. Dr. M. Adams) en een hoofdvak bij Kristal- en Structuurchemie aan de Universiteit Utrecht (o.l.v. Dr. J. van den Elsen, Prof. Dr. Piet Gros en wijlen Prof. Dr. J. Kroon). In juni 1998 begon zij als onderzoeker in opleiding bij de sectie Kristal- en Structuurchemie aan de Universiteit Utrecht ,gefinancierd door NWO. In deze functie werd het in dit proefschrift beschreven onderzoek verricht, onder begeleiding van Prof. Dr. P. Gros en Prof. Dr. M.R. Egmond. Vanaf 1 juni 2002 zet zij dit onderzoek voort, bij dezelfde sectie, als postdoctoraal onderzoeker.

List of publications

van den Elsen J., Vandeputte-Rutten L. Kroon J. and Gros P. (1999) Bacterial antibody recognition of meningococcal PorA by induced fit. Comparison of liganded and unliganded Fab structures. *J. Biol. Chem.* **274**(3):1495-1501

Au S.W., Naylor C.E. Gover S., Vandeputte-Rutten L., Scopes D.A., Mason P.J., Luzzatto L., Lam V.M. and Adams M.J. (1999) Solution of the structure of tetrameric human glucose 6-phosphate dehydrogenase by molecular replacement. *Acta Crystallogr. D Biol. Crystallogr.* **55** (Pt 4):826-834

Cosgrove M.S., Gover S., Naylor C.E., Vandeputte-Rutten L. Adams M.J. and Levy H.R. (2000) An examination of the role of Asp-177 in the His-Asp catalytic dyad of *Leuconostoc mesenteroides* glucose 6-phosphate dehydrogenase: X-ray structure and pH dependence of kinetic parameters of the D177N mutant enzyme. *Biochemistry* **39**(49):15002-15011

Vandeputte-Rutten L., Kramer R.A., Kroon J., Dekker N., Egmond M.R. and Gros P. (2001) Crystal structure of the outer membrane protease OmpT from *Escherichia coli* suggests a novel catalytic site. *EMBO J.* **20**(18):5033-5039

Kramer R.A., Vandeputte-Rutten L., de Roon G.J., Gros P., Dekker N. and Egmond M.R. (2001) Identification of essential acidic residues of outer membrane protease OmpT supports a novel active site. *FEBS Lett.* **505**(3):426-430

Kramer R.A., Brandenburg K., Vandeputte-Rutten L., Werkhoven M., Gros P., Dekker N. and Egmond M.R. (2002) Lipopolysaccharide regions involved in the activation of *Escherichia coli* outer membrane protease OmpT. *Eur. J. Biochem.* **269**(6):1746-1752

Vandeputte-Rutten L. and Gros P. (2002) Novel proteases: common themes and surprising features. *Curr. Opin. Struct. Biol.* **12**(6):704-708

Vandeputte-Rutten L., Bos M.P., Tommassen J., Gros P. (2003) Crystal structure of Neisserial surface protein A (NspA), a conserved outer membrane protein with vaccine potential. *J. Biol. Chem.* **278**(27):24825-24830

Vandeputte-Rutten L., Dekker N., Kramer R.A., Egmond M.R. and Gros P. Structural analysis of the outer membrane protease OmpT from *Escherichia coli* inhibited by zinc. *manuscript in preparation*